Generation of Human Aldose Reductase Mutants of Cys298

by

Daniel O. Oder

Submitted in Partial Fulfillment of the Requirements

for the Degree of

Master of Science

in the

Chemistry

Program

YOUNGSTOWN STATE UNIVERSITY

August 2015

Generation of Human Aldose Reductase Mutants of Cys298

Daniel O. Oder

I hereby release this thesis to the public. I understand that this thesis will be made available from the OhioLINK ETD Center and the Maag Library Circulation Desk for public access. I also authorize the University or other individuals to make copies of this thesis as needed for scholarly research.

Signature:

_____

Daniel O. Oder, Student Date

Approvals:

_____

Ganesaratnam K. Balendiran, Ph. D., Thesis Advisor Date

_____

Sherri Lovelace-Cameron, Ph. D., Committee Member Date

_____

Brian D. Leskiw, Ph. D., Committee Member Date

_____

Dr. Salvatore A. Sanders, Associate Dean of Graduate Studies Date

©

Daniel O. Oder

2015

Thesis Abstract

Human aldose reductase (hAR) uses the oxidation of NADPH to $NADP^+$ in order to catalyze the reduction of aldehydes to their corresponding alcohols. This enzyme is important because of its role in the polyol pathway and hyperglycemia-induced tissue damage. Several studies have shown that Cys298 has a role in the activation of hAR to its oxidized form. Even so, though it is not a catalytic residue the mechanism of hAR activation is not yet clearly understood. Structure, function and kinetic studies of Cys298 mutants will further our understanding of the role of this residue in substrate binding and interaction. This thesis project forms the foundation for future investigations since it provides an efficient, reproducible and reliable protein expression and protein purification system for three Cys298 mutants: Cys298Ala, Cys298Asp, and Cys298Gly.

Acknowledgements

I wish to express my sincere thanks to my research advisor, Dr. Ganesaratnam Balendiran, whose expertise, understanding and patience was invaluable to my graduate experience. I must also acknowledge Sudipti Gupta, without whose patience and tutelage I would not have developed such a mastery of the skills and experience needed to troubleshoot and succeed in this project. I am grateful for all the friendships I have encountered during this experience and for having a delightful group of graduate students to work with. Working with Amanda Sacco, Heather Folkwein, Emeka Udeigwe, DaVena Zivkovic, Niloufar Niknam, Victoria Boulos, and Aamber Hopson has been enjoyable and encouraging. I will miss the camaraderie we have shared during these past years and the countless stories we have told. I appreciate all the members of my thesis committee for their efforts in my progress towards graduation. Additionally, I appreciate the encouragement and support of my mom and dad. They had a role in persuading me to pursue this degree and without them I may have not succeeded it. In conclusion, I recognize that this research would not have been possible without the assistance of the Chemistry Department and School of Graduate Studies at Youngstown State University. Also, this research would not be possible without funding from the National Institutes of Health and the American Diabetes Association through grant DK088496.

Table of Contents

List of Tables

List of Figures

List of Symbols and Abbreviations:

%	percent
®	registered
µg	microgram
µL	microliter
µM	micromolar
3-DG	3-deoxyglucosone
A	adenosine
Abs	UV-Vis absorbance
AGEs	advanced glycation end-products
AKRs	aldo-keto reductases
Ala	alanine
Amp	ampicillin
Asp	aspartate
BME	β-mercaptoethanol
Bp	base pair
C	cytosine
C298A	cysteine to alanine mutant
C298D	cysteine to aspartate mutant
C298G	cysteine to glycine mutant
CEL	N^{ε}-(carboxyethyl)-lysine
CMA	N^{ε}-(carboxymethyl)-arginine
CML	N^{ε}-(carboxymethyl)-lysine
Cys	cysteine
ddH_2O	double-distilled H_2O
DNA	deoxyribonucleic acid
dsDNA	double stranded DNA
Ft	foot
G	guanine
GA	glycoaldehyde
Gly	glycine
GOLD	glyoxal-lysine dimer
GSH	tripeptide glutathione (Gly-Cys-Gly)
GSNO	S-nitrosoglutathione
GSSG	glutathione
hAR	human aldose reductase
HHE	4-hydroxy-2(E)-hexenal
HNE	4-hydroxy-2(E)-nonenal
HPHE	4-hydroperoxy-2(E)-hexenal
HPNE	4-hydroperoxy-2(E)-nonenal
IgG	bovine γ-globulin (immunoglobulin G)
IMAC	immobilized metal affinity chromatography
IPTG	isopropyl-1-thio-β-D-galactopyranoside
K	kilo

k_{cat}	turnover number
k_{cat}/K_m	catalytic efficiency
K_i	inhibition constant
K_m	Michaelis constant
LB	Luria-Broth
M	molar
MDA	malonaldehyde
MES	4-morpholineethanesulfonic acid
mg	milligram
mL	milliliter
mM	milimolar
MOLD	methylglyoxal-lysine dimer
MWCO	molecular weight cut-off
Ng	nanogram
OHE	4-oxo-2(E)-hexenal
ONE	4-oxo-2(E)-nonenal
PAGE	polyacrylamide gel electrophoresis
PBS	phosphate buffered saline
PCR	polymerase chain reaction
POVPC	1-palmitoyl-2-(5-oxovaleroyl)-sn-glycero-3-phosphocholine
rpm	revolutions per minute
S	second
SDS	sodium dodecyl sulfate
SOC	super optimal broth with catabolite repression
T	thymidine
TEMED	tetramethylethylenediamine
Tm	melting temperature
U	unit
V	volts
v/v	volume per volume
V_{max}	maximum velocity
w/v	weight per volume
X-Gal	5-bromo-4-chloro-3-indoyl-β-D-galactopyranoside

Chapter I: Introduction

I. Aldo-Keto Reductases

Human aldose reductase (hAR) belongs to a group of structurally similar proteins called aldo-keto reductases (AKRs). All plants, animals and fungi utilize AKRs to catalyze the reduction of aldehydes and ketones to primary or secondary alcohols.[1] These AKRs play an important role in the detoxification of toxic aldehydes and ketones that are produced endogenously (within the cell or organism) or exogenously (outside the cell or organism).[1] Humans express 13 AKR proteins: aldehyde reductase (AKR1A1), aldose reductases (AKR1B1, AKR1B10), hydroxysteroid dehydrogenases (AKR1C1, AKR1C2, AKR1C3, AKR1C4), Δ4-3-ketosteroid-5-β-reductase (AKR1D1), Kvβ voltage-gated potassium channel proteins (AKR6A3, AKR6A5, AKR6A9), and alflatoxin reductases (AKR7A2, AKR7A3).[1] Below is the phylogenetic tree of human aldo-keto reductases.

Figure 1.1: Phylogenetic Tree of Human Aldo-Keto Reductases[1]

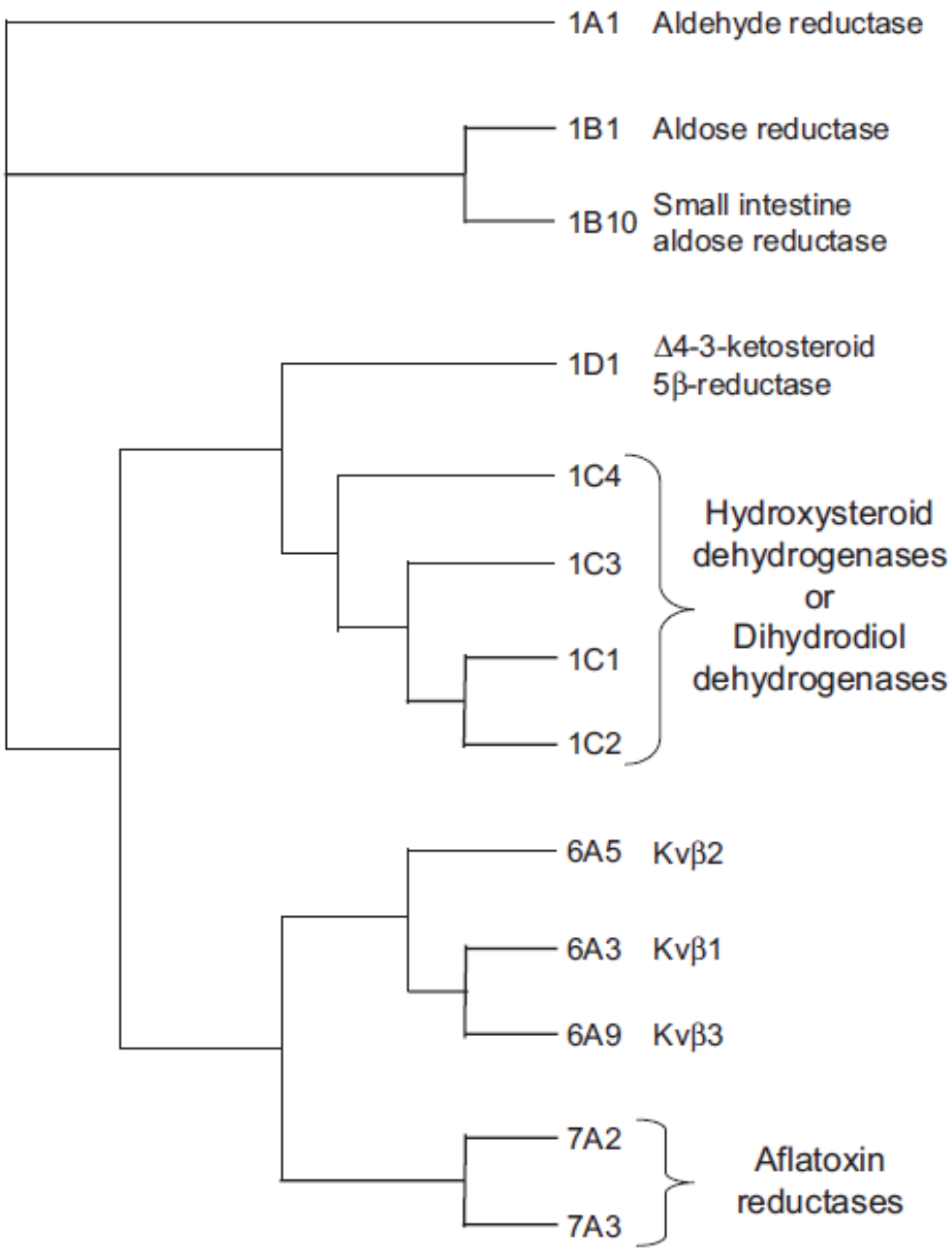

II. Natural Substrates

For aldose reductases like hAR (AKR1B1), the tight binding to NADPH predominantly provides the energy for catalysis.[1] This is why a wide range of aldehydes can be efficiently reduced even when there is little substrate affinity. Human aldose reductase's natural substrates include lipid peroxidation products and advanced glycation end-products (AGEs).[1] Lipid peroxidation is the oxidative degradation of lipids to yield aldehydes such as methylglyoxal, 3-deoxyglucosone (3-DG), 4-hydroxy-2(E)-nonenal (HNE) and 1-palmitoyl-2-(5-oxovaleroyl)-sn-glycero-3-phosphocholine (POVPC).[1] Chemical structures of various lipid peroxidation products are shown in the following figures (Figure 1.2 and Figure 1.3).

Figure 1.2: Lipid Peroxidation Products[1]

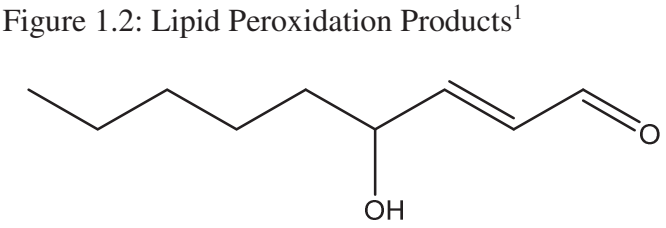

hydroxynonenal

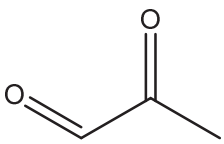

methylglyoxal

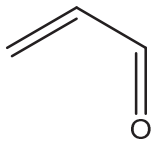

acrolein

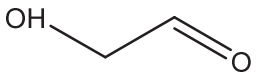

glycoaldehyde

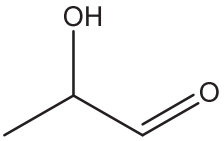

2-hydroxypropanal

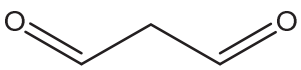

malondialdehyde

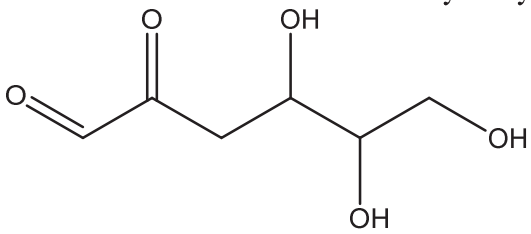

3-deoxyglucosone

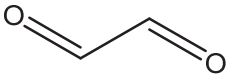

glyoxal

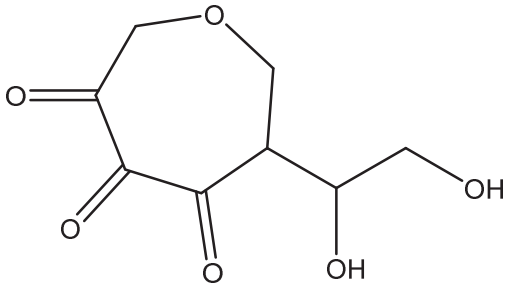

dehydroascorbic acid

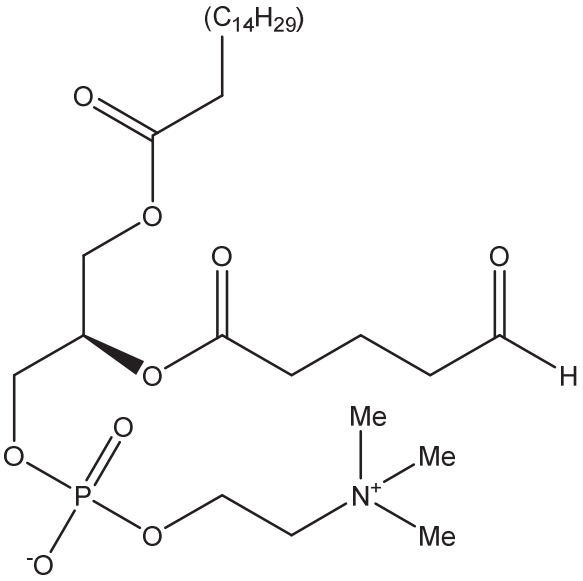

POVPC

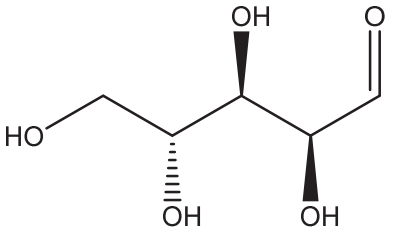

D-arabinose

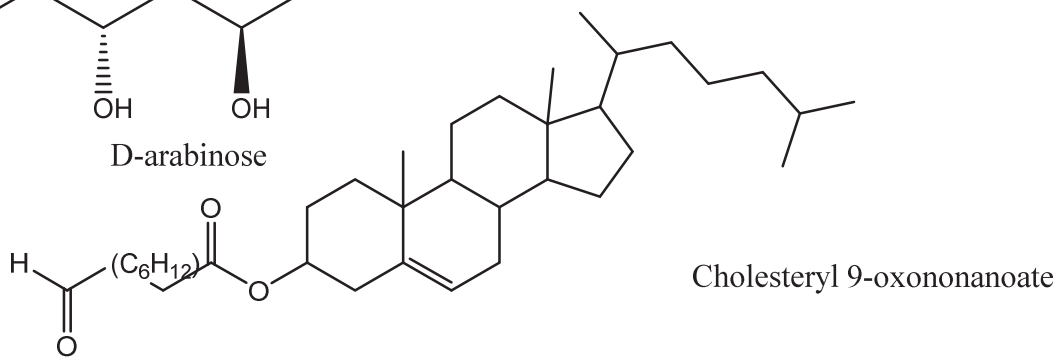

Cholesteryl 9-oxononanoate

Figure 1.3: Lipid Peroxidation Products[2]

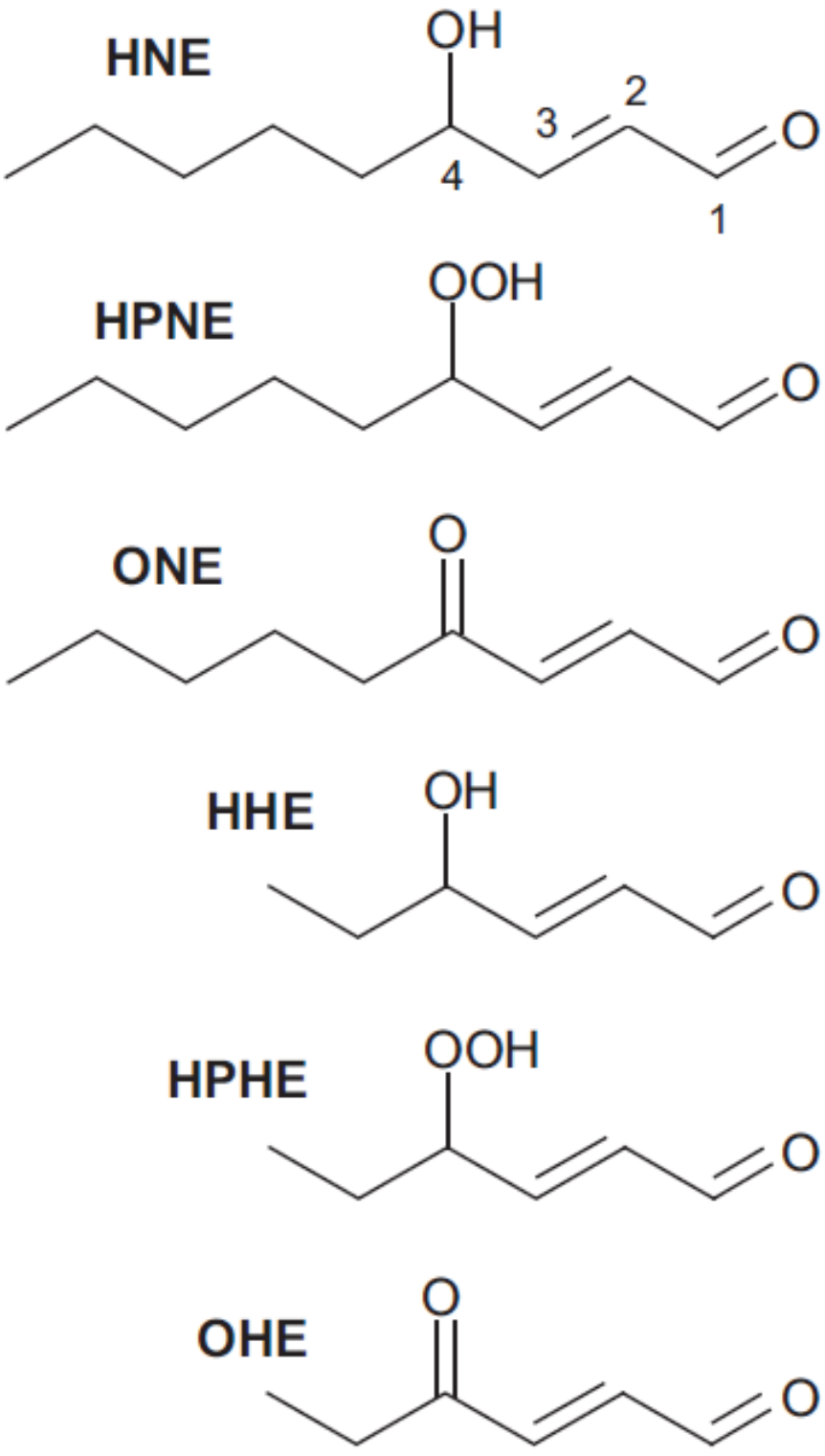

Meanwhile, AGEs are modifications of proteins or lipids that are produced when proteins or lipids react with aldose sugars through non-enzymatic glycosylation.[3] The figure below (Figure 1.4) illustrates the process by which an aldehyde (glucose) reacts with a protein to form a Schiff base (aldimine), undergoes Amadori rearrangement to become a more stable ketoamine and then is oxidatively cleaved by reactive nitrogen or oxygen species to produce an AGE.[1] Figure 1.5 and Figure 1.6 show both lysine-derived and arginine-derived AGEs.

Figure 1.4: Formation of Advanced Glycation End Products[1]

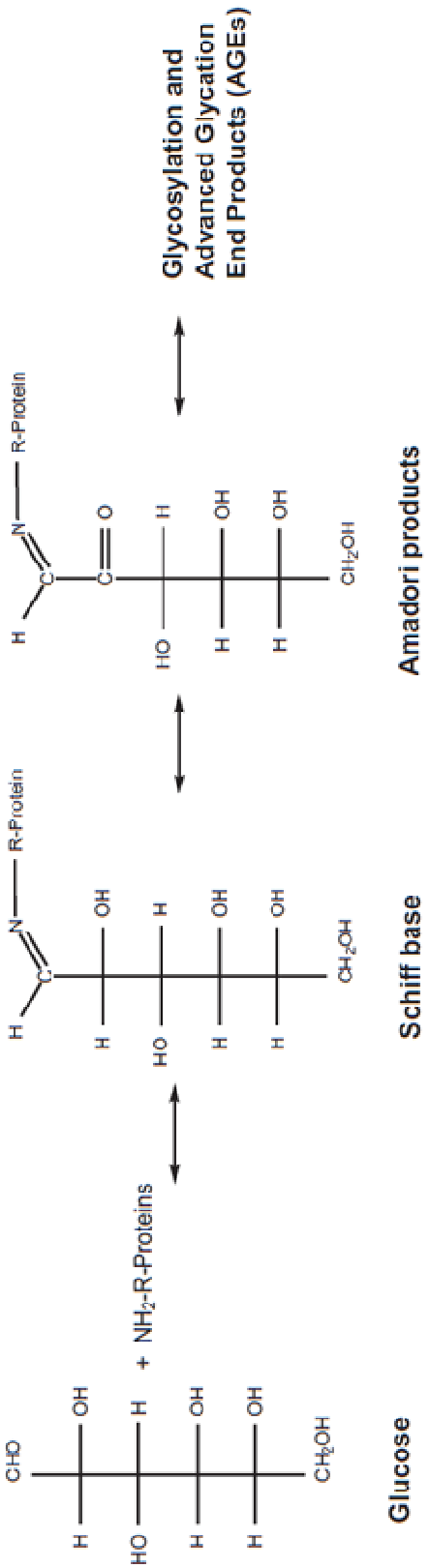

Figure 1.5: Lysine Derived AGEs[4]

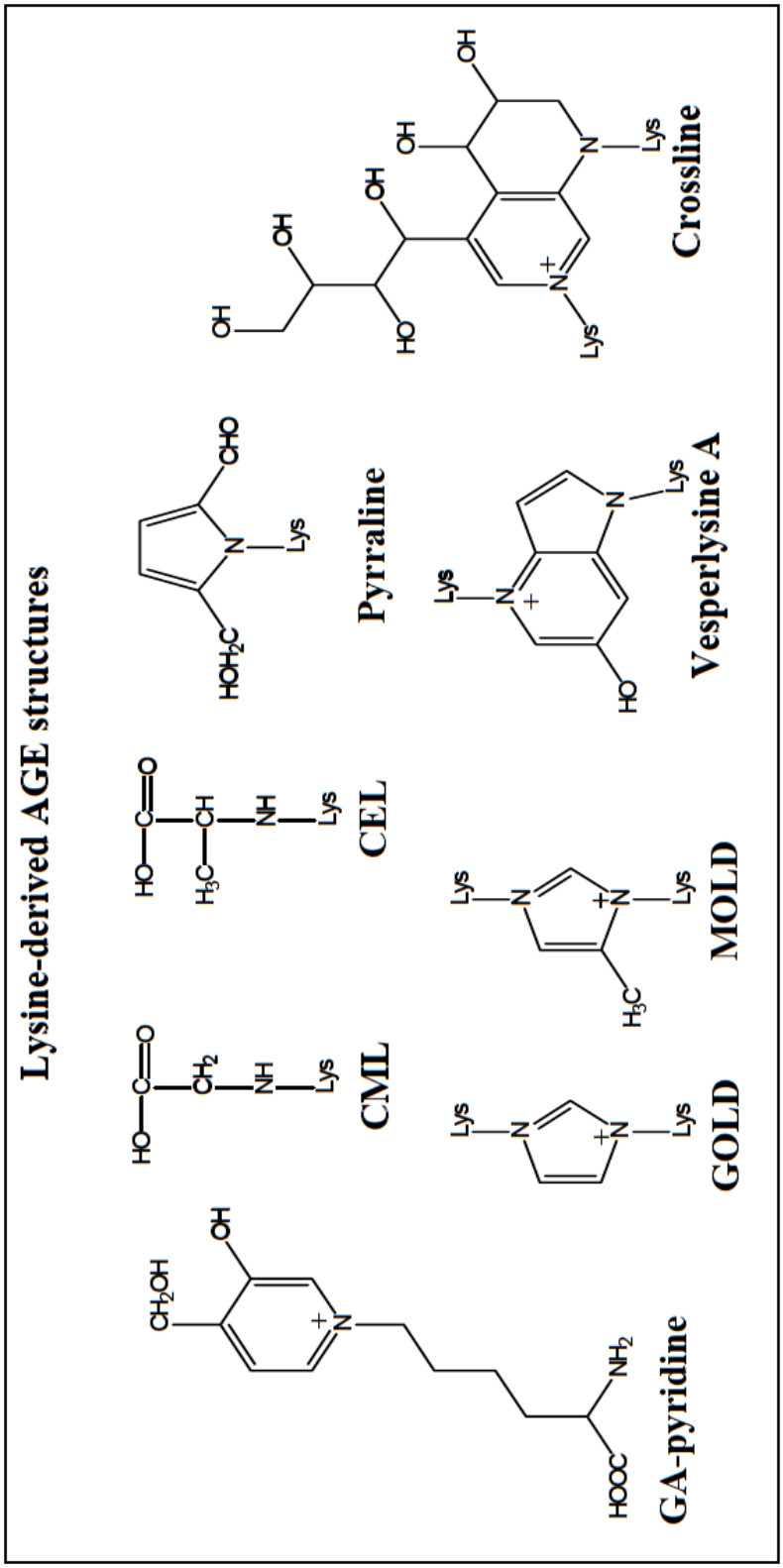

Figure 1.6: Arginine-derived AGEs[4]

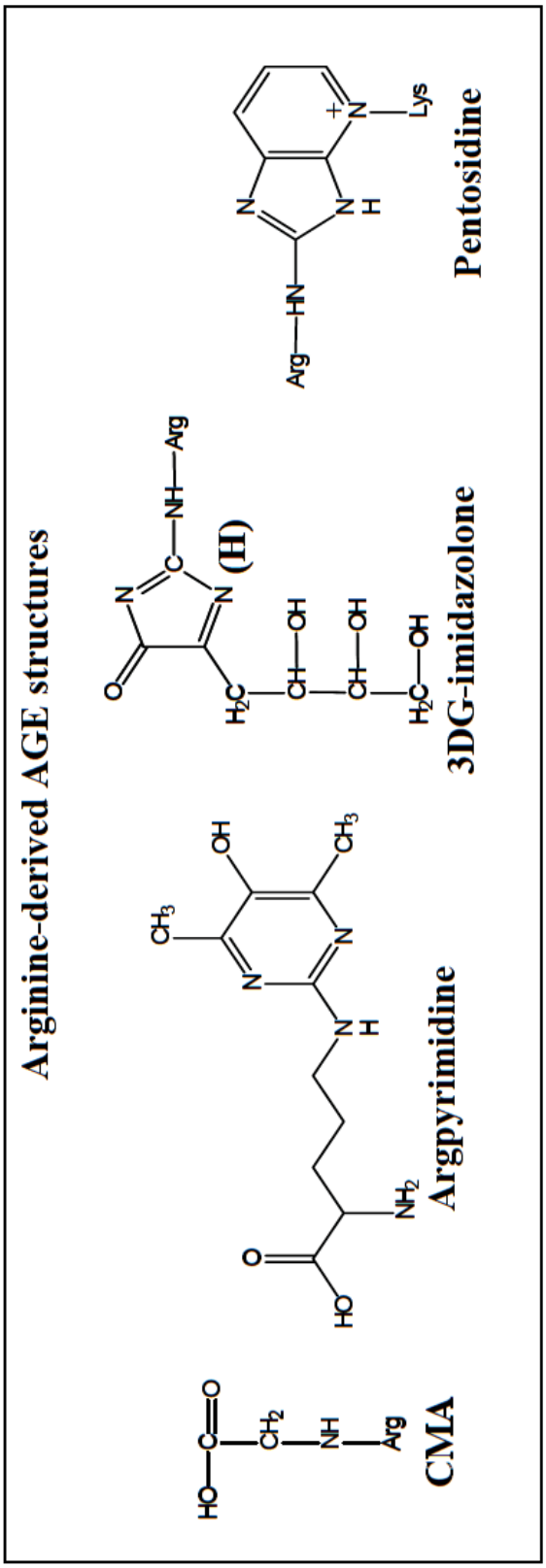

III. Polyol Pathway

Normally, humans use two important pathways for metabolizing excess glucose. Glycogenesis is for short-term energy storage and through this pathway the glucose is stored as glycogen. Meanwhile, triacylglycerol biosynthesis is for long-term energy storage and through this pathway the glucose is converted to triacylglycerols (fatty acids). However, when the human body is overwhelmed with excess glucose (hyperglycemia) it utilizes an additional pathway to metabolize glucose.[5] This supplementary pathway is the polyol pathway (Figure 1.7).[5] During normoglycemia (normal glucose levels) less than 3% of glucose is metabolized through this pathway, but during hyperglycemia as much as 30% of the total glucose is metabolized through this pathway.[6,7]

Figure 1.7: Polyol Pathway

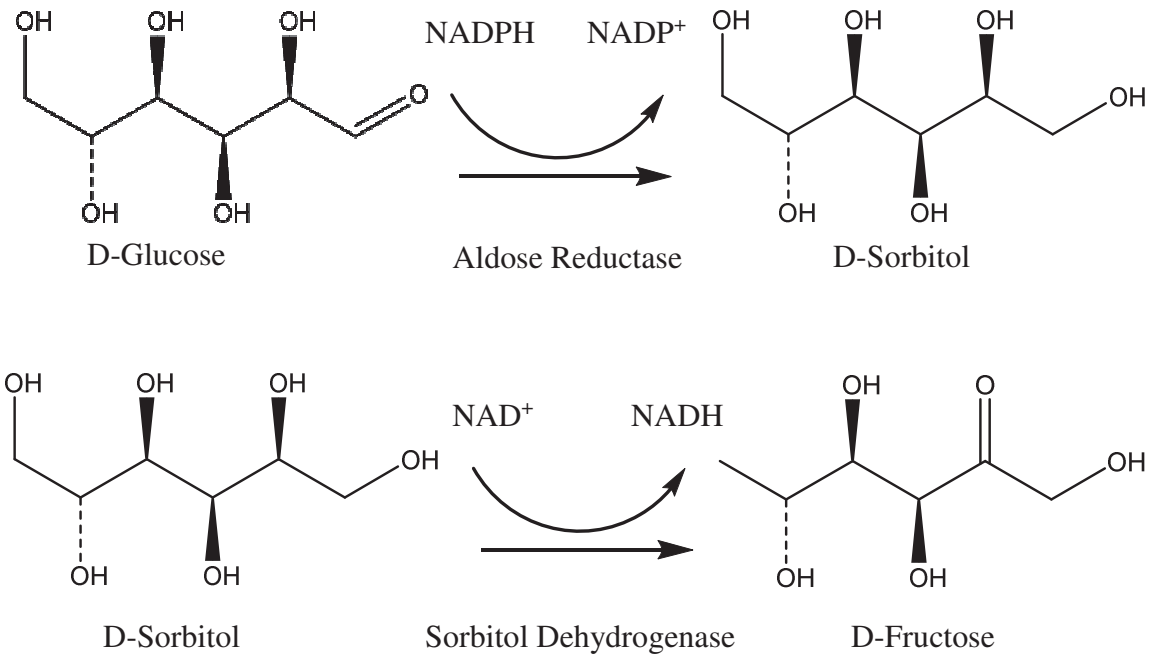

Aldose reductase is an important enzyme in the polyol pathway because it catalyzes the rate-determining step, which is the first step in this pathway. Aldose reductase uses the oxidation of NADPH to $NADP^+$ to catalyze the reduction of aldose aldehydes to their corresponding alcohols.[8]

IV. Human Aldose Reductase and Hyperglycemic Tissue Damage

Even with the assistance of the polyol pathway the body cannot keep pace with the excess glucose. When this situation occurs tissues are damaged and diabetic complications ensue.[5,6,7] The "role of [human] aldose reductase in mediating hyperglycemic injury remains obscure," but there are several hypotheses for how it is involved in tissue damage.[7] One idea is that tissue damage is caused by the buildup of sorbitol from increased hAR activity. Sorbitol is impermeable to the cell membrane and when it accumulates inside the cell it causes oxidative stress, protein insolubilization, glycation and diabetic complications.[7] Moreover, sorbitol buildup leads to increased osmotic pressure in the kidneys because of its role in balancing the osmotic pressure of extracellular NaCl during urine concentration.[6] Another theory is that tissue damage is caused by oxidative stress induced by the depletion of NADPH and NAD^+ from increased hAR and sorbitol dehydrogenase activity.[6] Utilization of the polyol pathway depletes NADPH and NAD^+, which results in "metabolic imbalances" in "tissues that undergo insulin-independent uptake of glucose." [6] Glucose transport proteins 1, 2, 3 and 5 (SLC2A1, SLC2A2, SLC2A3, SLC2A5) are insulin-independent and transport glucose across various tissues of the body such as the eyes, nerves and kidneys.[9] So with diminished quantities of these important cofactors (NADPH and NAD^+) less glucose is transported to various areas of the body. This is why diabetes is often associated with

damage in the ocular lens, retina, peripheral nervous system, and renal glomerulus.[6] Additionally, NADPH depletion "compromises antioxidative defenses." [7] Glutathione reductase uses NADPH to reduce glutathione disulfide to glutathione.[7,10] Glutathione is important for resisting oxidative stress, maintaining the reducing environment of the cell, and is a major reducing agent for disulfides and peroxides.[10] Clearly, hAR does have a role in causing hyperglycemic tissue damage and inhibitors of hAR have been proven to prevent, delay and reverse tissue damage due to diabetic complications.[7]

V. Kinetic Properties of Native and Activated hAR

At normal glucose levels, human aldose reductase (hAR) exists mainly in its native (unoxidized) form.[8] During hyperglycemia, native human aldose reductase is oxidized to its activated, inhibitor-resistant form.[8]

In a study done by Grimshaw et al. (1996), they examined the kinetic properties of naturally occurring activated and native human placental aldose reductase. They observed that with DL-glyceraldehyde as substrate the activated hAR had a significantly higher Michaelis constant (K_m), and higher maximum velocity (V_{max}) than that of the native hAR (Figure 1.8).[8] Also with sorbinil as the inhibitor the activated hAR had a higher inhibition constant (K_i) (Figure 1.8).[8]

Figure 1.8: Kinetic Properties of Native and Activated Human Aldose Reductase[8]

Comparison of Kinetic Parameters for Native and Oxidized Aldose Reductase

	Recombinant enzyme		Human placenta	
Parameter[a]	Native	Oxidized	Native[b]	Oxidized[c]
V (s^{-1})	0.45	0.50	0.62	1.5
K (mM)	0.047	2.4	0.024	6.8
V/K (mM^{-1} s^{-1})	9.6	0.21	26	0.22
K_i Sorbinil (μM)	0.5	380	0.5	400

The higher V_{max} of activated hAR indicates that it can catalyze the corresponding forward reduction reaction at a faster maximum rate than native hAR. The higher K_m of activated hAR indicates that it has a lower affinity for the substrate.[8] Sorbinil is a non-competitive inhibitor for the forward reduction reaction and it interacts with the enzyme regardless of whether substrate is bound to it. The higher K_i for the activated hAR shows that a higher concentration of sorbinil was required to decrease the V_{max} by one-half.[8] So clearly, activated hAR has a detrimental effect on inhibitor potency and enzyme-substrate interaction.

VI. A Specific Post-Translational Modification

The work done by Pretrash et al. (1992) located a specific residue that contributes to hAR activation *in vitro*. Petrash et al. (1992) carried out kinetic studies of recombinant C80S, C298S, and C303S mutants to determine which residue modifications likely contributes to the activation of hAR.[11] These three residues were selected as potential candidates because they are located in the vicinity of the active site and prone to oxidation.[11] Also, all of these residues were modified from a cysteine (thiol side chain) to a serine (hydroxyl side chain) (Figure 1.9).

Figure 1.9: Cysteine and Serine Amino Acids[13]

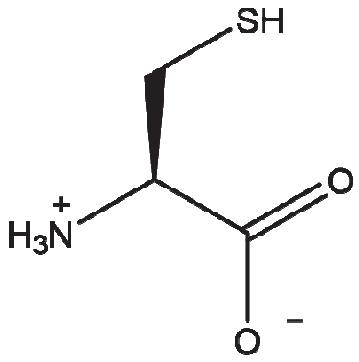

Cysteine

side chain pKa: 8

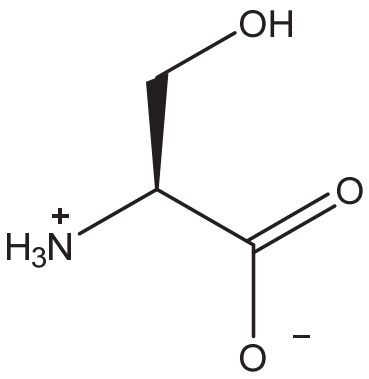

Serine

side chain pKa: 13

Figure 1.10: Kinetic Studies of Cysteine Mutants with Different Substrates[11]

Kinetic constants for wild type and mutant aldose reductases

Values of kinetic constants are mean ± S.E. (n = 15). The indicated substrates were varied over a concentration range of at least 0.1–2 times K'_m. K'_m values are apparent Michaelis constants for the indicated substrate.

	Wild type	C80S	C298S	C303S
D-Xylose				
K'_m (mM)	10.2 ± 1.49	15.6 ± 1.55	543 ± 102[a]	290 ± 36[a]
k_{cat} (s^{-1})	1.24 ± 0.06	1.52 ± 0.04	8.48 ± 0.85[a]	0.81 ± 0.4
k_{cat}/K'_m (s^{-1} M^{-1})	122 ± 13.5	97.6 ± 8.07	15.7 ± 1.52[a]	2.77 ± 0.23[a]
D-Glucose				
K'_m (mM)	212 ± 26.7	196 ± 24	>1000[a]	881 ± 277[a]
k_{cat} (s^{-1})	0.086 ± 0.004	0.359 ± 0.026[a]	>1.95[a]	0.037 ± 0.004[a]
k_{cat}/K'_m (s^{-1} M^{-1})	0.407 ± 0.033	1.87 ± 0.269[a]	ND[b]	0.085 ± 0.010[a]
p-Nitrobenzaldehyde				
K'_m (μM)	15.7 ± 1.70	34.6 ± 6.79[a]	202 ± 14.1[a]	254 ± 20.2[a]
k_{cat} (s^{-1})	0.469 ± 0.011	0.377 ± 0.014	3.33 ± 0.092[a]	0.486 ± 0.016
k_{cat}/K'_m (s^{-1} M^{-1})	29,738 ± 2,689	10,865 ± 1.881[a]	16,432 ± 741[a]	1,912 ± 94[a]
Benzaldehyde				
K'_m (μM)	72.8 ± 11.3	27.6 ± 3.49[a]	1,061 ± 208[a]	67.7 ± 9.39
k_{cat} (s^{-1})	0.443 ± 0.044	0.758 ± 0.018[a]	4.62 ± 0.121[a]	0.299 ± 0.011[a]
k_{cat}/K'_m (s^{-1} M^{-1})	6,093 ± 742	27,473 ± 3,033[a]	4,404 ± 377[a]	4,420 ± 501

[a] $p < 0.001$ compared to ALR2:wild type.
[b] ND, value could not be accurately computed due to uncertainty in K'_m and k_{cat} components.

From kinetic studies of these recombinant mutants of hAR with different substrates, the researchers noted that the greatest changes to K_m, turnover number (k_{cat}) and catalytic efficiency (k_{cat}/K_m) correspond with the C298S mutant (Figure 1.10).[11] This C298S mutant had a significantly higher K_m, higher k_{cat} and lower catalytic efficiency for all the substrates (Figure 1.10).[11] If you focus on the values for C298S with D-glucose as substrate you will notice that its K_m and k_{cat} are significantly larger and its catalytic efficiency is so small that it could not be accurately determined.[11] The researchers attributed these unsubtle changes to the altered interaction of residue 298 with the nicotinamide ring of NADPH and the changed characteristics of the active site.[11]

VII. Hypotheses on Cys298 Oxidation

Studies have shown that oxidation of Cys298 prevents the NADPH-binding loop from completely closing.[1,11] This modification allows $NADP^+$ to be released faster. Also, since $NADP^+$ release is the rate limiting step in hAR catalysis this alteration leads to increased turnover rate, increased catalysis, and increased inhibition constant.[1,11] Cys298 mutants like C298S model the oxidation of cysteine (S^{-2}) to its various oxidation states: sulfenic acid (S^0), sulfinic acid (S^{+2}) and sulfonic acid (S^{+4}).[1] Even so, no one is certain of how exactly Cys298 becomes oxidized, but oxidative post-translational modification of cysteine residues can occur via sulfur-nitrosylation, sulfhydration, sulfur-glutathionylation, disulfide bond formation, sulfenylation, and oxidation to sulfur acids.[1, 12] These oxidative post-translational modifications are often induced by reactive nitrogen and oxygen species and glutathiolated and sulfenic acid forms of hAR have been discovered *in vivo*.[1, 12] Figure 1.11 shows common oxidative post-translational modifications that occur to cysteine residues in other proteins.

Figure 1.11: Oxidative Post-Translational Modifications to Cysteine in Proteins[12]

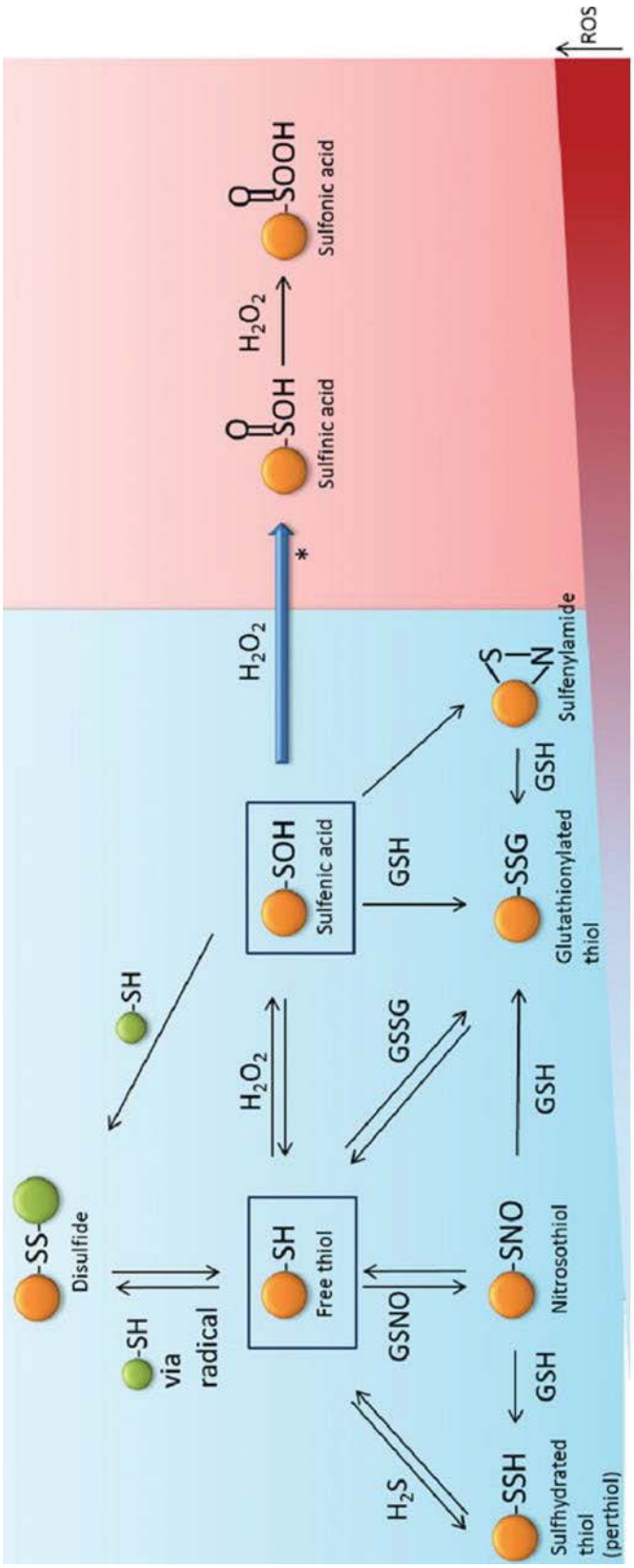

VIII. Previous Work: Kinetic Studies

The work done by Dr. Balendiran and Richard Cuckovich was published in 2011 and further confirmed that Cys298 plays a crucial role in the activation of hAR. They conducted kinetic studies on the hAR C298S mutant with four different substrates: DL-glyceraldehyde, HNE, D-glucose, and benzyl alcohol (Figure 1.12). For all the substrates the C298S mutant has a significantly larger K_m than that of the wild-type.[13] The k_{cat} of the C298S mutant was remarkably higher for only DL-glyceraldehyde and benzyl alcohol; so the mutant required more time to turnover one molecule of those substrates. k_{cat}/K_m is a measure of the catalytic efficiency of the enzyme and for the mutant this value was lower for all the substrates.[13] Also, benzyl alcohol was the only substrate studied for the reverse oxidation reaction and it is interesting that the C298S mutant had a lower affinity for it when compared to that of the wild-type.[13]

Figure 1.12: Kinetic Study of C298S Mutant with Different Substrates[13]

Comparison of catalytic activity of wild-type and C298S mutant hAR for carbonyl reduction and alcohol oxidation reactions at 25 °C

The uncertainties are S.D. of the average value.

hAR Protein	Substrate	K_m	k_{cat}	k_{cat}/K_m
			s^{-1}	
Wild-type	DL-Glyceraldehyde	0.1 ± 0.01 mM	1.55 ± 0.01	14.5 $mM^{-1}s^{-1}$
C298S		1.2 ± 0.05 mM	3.72 ± 0.3	3.10 $mM^{-1}s^{-1}$
Wild-type	D-Glucose	55.0 ± 6.0 mM	0.64 ± 0.05	0.011 $mM^{-1}s^{-1}$
C298S		800 ± 50.0 mM	0.42 ± 0.04	0.0005 $mM^{-1}s^{-1}$
Wild-type	HNE	48.0 ± 4.0 μM	0.90 ± 0.06	0.019 $\mu M^{-1}s^{-1}$
C298S		110.0 ± 8.0 μM	0.60 ± 0.02	0.006 $\mu M^{-1}s^{-1}$
Wild-type	Benzyl alcohol	1.62 ± 0.1 mM	0.35 ± .025	0.215 $mM^{-1}s^{-1}$
C298S		4.55 ± 0.3 mM	0.42 ± .02	0.092 $mM^{-1}s^{-1}$

From this table (Figure 1.12) Balendiran et al. (2011) concluded that the affinity of the substrate-enzyme complexes for both the forward and reverse reactions are weakened in the C298S mutant.[13] Furthermore, since the mutant had similar trends for K_m and catalytic efficiency that had been observed by other researchers for activated hAR, the authors concluded that Cys298 was oxidized during the activation of hAR.[7,8,11,13] Moreover, from crystal structures of wild-type and C298S mutant hAR Balendiran et al. (2011) observed that in the wild-type the Cys298 side chain is near the nicotinamide ring of NADPH and is surrounded by hydrophobic residues: Trp20, Trp209, and Trp219.[13] Meanwhile, in the C298S mutant the Ser298 side chain is further away from those hydrophobic residues and forms a hydrogen bond with the phenol side chain of Tyr209.[13] Figure 1.13 shows the interactions between Tyr209 and the wild-type and C298S mutant.

Figure 1.13: Omit Map of Tyr209 in wild-type and C298S hAR[13]

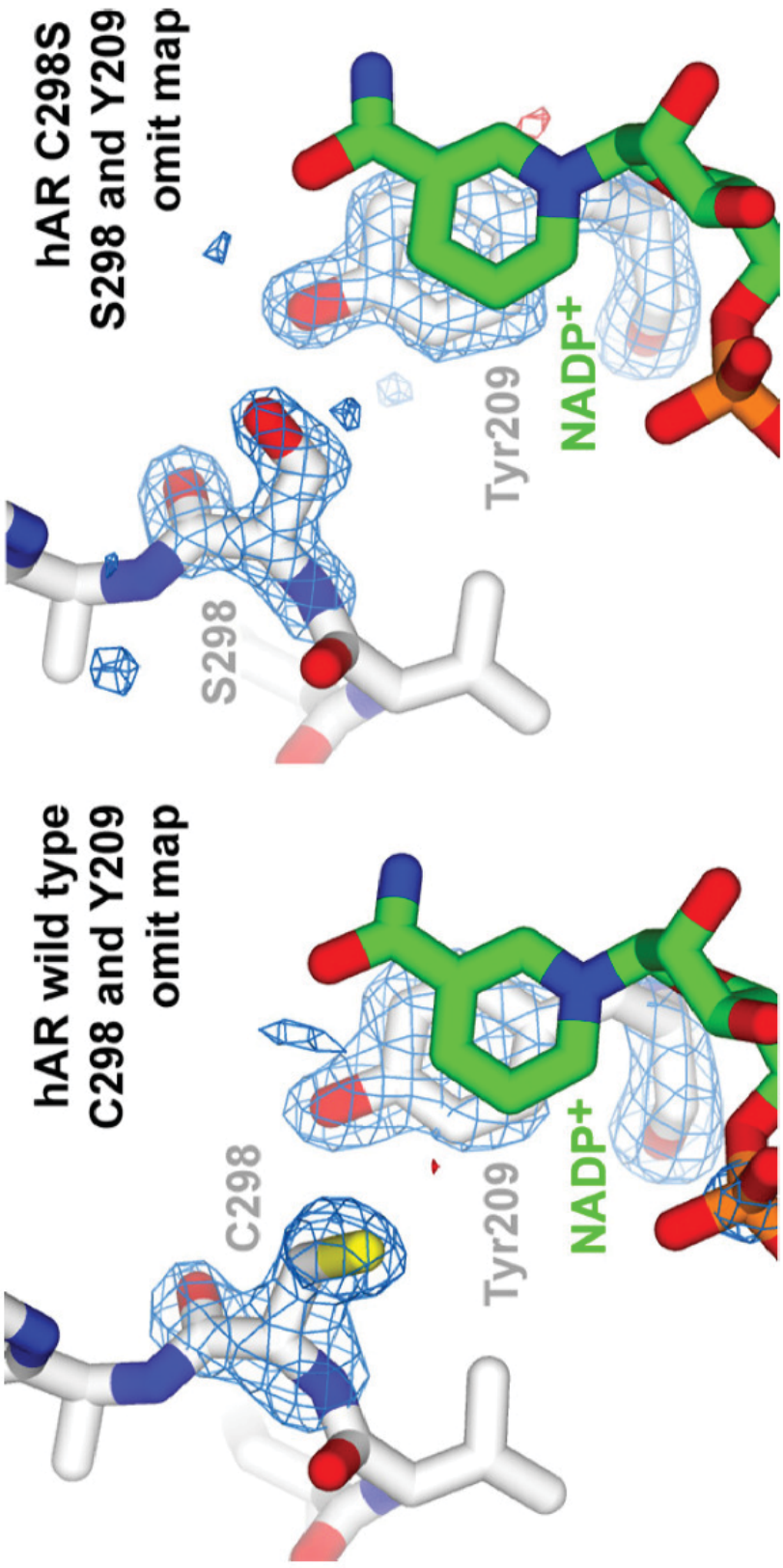

From this crystal structure map (Figure 1.13) Balendiran et al. (2011) concluded that formation of the hydrogen bond makes residue 298 more rigid and greatly increases the polarity of the NADPH binding pocket.[13] This increase in polarity is then likely responsible for decreasing the strength of the enzyme-NADPH and enzyme-substrate interactions due to the conflicting polarities of the hydrophilic serine side chain with the hydrophobic binding pockets.[13]

Chapter II: Materials and Methods

I. Materials

Difco Yeast Extract UF, Bacto Tryptone, Bacto Agar, and 10 mL BD slip-tip disposable syringes were purchased from BD Biosciences, San Jose, CA; ampicillin sodium salt, 4-morpholineethanesulfonic acid, Trizma base (Sigma 7-9), imidazole, and Luria Broth (Miller) were purchased from Sigma-Aldrich Corporation, St. Louis, MO; Fisherbrand 50 mL graduated polypropylene centrifuge tubes, Falcon 15 mL conical centrifuge tubes, PageRuler Plus Prestained Protein Ladder, sodium chloride, magnesium sulfate, potassium chloride, glucose, and glycerol were purchased from Thermo Fisher Scientific Inc., Waltham, MA; Novagen Thrombin Restriction Grade, Novagen 4x SDS sample buffer, Novagen pET-15b DNA, Millex-HV Syringe Filter Unit (0.45 µm), and Millex-GV Syringe Filter Unit (0.22 µm) were purchased from EMD Millipore, Darmstadt, Germany; Bio-Rad Protein Assay Dye Reagent Concentrate, Protein Standard I Globulin (bovine γ-globulin), Coomassie Brilliant Blue G-250, sodium dodecyl sulfate, TEMED, Resolving Gel Buffer (1.5 M Tris-HCl pH 8.8), Stacking Gel Buffer (0.5 M Tris-HCl pH 6.8), 10x Tris/Glycine/SDS Electrophoresis Buffer and bromophenol blue were purchased from Bio-Rad Laboratories Inc., Hercules, CA; isopropyl-1-thio-β-D-

galactopyranoside was purchased from BioPioneer Inc., San Diego, CA; ammonium persulfate, sodium hydrogen phosphate, potassium dihydrogen phosphate, magnesium chloride, and sodium hydroxide were purchased from Avantor Performance Materials Inc., Center Valley, PA; acrylamide/bisacrylamide liquid (37.5:1) was purchased from Roche Diagnostics Corporation, Indianapolis, IN; methanol (absolute), ethyl alcohol (190 proof), acetic acid, and hydrochloric acid were purchased from Pharmco-Aaper, Toronto, Canada; Spectra/Por 1 dialysis tubing (6-8 k MWCO, 23 mm flat width, 100 ft) was purchased from Spectrum Laboratories Inc., Rancho Dominguez, CA; Talon CellThru (IMAC) resin was purchased from Clontech Laboratories Inc., Mountain View, CA; β-mercaptoethanol was purchased from Amresco Inc., Solon, OH; BL21 (DE3) competent *E. coli* and the QuikChange II Site-Directed Mutagenesis Kit were purchased from Agilent Technologies, Santa Clara, CA; QIAprep Spin Miniprep Kit and TE buffer was purchased from Qiagen, Venlo, Netherlands.

II. Strains, Media and Buffers

The XL1-Blue supercompetent *E. coli* strain was included with the QuikChange II Site-Directed Mutagenesis Kit and it was used in all experiments involving the pWhitescript, pUC18 and pET-15b plasmids. The cells were cultured in Luria Broth (Miller) with ampicillin (1% w/v tryptone, 1% w/v NaCl, 0.5% w/v yeast extract, 100 µg/mL ampicillin) [LB-Amp]. Transformants were selected on Luria Broth Agar with ampicillin (Luria Broth (Miller), 0.9% w/v bacto agar, 100 µg/mL ampicillin) [LB-Amp plates]. Blue-white screening was done with 40 µL of 100 mM IPTG and 40 µL of 40 mg/mL X-Gal on LB-Amp plates. The BL21(DE3) competent *E. coli* cells were cultured in 2X YT Media with ampicillin (1.6% w/v bacto tryptone, 1% w/v yeast extract, 0.5%

w/v NaCl, pH 7.0, 100 µg/mL ampicillin) and transformants were selected on LB-Amp plates. For protein overexpression, BL21(DE3) transformants were grown in 2X YT media with ampicillin (100 µg/mL) [YT-Amp]. Protein expression was induced in YT-Amp culture with IPTG (1 mM). These following buffers were used for protein purification: extraction buffer (50 mM Tris, 300 mM NaCl, 2 mM BME, pH 7), wash 1 buffer (50 mM Tris, 300 mM NaCl, 2 mM BME, pH 7), wash 2 buffer (10 mM imidazole, 50 mM Tris, 300 mM NaCl, 2 mM BME, pH 7), elution buffer (300 mM imidazole, 50 mM Tris, 300 mM NaCl, 2 mM BME, pH 7), dialysis buffer (50 mM Tris, 300 mM NaCl, 2 mM BME, pH 7).

III. pET-15b Vector

This 5,708 base pair cloning vector (Figure 2.1) contains the ampicillin resistance gene, His-Tag coding sequence, multiple cloning sites and a thrombin cleavage site.

Figure 2.1: Map of pET-15b Vector

Figure adapted from www.chem.agilent.com

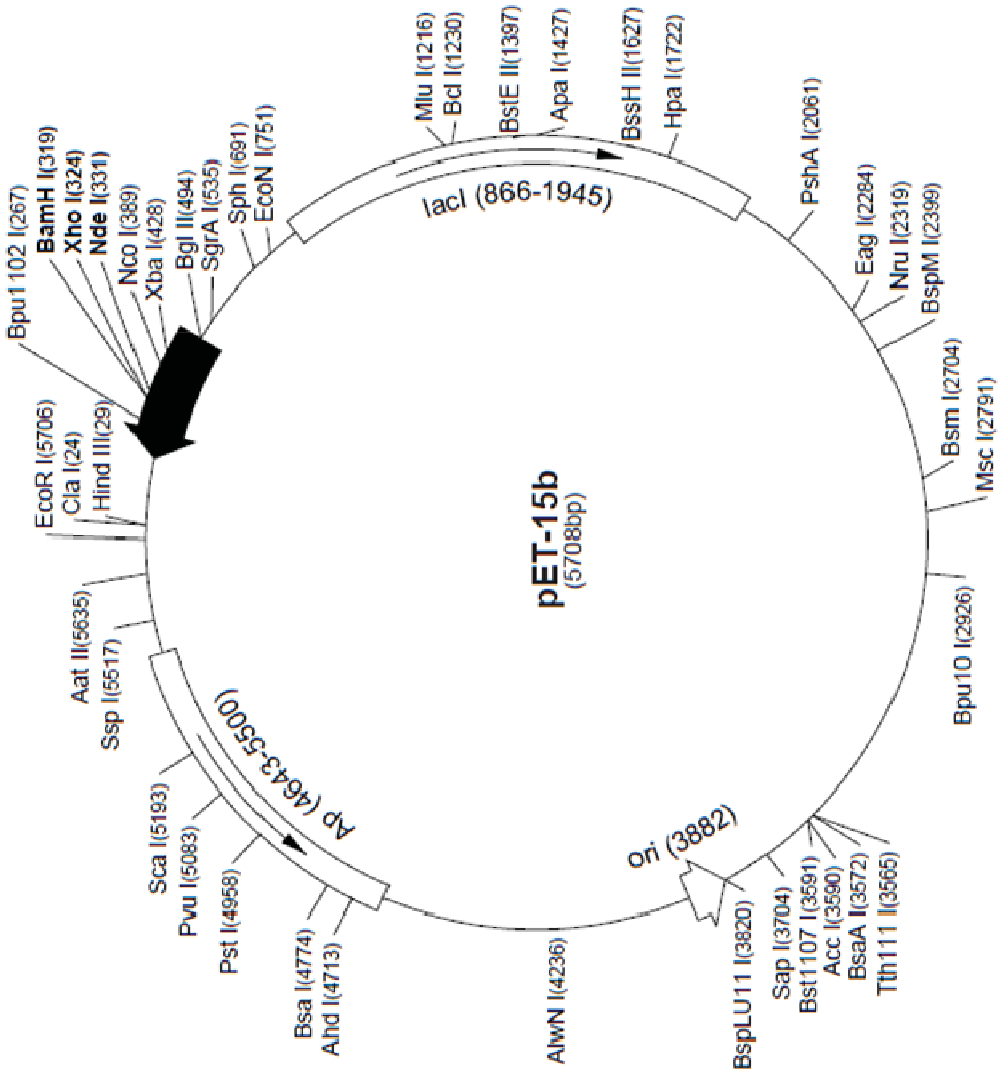

pET-15b sequence landmarks	
T7 promoter	453-469
T7 transcription start	452
His•Tag coding sequence	362-380
Multiple cloning sites (*Nde* I - *BamH* I)	319-335
T7 terminator	213-259
lacI coding sequence	(866-1945)
pBR322 origin	3882
bla coding sequence	4643-5500

IV. pWhitescript

This 4.5 kbp mutagenesis control plasmid contains the ampicillin resistance gene for antibiotic selection and the *lac*Z gene for blue-white screening. XL1-Blue cells transformed with this plasmid and the oligonucleotide control primers appear blue on LB-Amp plates containing IPTG and X-Gal.

V. pUC18

This 2,686 bp transformation control plasmid (Figure 2.2) contains the ampicillin resistance gene, *lac*Z gene, and multiple cloning sites. Insertion of the bacterial host's DNA into the multiple cloning site disrupts the *lac*Z gene, resulting in white XL1-Blue cells.

Figure 2.2: Map of pUC18

Figure adapted from www.snapgene.com

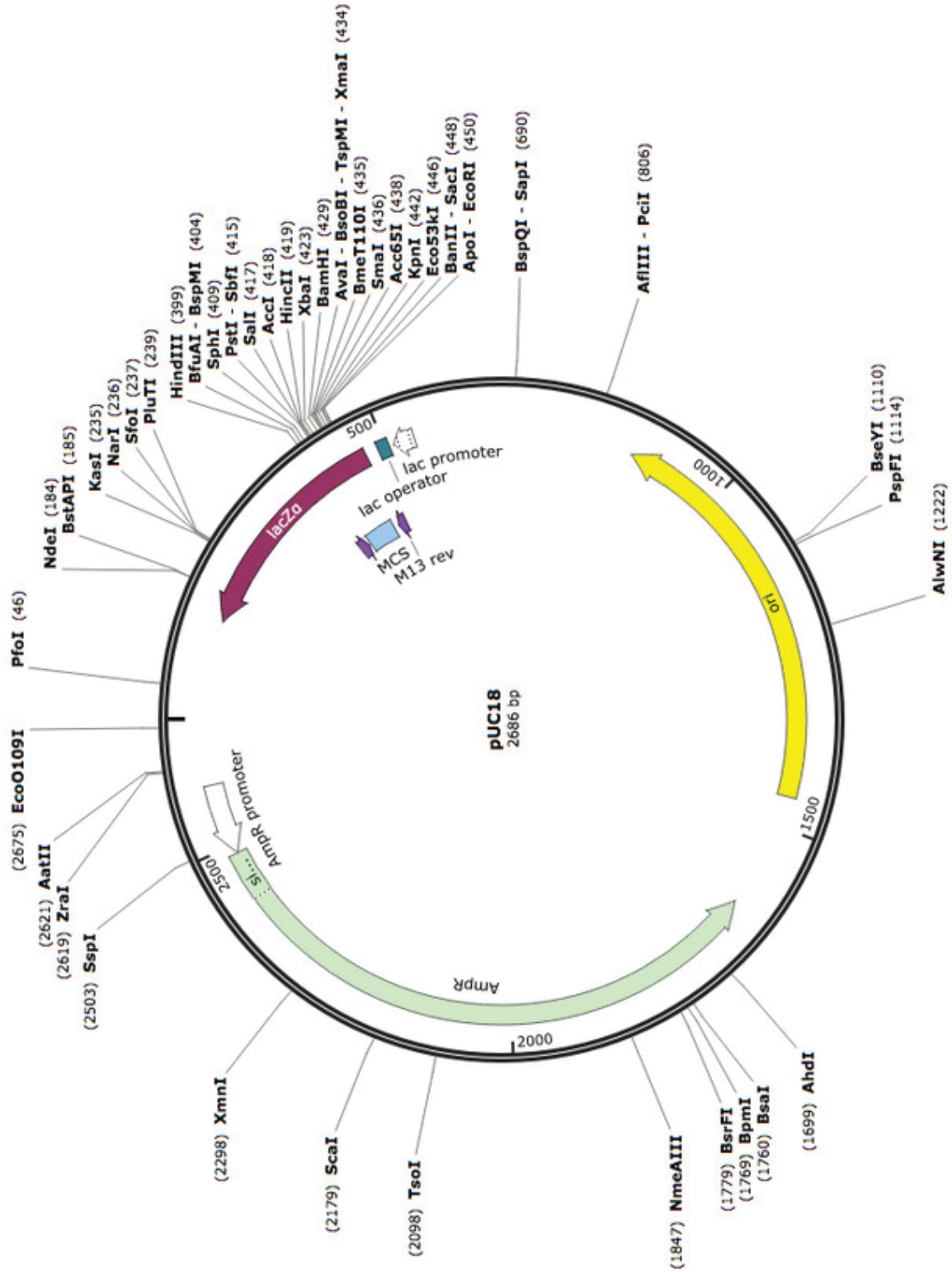

VI. Polymerase Chain Reaction

A QuikChange II Site-Directed Mutagenesis Kit was used to prepare the mutant and control reactions. Polymerase chain reaction (PCR) was performed in a programmable thermal cycler with the following primers that were synthesized by Eurofins Genomics. Shown below are the primers and underlined are the mutation sites:

C298A Forward: 5'AACAGGAACTGGAGGGTC**GCC**GCCTTGTTGAGCTGTACC 3'

C298A Reverse: 5'GGTACAGCTCAACAAGGC**GGC**GACCCTCCAGTTCCTGTT 3'

Tm: 88.4°C

C298D Forward:

5'CAACAGGAACTGGAGGGTC**GAC**GCCTTGTTGAGCTGTACCT 3'

C298D Reverse:

5'AGGTACAGCTCAACAAGGC**GTC**GACCCTCCAGTTCCTGTTG 3'

Tm: 88.0°C

C298G Forward: 5'CAGGAACTGGAGGGTC**GGA**GCCTTGTTGAGCTGTA 3'

C298G Reverse: 5'TACAGCTCAACAAGGC**TCC**GACCCTCCAGTTCCTG 3'

Tm: 85.6°C

The mutagenesis control reaction and the mutant reaction was prepared as indicated below in Table 2.1 and Table 2.2:

Table 2.1: Mutagenesis Control Reaction

Volume (µL)	Reagents
5	10x reaction buffer
2	(5 ng/µL) pWhitescript 4.5-kb control plasmid
1.25	(100 ng/µL) oligonucleotide control primer #1
1.25	(100 ng/µL) oligonucleotide control primer #2
1	dNTP mix
38.5	ddH_2O

Table 2.2: Mutant Reaction

Volume (µL)	Reagents
5	10x reaction buffer
3	(5 ng/µL) hAR dsDNA template
1.25	(10 µM) mutant forward primer
1.25	(10 µM) mutant reverse primer
1	dNTP mix
37.5	ddH_2O

Afterwards, 1 µL of 2.5U/µL *PfuUltra* High-Fidelity DNA polymerase was added to each reaction and PCR was initiated with the following thermal cycling parameters (Table 2.3):

Table 2.3: Thermal Cycling Parameters

Cycles	Temperature (°C)	Time
1	95	30 s
25	95	30 s
	55	1 min
	68	7 min
1	4	30 min

After thermal cycling, the mutant and control reactions were treated with 1 µL of 10 U/µL of *Dpn* I restriction enzyme to digest the unmutated, methylated DNA. Next, the reactions were gently mixed by pipetting up and down and incubated in the thermal cycler at 37°C for 1 hour. All *Dpn* I-treated DNA was stored at -20°C.

VII. Preparation of -80°C Bacterial Glycerol Stock

With a sterile wire loop, splinters of ice containing the cells were streaked onto a LB-Amp plate. The plate was incubated overnight at 37°C. A colony was selected from the plate and it was inoculated in 5 mL of LB-Amp. The cells were incubated at 37°C and 200 rpm until the Abs_{600} reached 0.4-0.6. 4 mL of cell culture was added to 4 mL of 40% v/v glycerol and 800 µL of the bacterial glycerol stocks were dispensed into 10 microcentrifuge tubes. These tubes of bacterial glycerol stocks were stored at -80°C.

VIII. Preparation of Competent Cells with Calcium Chloride Treatment

This following protocol was used to make the XL1-Blue and BL21(DE3) cells transiently permeable to DNA. With a sterile wire loop, splinters of ice from the bacterial glycerol stock were inoculated in 100 mL LB-Amp (in 500 mL Erlenmeyer flask). The cells were incubated at 37°C and 200 rpm until the Abs_{600} was 0.4-0.6. The cell culture was chilled on ice for 30 minutes and then transferred into two 50 mL graduated centrifuge tubes. The cell culture was centrifuged at 4°C and 5,000 rpm for 10 minutes and the supernatant was discarded. The cell pellet was resuspended in 35 mL of 0°C 100 mM calcium chloride solution, gently tapped and incubated on ice for 20 minutes. This mixture was centrifuged at 4°C and 5,000 rpm for 10 minutes and the pellet was resuspended in 1.5 mL of cold (0°C) 100 mM calcium chloride solution. For long-term storage, this cell culture mixture was kept at -80°C in 40% v/v glycerol that was 1:1 with the cell culture.

IX. XL1-Blue *E. coli* Transformation

The XL1-Blue glycerol stock was gently thawed on ice and 100 µL was aliquoted into two prechilled microcentrifuge tubes: one for the mutagenesis control reaction and one for the mutant reaction. Also, 50 µL of XL1-Blue supercompetent cells was aliquoted into one prechilled microcentrifuge tube for the transformation control reaction. The 5-10 µL of *Dpn* I-treated mutant DNA was added to the mutant reaction tube and 5 µL of *Dpn* I-treated control DNA was added to the mutagenesis control tube. For successful transformations, the C298A and C298G mutant reactions required 5 µL of Dpn I-treated DNA, while the C298D mutant reaction needed 10 µL of Dpn I-treated DNA. No DNA was added to the transformation control tube, but 1 µL of pUC18 control plasmid was

added to it. All three tubes were swirled gently and incubated on ice for 30 minutes. The tubes were heat pulsed for 90 seconds in a 42°C water bath and then placed on ice for 2 minutes. The 450 µL of 42°C preheated SOC media (2% w/v bacto tryptone, 0.5% w/v yeast extract, 0.01 M NaCl, 0.004 mM KCl, 0.01 M $MgCl_2$, 0.01 M $MgSO_4$, 0.02 M glucose) was added to each tube and they were incubated at 37°C for 1 hour with shaking at 200 rpm. About 250-400 µL of the mutant reaction, 200 µL of the mutagenesis control reaction, and 50 µL of the transformation control reaction were spread onto LB-Amp plates containing X-Gal and IPTG. The plates were incubated overnight at 37°C and successful XL1-Blue transformants appeared white since their *lac*Z gene was disrupted by the insertion of mutant DNA.

X. Isolation of Plasmid DNA (QIAprep ® Spin Miniprep Kit)[14]

Six white colonies from the XL1-Blue LB-Amp plate were streaked onto one LB-Amp plate (subdivided into 6 sections). Three colonies (one from 3 separate sections) were selected and inoculated in 5 mL of LB-Amp. The cell cultures were incubated at 37°C with 200 rpm shaking overnight. The 4 mL of cell culture from each section was equally dispensed into 3 microcentrifuge tubes. There are now 3 microcentrifuge tubes from each section (9 tubes total) and each tube contains 1.333 mL of cell culture. The tubes were centrifuged at 8,000 rpm and 25°C for 3 minutes. The pellets from each section were combined, resuspended in 250 µL of Buffer P1 (resuspension buffer) and transferred to a microcentrifuge tube. The following procedures refer to what was performed to each of the 3 microcentrifuge tubes. For the lysis reaction, 250 µL of Buffer P2 (lysis buffer) was added and the mixture was gently mixed until it turned clear. For the neutralization reaction, 350 µL of Buffer N3 (neutralization buffer) was added and

the tube was gently inverted 5 times. Later, the solution was centrifuged at 13,000 rpm and 25°C for 10 minutes. All subsequent centrifugations were done at 13,000 rpm and 25°C. The supernatant was pipetted into a QIAprep spin column, centrifuged for 1 minute and the flow-through was discarded. The 500 µL of Buffer PB (binding buffer) was added to the spin column, it was centrifuged for 1 minute and the flow-through was discarded. The 750 µL of Buffer PE (wash buffer) was added to the spin column, it was centrifuged for 1 minute and the flow-through was discarded. To remove residual buffer, the spin column was centrifuged for 1 minute and the flow-through was discarded. The spin column was placed in an empty microcentrifuge tube and 50 µL of Buffer EB (10 mM Tris-Cl, pH 8.5) was added to elute the DNA. The tube was left undisturbed for 1 min and centrifuged for 1 min. The isolated DNA was stored at -20°C.

XI. DNA Sequencing

Nine tubes of isolated DNA (3 from each Cys298 mutant) were sent to Eurofins Genomics for DNA sequencing. After DNA sequencing, the sequences of mutants were analyzed by BioEdit Sequence Alignment Editor Version 7.2.5 to check for the correct mutation and quality of the sequences. With this software, a ClustalW multiple sequence alignment was performed to compare each mutation sequence with the hAR wild-type sequence. The sequences that matched more closely with the wild-type were chosen and used to select the *Dpn* I-treated DNA samples for the transformation of BL21(DE3) competent cells.

XII. BL21(DE3) *E. coli* Transformation

The 2 µL of Dpn I-treated DNA was added to 50-200 µL of BL21(DE3) glycerol stock (in microcentrifuge tube) and incubated on ice for 30 minutes. The C298A and C298D mutant reactions required 50 µL of bacterial glycerol stock, while the C298G mutant reaction required 200 µL of bacterial glycerol stock. Next, the mutant reaction was heat pulsed for 90 seconds at 42°C and then placed on ice for 2 minutes. The 450 µL of preheated 42°C SOC media was added to the mutant reaction and it was incubated at 37°C for one hour. 50-75 µL of the reaction was spread onto a LB-Amp plate. The plates were incubated overnight at 37°C.

XIII. SDS-PAGE

Protein samples were resolved on a 10% w/v sodium dodecyl sulfate (SDS) polyacrylamide gel. Below are the protocols for preparing the separating and stacking gel (Table 2.4 and Table 2.5).

Table 2.4: Separating Gel (10 mL)

Reagents	Volume (mL)
ddH_2O	3.8
acrylamide/bisacrylamide liquid (37.5:1)	3.4
Resolving Gel Buffer (1.5 M Tris-HCl, pH 8.8)	2.6
10% w/v SDS	0.1
10% w/v ammonium persulfate	0.1
TEMED	0.01

Table 2.5: Stacking Gel (5 mL)

Reagents	Volume (mL)
ddH_2O	2.975
acrylamide/bisacrylamide liquid (37.5:1)	0.67
Stacking Gel Buffer (0.5 M Tris-HCl pH 6.8)	1.25
10% w/v SDS	0.05
10% w/v ammonium persulfate	0.05
TEMED	0.005

The running buffer was prepared by diluting the 10x Tris/Glycine/SDS Electrophoresis Buffer (25 mM Tris, 192 mM glycine, 0.1% w/v SDS, pH 8.3) to 1x with ddH_20. The staining solution was prepared with 0.3% w/v Coomassie Brilliant Blue G-250, 50% v/v

methanol, 40% v/v H_2O, and 10% v/v acetic acid. The de-staining solution was prepared with 30% v/v methanol, 60% v/v H_2O, and 10% v/v acetic acid. The 4x SDS protein sample buffer was prepared with 40% v/v glycerol, 240 mM Tris (pH 6.8), 8% w/v SDS, 0.04% w/v bromophenol blue, and 5% v/v BME. The 2x SDS protein sample buffer was prepared by diluting the 4x SDS protein sample buffer with 1x PBS buffer. The 1x phosphate buffered saline (PBS) buffer was prepared with 0.8% w/v sodium chloride, 0.02% w/v potassium chloride, sodium phosphate 0.144% w/v, and 0.024% w/v potassium diphosphate with the pH adjusted to 7.4. Protein gel samples from protein purification were prepared by mixing 75 µL of the sample with 25 µL of the 4x SDS protein sample buffer. Protein gel samples from protein expression were prepared by adding 60 µL of the 2x SDS protein sample buffer to the cell pellets (1 mL of cell culture that had been centrifuged for 2 minutes). PageRuler Plus Prestained Protein Ladder was used as the molecular weight marker and all gel samples were boiled for 3 min before being loaded into the wells. Initially, the electrical voltage was set to 70 V, but once the separating gel had been crossed it was increased to 100 V. Once the protein samples had run the entire length of the gel, the gel was removed and rinsed with water. The gel was placed in the staining solution and microwaved for 45 seconds on high power. It was placed on a low speed laboratory shaker to shake for 5 minutes. Next, the gel was placed in the de-staining solution, microwaved for 45 seconds on high power and gently shaken for 5 minutes. This cycle was repeated 3-4 times with fresh de-staining solution and then left to gently shake overnight. The following day the bands on the gel were visualized with an ultraviolet illuminator. For long-term storage, SDS gels were kept submerged in water.

Chapter III: Protein Expression

I. Protein Expression

A single colony of BL21(DE3) was picked from a LB-Amp plate and inoculated in 50 mL of 2YT media (in 125 mL Erlenmeyer flask). It was incubated overnight at 37°C and 200 rpm. The 10 mL of the cell culture was inoculated in 1 L of 2YT media (in 2,800 mL Erlenmeyer flask) and incubated for 2.5-3 hours at 37°C and 200 rpm. Once the Abs_{600} reached 0.6-0.8, protein expression was induced with 10 mL of 100 mM IPTG and the cell culture was incubated for 4 hours at 37°C and 200 rpm. Gradually, the cell culture was added to two 250 mL centrifuge bottles and centrifuged at 4°C and 6000 rpm in 5 minute cycles. The collected cell pellets were stored at -80°C.

Chapter IV: Protein Purification

I. Sonication

The cell pellets were thawed on ice and resuspended with the extraction buffer to yield a total volume of 60-80 mL. This suspension was mixed with a vortex mixer and pipetted until the solution had no clumps. The suspension was poured into a 100 mL beaker and this beaker was then placed inside a 1 L beaker that was filled with ice. The 1 L beaker was placed inside the sonicator and the probe was lowered into the smaller beaker until it was within a ½ inch from the bottom of the beaker. The suspension was sonicated in a 30 second burst and allowed to cool for 30 seconds. This first cycle was repeated 15 times. Next, the suspension was sonicated in a 1 minute burst and allowed to cool for 1 minute. This second cycle was repeated 10 times. The sonicated suspension was centrifuged at 12,000 rpm and 4°C for 30 minutes. The supernatant was collected in a plastic bottle and the pellets were combined and resuspended with extraction buffer. For

the resuspended pellets, the entire sonication and centrifugation process was repeated as before and the all the supernatant was collected in one plastic bottle.

II. Immobilized Metal Affinity Chromatography

The 5 mL of Talon CellThru Immobilized Metal Affinity Chromatography (IMAC) resin was washed with 15 mL of extraction buffer. This process was repeated 3 times and each time the liquid was discarded with a syringe. This resin was added to the supernatant and it was gently shaken with a small laboratory rocker for 12-16 hours at 4°C. This procedure was done to bind the affinity resin with the histidine tag of the protein. A 30 mL gravity-flow column was washed with these solutions in the following order: 50 mL of 2 M NaOH, 50 mL of ddH_2O, and 25 mL of extraction buffer. In a 4°C cold room, the supernatant/resin mixture was added to the column and the flow-through was collected at a slow, steady rate. The 50 mL wash 1 buffer was added to the column and wash 1 was collected in one fraction. The 50 mL of wash 2 buffer was added to the column and wash 2 was collected in one fraction. The 50 mL of elution buffer was added to the column and 5 eluates were collected in 10 mL fractions. All of the fractions were stored at 4°C.

III. Dialysis

SDS-PAGE was used to confirm which of the elution fractions had the most protein and these fractions were loaded into Spectra/Por 1 dialysis tubing. The protein was dialyzed for 8-12 hours in 2 L of dialysis buffer that was slowly stirred at 4°C. The dialysis buffer was changed for a total of 3 times and the protein was transferred to 50 mL graduated centrifuge tubes.

IV. Protein Quantification: Bradford Reagent Assay

The 20% v/v dye reagent was prepared by diluting the Dye Reagent Concentrate with ddH_2O and filtering it with filter paper. Six dilutions of IgG protein standard were prepared that ranged from 0.2 mg/mL to 1.2 mg/mL. The 100 µL of protein sample and 100 µL of IgG protein standard were pipetted into glass tubes. The 5 mL of 20% v/v dye reagent was added to each tube and they were vortexed and incubated at 37°C for 5 minutes. The absorbance at 595 nm was recorded and the protein concentration of the protein sample was calculated from an IgG standard graph of Abs_{595} versus concentration.

V. Thrombin Cleavage of Histidine Tag

After the protein concentration of the dialysis protein sample was determined, 1 µL of thrombin for every 4 mg of protein was added to the dialysis protein sample. The pre-digested protein was kept overnight at room temperature. Next, the IMAC resin was added to the digested protein and it was gently shaken with a small laboratory rocker for 12-16 hours at 4°C. This procedure was done to bind the affinity resin with the cleaved histidine tag of the protein. At room temperature the protein/resin mixture was added to the column and the flow-through was collected at a slow, steady rate.

Chapter V: Results

I. DNA Sequencing

Below, are the DNA sequences (Figures 5.1, 5.3, 5.5, 5.7, 5.9, 5.11) of the isolated DNA that was used for the protein expression of each Cys298 mutant. Underlined in these sequences are the mutation sites. Also, the DNA chromatograms (Figures 5.2, 5.4, 5.6, 5.8, 5.10, 5.12) of each Cys298 mutant have well-resolved peaks and no ambiguities within the protein coding sequences. In the following DNA chromatograms T represents thymidine, A represents adenosine, G represents guanine, C represents cytosine and N represents an undetermined nucleotide.

Figure 5.1: C298A Tube 1 Forward Sequence

NNNNNNNNNNNNNNNNNNNNNNNNNCNNNNNNATTTTGTTTAACTTTAA
GAAGGAGATATACCATGGGCAGCAGCCATCATCATCATCATCACAGCAGCGG
CCTGGTGCCGCGCGGCAGCCATATGGCTAGCCGTATCCTGCTCAACAACGGC
GCCAAGATGCCCATCCTGGGGTTGGGTACCTGGAAGTCCCCTCCAGGGCAGG
TGACTGAGGCCGTGAAGGTGGCCATTGACGTCGGGTACCGCCACATCGACTG
TGCCCATGTGTACCAGAATGAGAATGAGGTGGGGGTGGCCATTCAGGAGAAG
CTCAGGGAGCAGGTGGTGAAGCGTGAGGAGCTCTTCATCGTCAGCAAGCTGT
GGTGCACGTACCATGAGAAGGGCCTGGTGAAAGGAGCCTGCCAGAAGACAC
TCAGCGACCTGAAGCTGGACTACCTGGACCTCTACCTTATTCACTGGCCGACT
GGCTTTAAGCCTGGGAAGGAATTTTTCCCATTGGATGAGTCGGGCAATGTGG
TTCCCAGTGACACCAACATTCTGGACACGTGGGCGGCCATGGAAGAGCTGGT
GGATGAAGGGCTGGTGAAAGCTATTGGCATCTCCAACTTCAACCATCTCCAG
GTGGAGATGATCTTAAACAAACCTGGCTTGAAGTATAAGCCTGCAGTTAACC
AGATTGAGTGCCACCCATATCTCACTCAGGAGAAGTTAATCCAGTACTGCCA
GTCCAAAGGCATCGTGGTGACCGCCTACAGCCCCCTCGGCTCTCCTGACAGG
CCCTGGGCCAAGCCCGAGGACCCTTCTCTCCTGGAGGATCCCAGGATCAAGG
CGATCGCAGCCAAGCACAATAAAACTACAGCCCAGNTCCTGATCCGGTTCCC
CATGCAGAGGAACTTGGTGGTGATCCCCAAGTCTGTGACACCAGAACGCATT
GCTGANAACTTTAAGGTCTTTGACTTTGAACTGAGCAGCCAGGATATGACCA
CCTTACTCAGCTACANNAGGAACTGGAGGGTC**GCC**GCCNNTTGAGCTGTACC
TCCCACAAGGATTACCCCTTCCATGANANTTTNAGCTGTGGNNCCTGNTCNTC
CCNNNNACNNTACNGNNNTTCNTGCCNNATTTTNNNNNNNNTANNNNNNNN
NNTCNNNCANCNNNGGNNNNCNANCNNNNNNANNNGGCNNNNNNNNGGGN
CNTNNNNNTNNCNTTGNNNNNNNNN

Figure 5.2 C298A Forward DNA Chromatogram

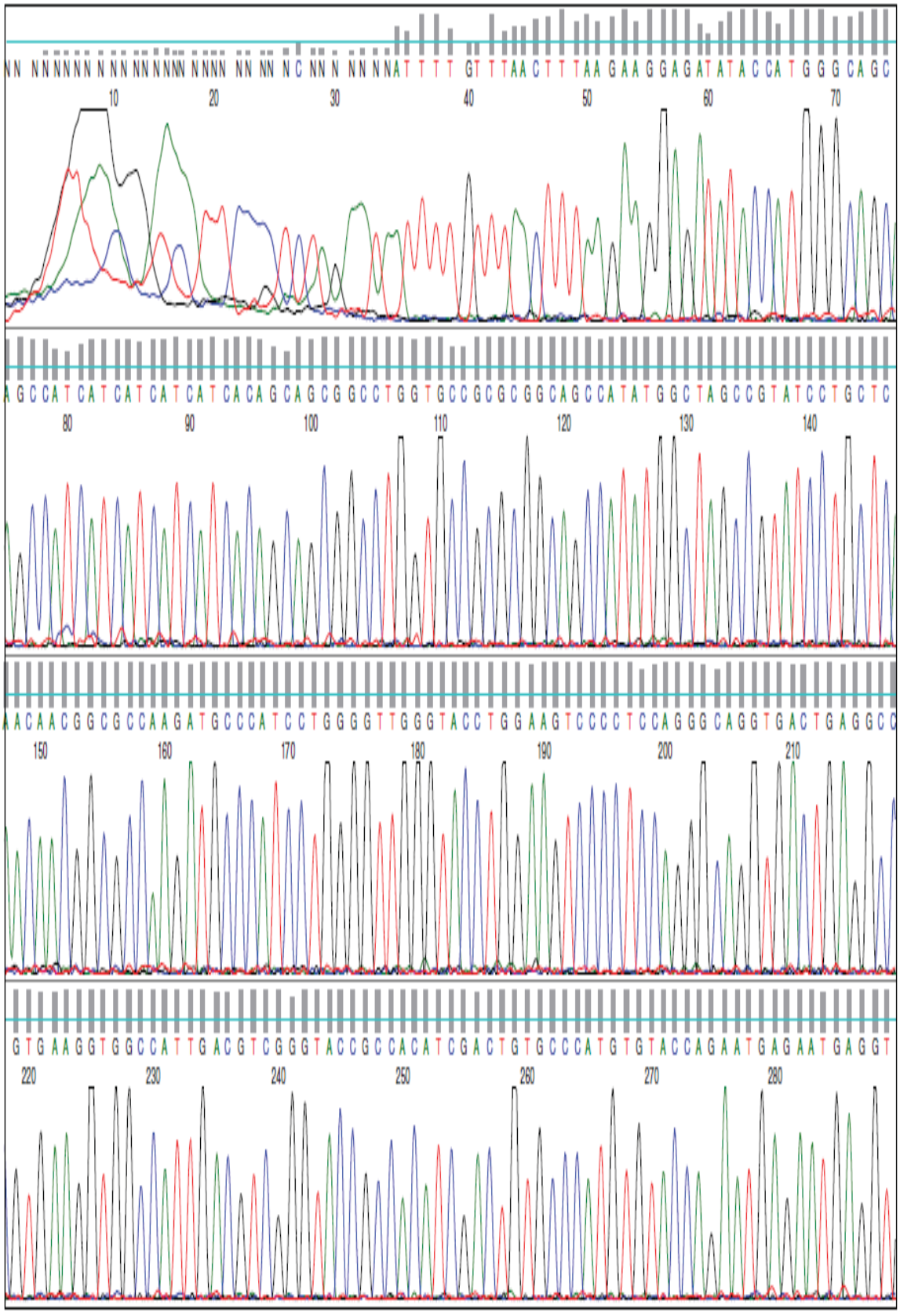

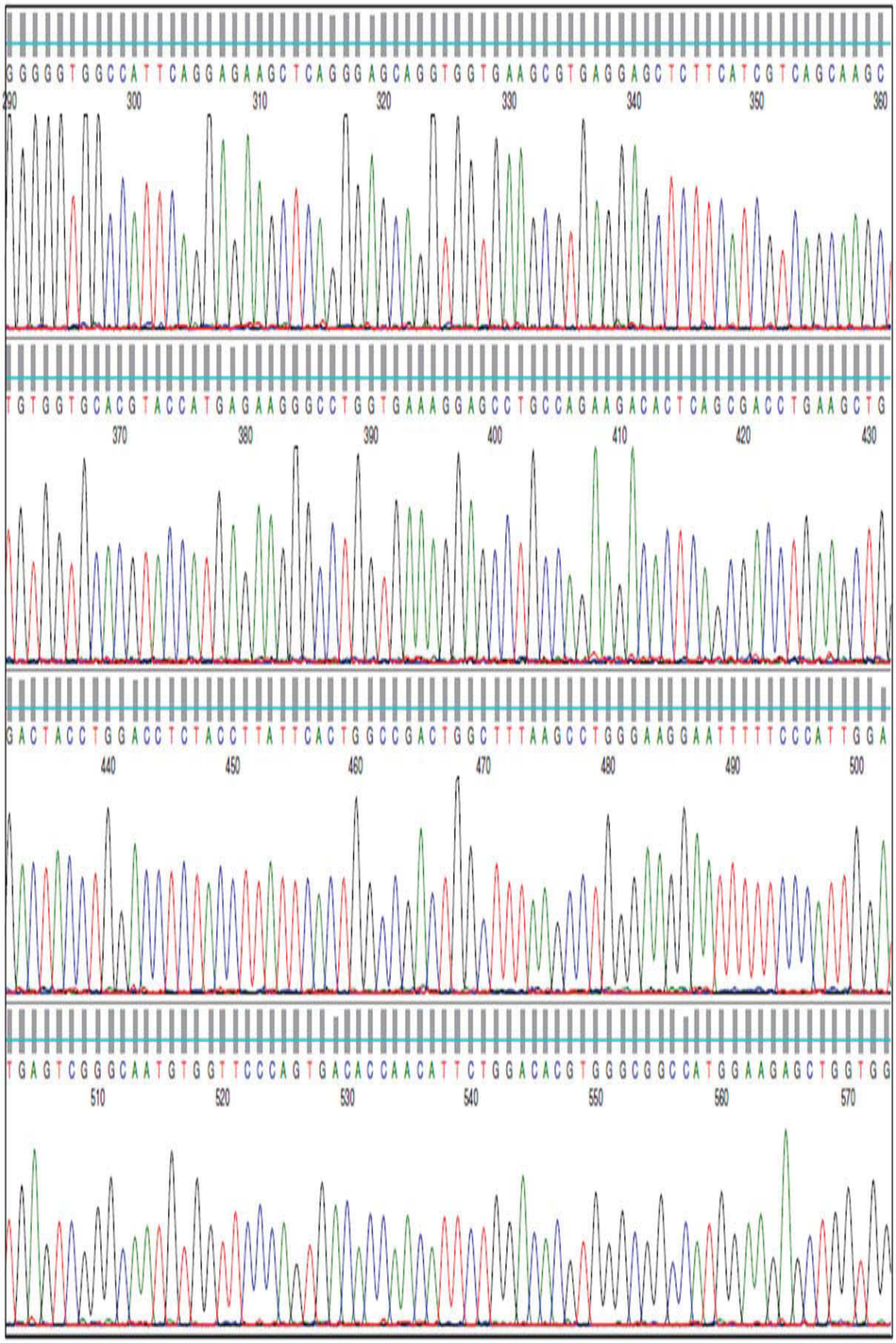
GGGGGTGGCCATTCAGGAGAAGCTCAGGGAGCAGGTGGTGAAGCGTGAGGAGCTCTTCATCGTCAGCAAGC
290
300
310
320
330
340
350
360
TGTGGTGCACGTACCATGAGAAGGGCCTGGTGAAAGGAGCCTGCCAGAAGACACTCAGCGACCTGAAGCTG
370
380
390
400
410
420
430
GACTACCTGGACCTCTACCTTATTCACTGGCCGACTGGCTTTAAGCCTGGGAAGGAATTTTTCCCATTGGA
440
450
460
470
480
490
500
TGAGTCGGGCAATGTGGTTCCCAGTGACACCAACATTCTGGACACGTGGGCGGCCATGGAAGAGCTGGTGG
510
520
530
540
550
560
570

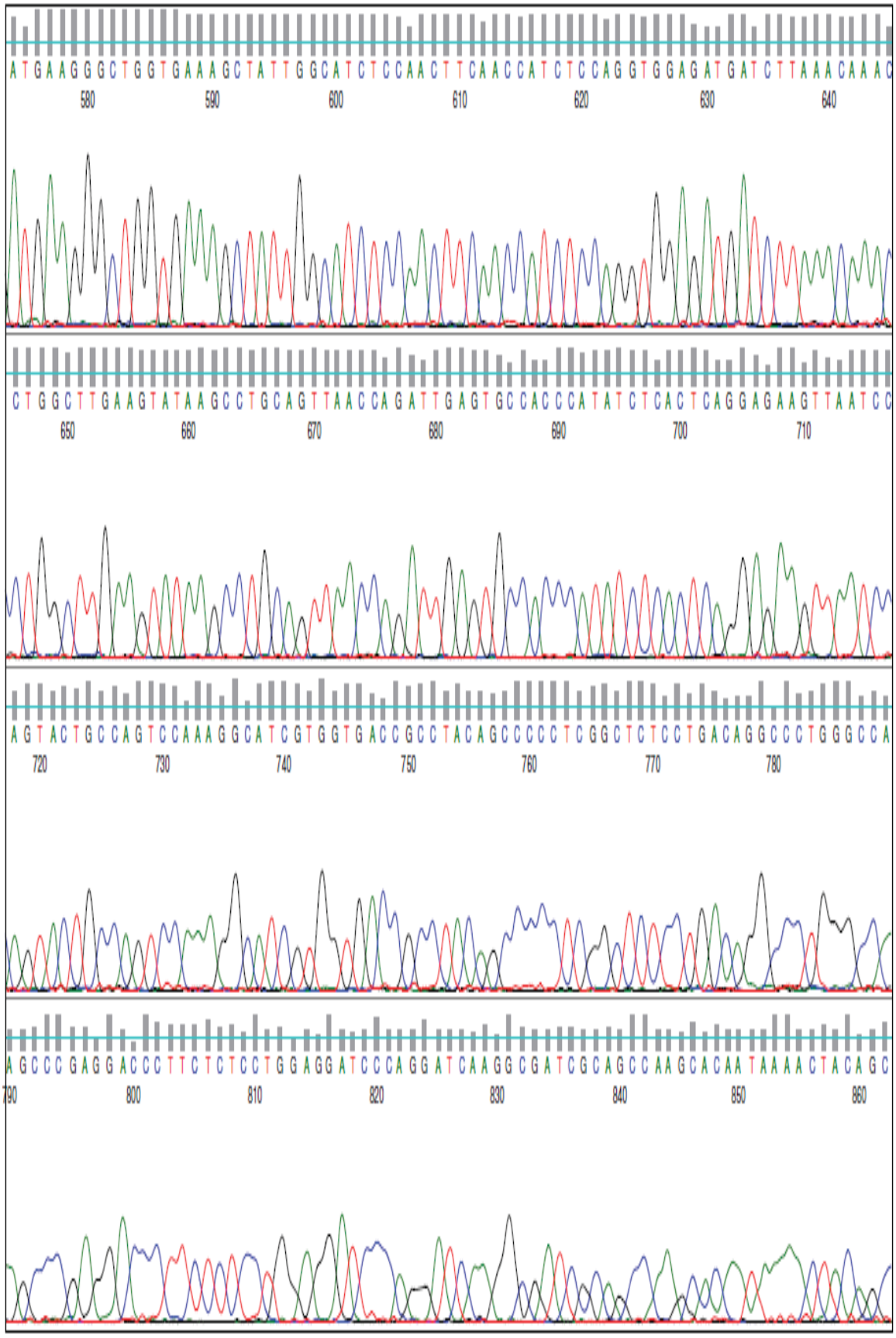
ATGAAGGGCTGGTGAAAGCTATTGGCATCTCCAACTTCAACCATCTCCAGGTGGAGATGATCTTAAACAAAC
580
590
600
610
620
630
640
CTGGCTTGAAGTATAAGCCTGCAGTTAACCAGATTGAGTGCCACCCATATCTCACTCAGGAGAAGTTAATCC
650
660
670
680
690
700
710
AGTACTGCCAGTCCAAAGGCATCGTGGTGACCGCCTACAGCCCCCTCGGCTCTCCTGACAGGCCCTGGGCCA
720
730
740
750
760
770
780
AGCCCGAGGACCCTTCTCTCCTGGAGGATCCCAGGATCAAGGCGATCGCAGCCAAGCACAATAAAACTACAGC
790
800
810
820
830
840
850
860

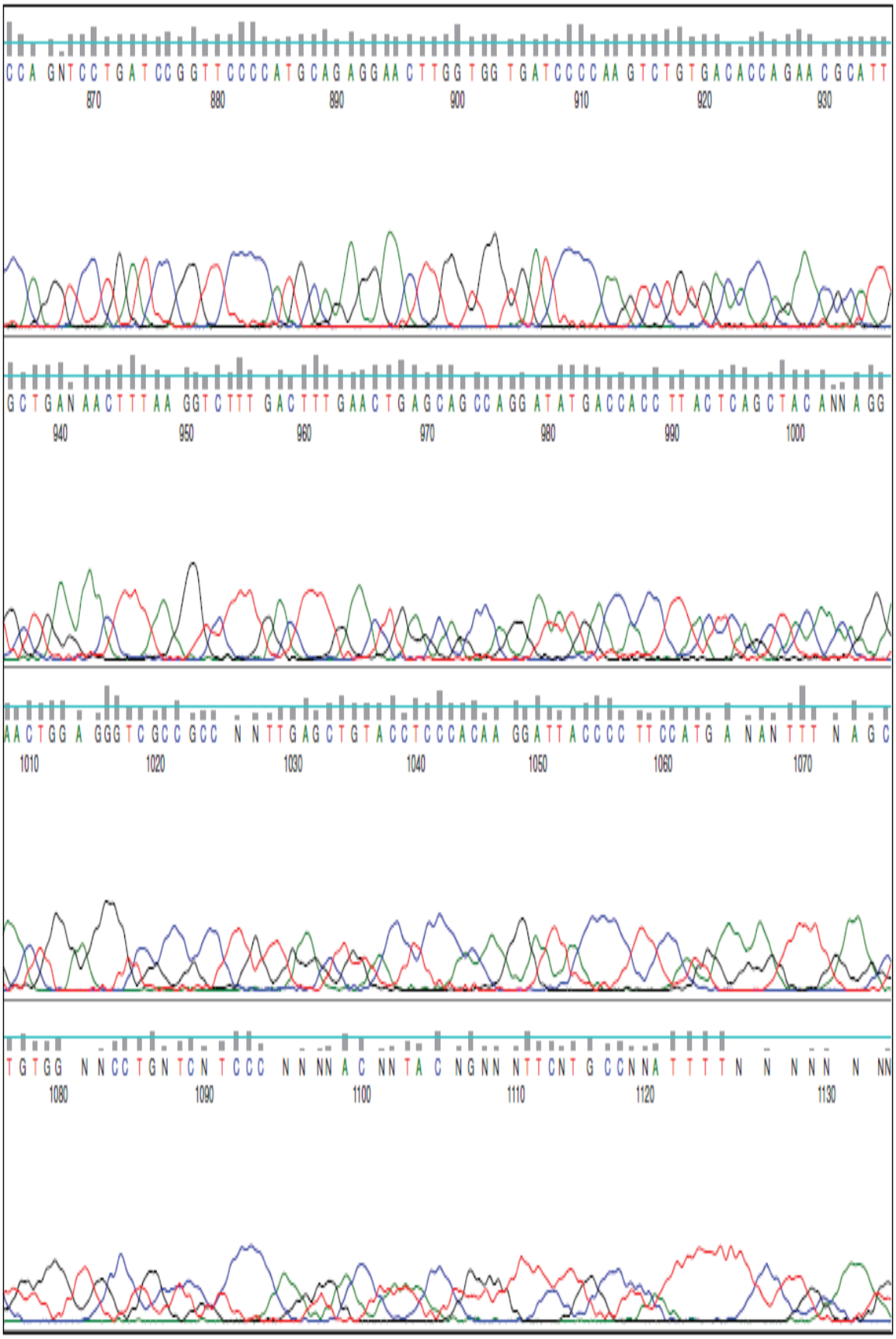
CCA GNTCCTGATCCGGTTCCCCATGCAGAGGAACTTGGTGGTGATCCCCAAGTCTGTGACACCAGAACGCATT
870 880 890 900 910 920 930
GCTGANAACTTTAA GGTCTTT GACTTTGAACTGAGCAGCCAGGATATGACCACC TT ACTCAGCTAC ANN A GG
940 950 960 970 980 990 1000
AACTGG A GGGTCGCC GCC N NTTGAGCTGTACCTCCCACAA GGATTACCCC TTCCATG A NAN TTT N A G C
1010 1020 1030 1040 1050 1060 1070
TGTGG N NCCTGNTCN TCCC N N NN A C NN TA C NGNN NTTCNT G CCNNA TTTTN N N N N N NN
1080 1090 1100 1110 1120 1130

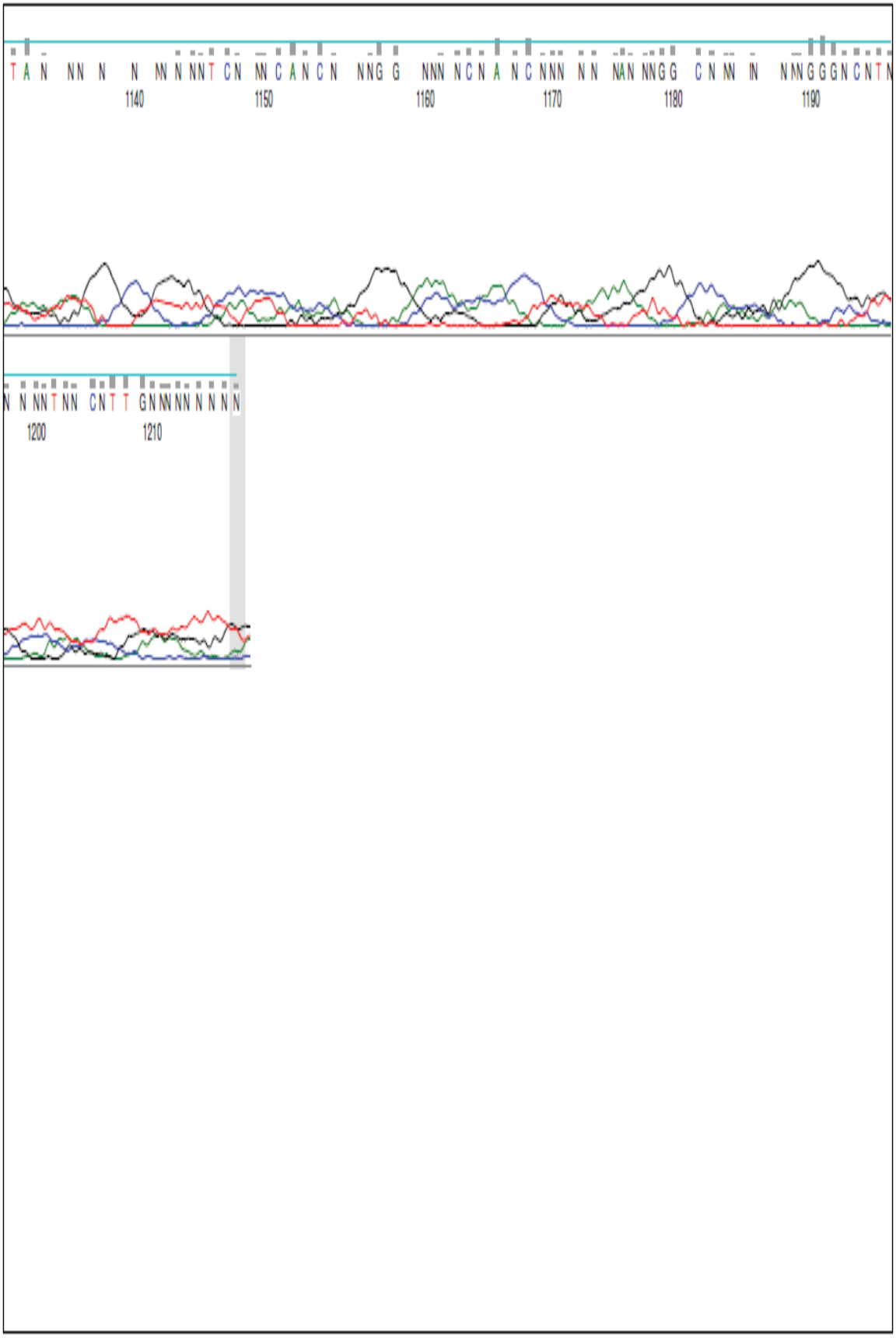
1140
1150
1160
1170
1180
1190
1200
1210

Figure 5.3: C298A Tube 1 Reverse Sequence

NNNNNNNNNNNNNTTTCGGGCTTTGTTAGCAGCCGGATCCTCGAGGCAAAG
AGAAGTCTTGCTGAAAGGATTCCAGTTCCAAGCAGTCAAAACTCAACCGTTA
GTGGCACTATTTTGACCTGGTAGATTTTGCTTCTCTTTGGTCAGAAAAGGGTA
TTCAGGTTGTACTTTCCCCAGCAGGGTAGAAAGAAGGGCAAAGCAAACTGGA
AGAGACTTCTACTCTACTGACAGGGCTCTTGAGATCCAACATCAAGCTAGAC
ACGCCCTCGCTGGCCACTCTACAGGTTGCTGTCCCACTGCTGAGTGACACAG
GCCATACTACATTTGCAAGGAAAAAAATGAGGCAAGAAACACAGGTATAGG
TCACTTGGGGACGAGCAGGCAACCACAGCTTCAAAACTCTTCATGGAAGGGG
TAATCCTTGTGGGAGGTACAGCTCAACAAGGC**GGC**GACCCTCCAGTTCCTGT
TGTAGCTGAGTAAGGTGGTCATATCCTGGCTGCTCAGTTCAAAGTCAAAGAC
CTTAAAGTTCTCAGCAATGCGTTCTGGTGTCACAGACTTGGGGATCACCACCA
AGTTCCTCTGCATGGGGAACCGGATCAGGACCTGGGCTGTAGTTTTATTGTGC
TTGGCTGCGATCGCCTTGATCCTGGGATCCTCCAGGAGAGAAGGGTCCTCGG
GCTTGGCCCAGGGCCTGTCAGGAGAGCCGAGGGGGCTGTAGGCGGTCACCAC
GATGCCTTTGGACTGGCAGTACTGGATTAACTTCTCCTGAGTGAGATATGGGT
GGCACTCAATCTGGTTAACTGCAGGCTTATACTTCAAGCCAGGTTTGTTTAAG
ATCATCTCCACCTGGNGATGGTTGAAGTTGGAGATGCCAATAGCTTTCACCA
GCCCTTCATCCACCAGCTCTTCCATGGCCGCCCACGTGTCCAGAATGTTGGTG
TCACTGGGAACCACATTGCCCGACTCATCCNATGGNAAATTCCTTCCCAGGCT
TAAAGCCAGTCGGCCAGTGAATAANNAGAGTCCAGTAGTCCAGCTTCAGTCG
CTGAGTGTCTCTGNAGCTNCTTTCACCAGGCCCTNTCATGGNACNNGCACNN
CAGCTGCTGACGATGAAGANCNNCCTNNNNNNNNCNCNGNTCCNNNNCTTC
NCNGAANTGNNNNCCCCCNCNNNNTNNCNNTNNGNNNNNANGNNNNNTNNN
NTNNNNNGNNNCCNNANNNNNANGNNCNNNTTNNNNGGCNNTNNANNNNC
NNNNNNNNCCNNNNNNNNGGNNNNNNNNNTNNNN

Figure 5.4: C298A Reverse DNA Chromatogram

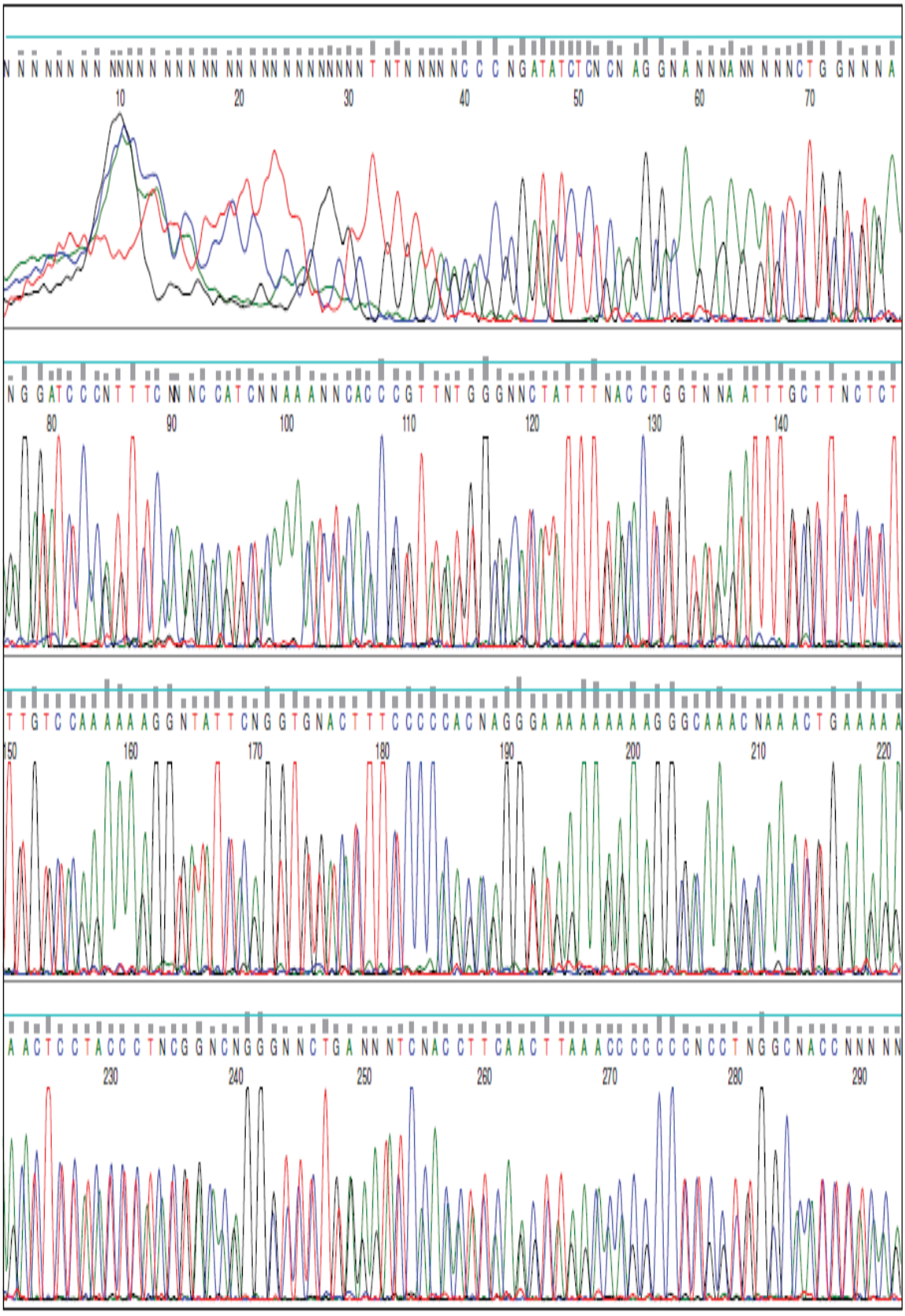

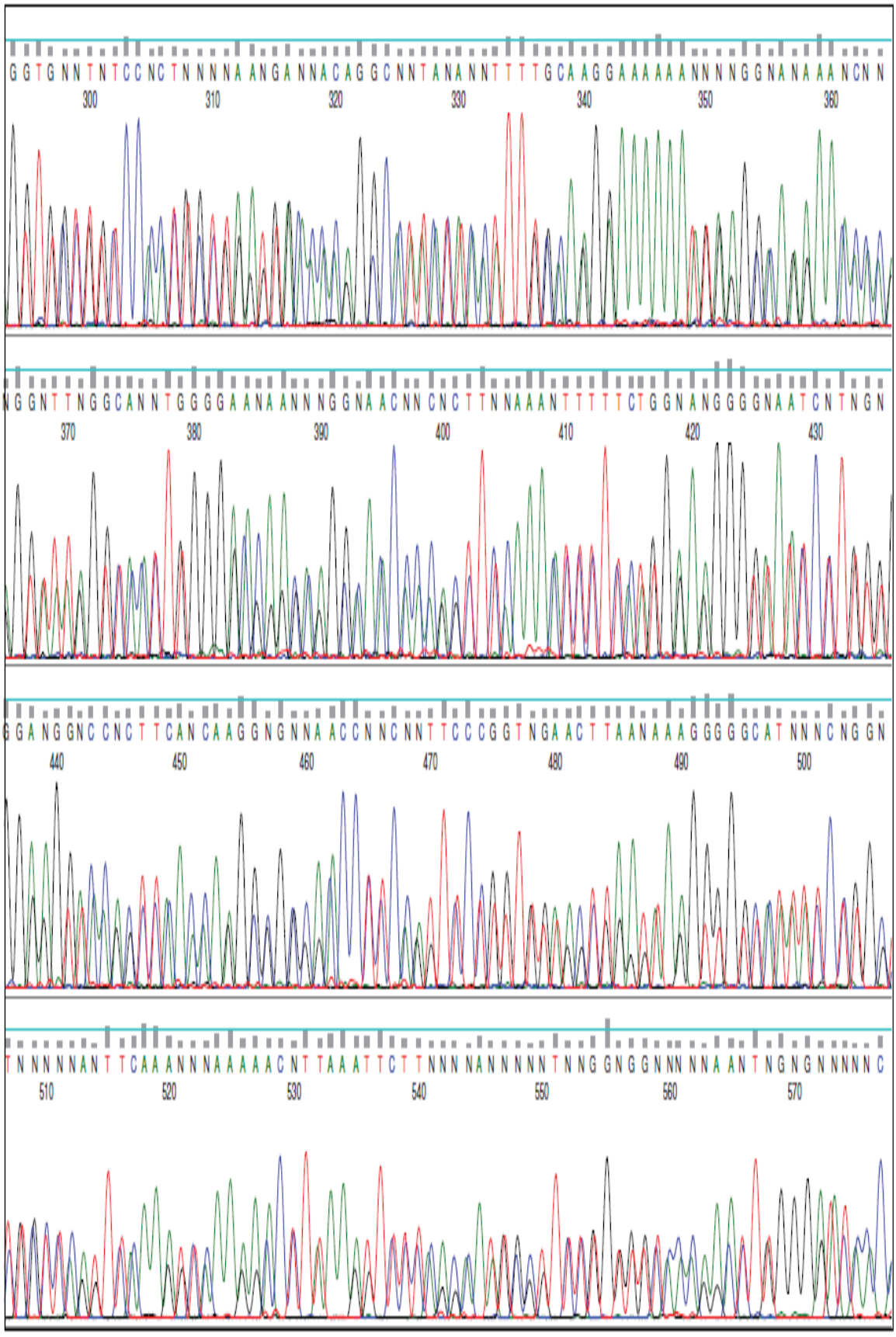
GGTGNNTNTCCNCTNNNNAANGANNACAGGCNNTANANNTTTTGCAAGGAAAAAANNNNGGNANAAANCNN
300 310 320 330 340 350 360
NGGNTTNGGCANNTGGGGAANANANNNGGNAACNNCNCTTNNAAANTTTTTCTGGNANGGGGNAATCNTNGN
370 380 390 400 410 420 430
GGANGGNCCNCTTTCANCAAGGNGNNNAACCNNCNNTTCCCGGTNGAACTTAANAAAGGGGGCATNNNCNGGN
440 450 460 470 480 490 500
TNNNNNANTTCAAANNNAAAAACNTTAAATTCTTNNNNANNNNNTNNGGNGGNNNNNAANTNGNGNNNNNC
510 520 530 540 550 560 570

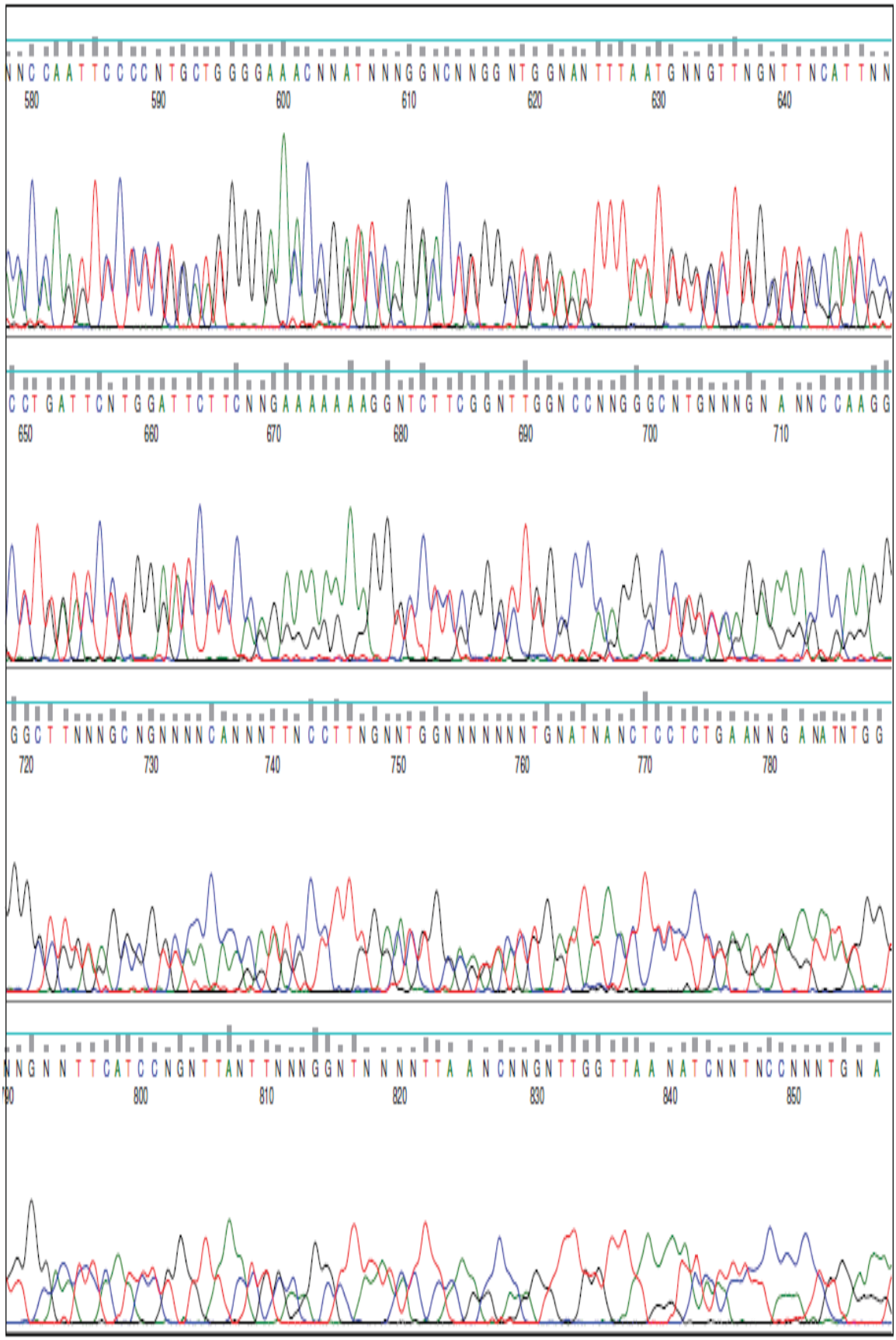
580
590
600
610
620
630
640
650
660
670
680
690
700
710
720
730
740
750
760
770
780
800
810
820
830
840
850

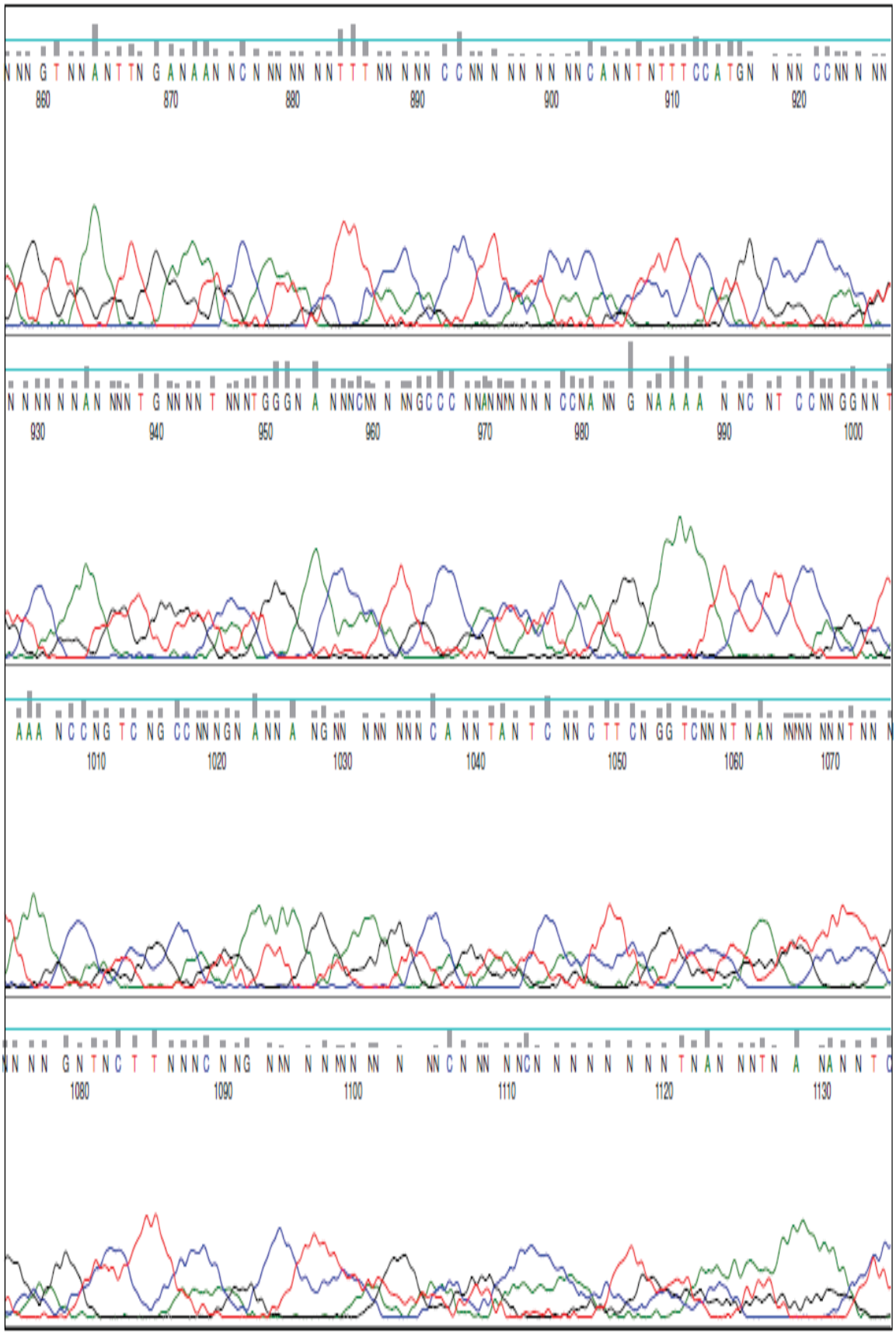

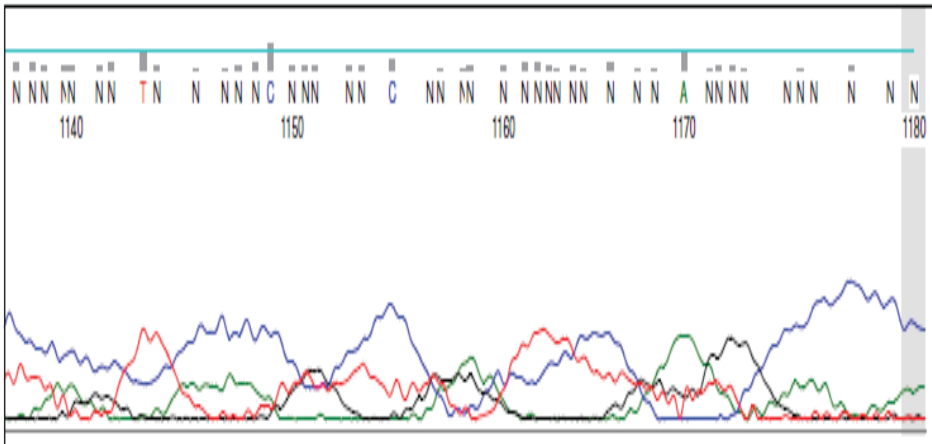
1140
1150
1160
1170
1180

Figure 5.5: C298D Tube 2 Forward Sequence

NNNNNNNNNNNNNNTNCCTCTAGANTAATTTTGTTTAACTTTAAGAAGGAG
ATATACCATGGGCAGCAGCCATCATCATCATCACAGCAGCGGCCTGGTG
CCGCGCGGCAGCCATATGGCTAGCCGTATCCTGCTCAACAACGGCGCCAAGA
TGCCCATCCTGGGGTTGGGTACCTGGAAGTCCCCTCCAGGGCAGGTGACTGA
GGCCGTGAAGGTGGCCATTGACGTCGGGTACCGCCACATCGACTGTGCCCAT
GTGTACCAGAATGAGAATGAGGTGGGGGTGGCCATTCAGGAGAAGCTCAGG
GAGCAGGTGGTGAAGCGTGAGGAGCTCTTCATCGTCAGCAAGCTGTGGTGCA
CGTACCATGAGAAGGGCCTGGTGAAAGGAGCCTGCCAGAAGACACTCAGCG
ACCTGAAGCTGGACTACCTGGACCTCTACCTTATTCACTGGCCGACTGGCTTT
AAGCCTGGGAAGGAATTTTTCCCATTGGATGAGTCGGGCAATGTGGTTCCCA
GTGACACCAACATTCTGGACACGTGGGCGGCCATGGAAGAGCTGGTGGATGA
AGGGCTGGTGAAAGCTATTGGCATCTCCAACTTCAACCATCTCCAGGTGGAG
ATGATCTTAAACAAACCTGGCTTGAAGTATAAGCCTGCAGTTAACCAGATTG
AGTGCCACCCATATCTCACTCAGGAGAAGTTAATCCAGTACTGCCAGTCCAA
AGGCATCGTGGTGACCGCCTACAGCCCCCTCGGCTCTCCTGACAGGCCCTGG
GCCAAGCCCGAGGACCCTTCTCTCCTGGAGGATCCCAGGATCAAGGCGATCG
CAGCCAAGCACAATAAAACTACAGCCCAGGTCCTGATCCGGTTCCCCATGCA
GAGGAACTTGGTGGTGATCCCCAAGTCTGTGACACCAGAACGCATTGCTGAG
AACTTTAANGNCTTTGACTTTGAACTGAGCAGCCAGGATATGACCACCTTACT
CAGCTACAACAGGAACTGGAGGGTC**GAC**GCCTTGTTGAGCTGTACCTCCCAC
AAGGATTACCCCTTCCATGAAGAGTTTGAAGCTGTNGGTTGCCTGCTCNTCCC
CANNTGAACNATACCTNNGTTTCTTGCCTCNNTTTTNNNNNAATGTAGNANG
GNNNGNGNNACTCANCAGNGGGNCNNNCANCNNNNNNANNNNCNANNNNN
GGGCGNNNCTAGCTNNNNNTNNNNTNNNNANNNNNNNNNNCNNNTANNNN
NNNANNNNNNTNNNCNNNNNNNNNNNNNNNNNNN

Figure 5.6: C298D Forward DNA Chromatogram

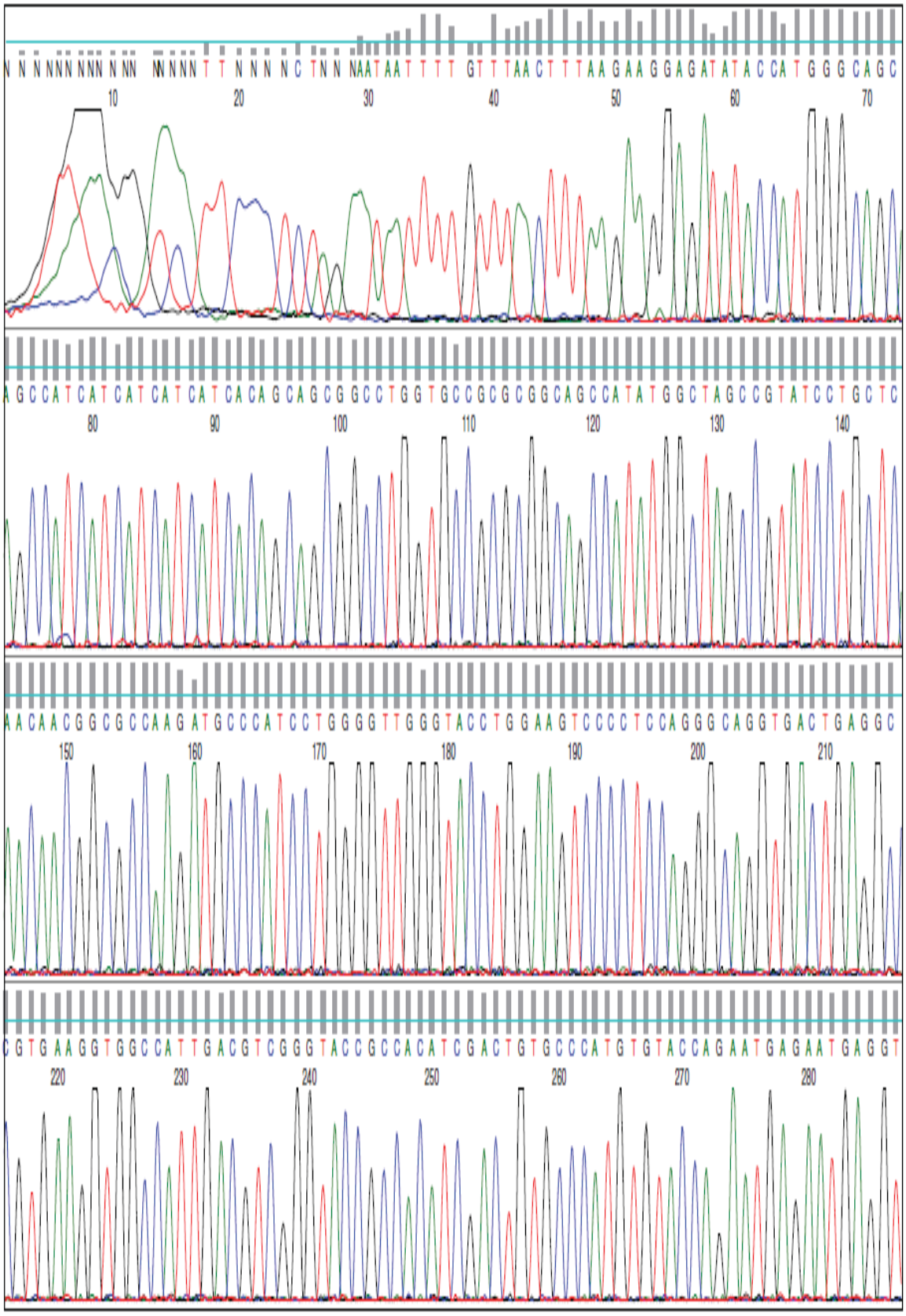

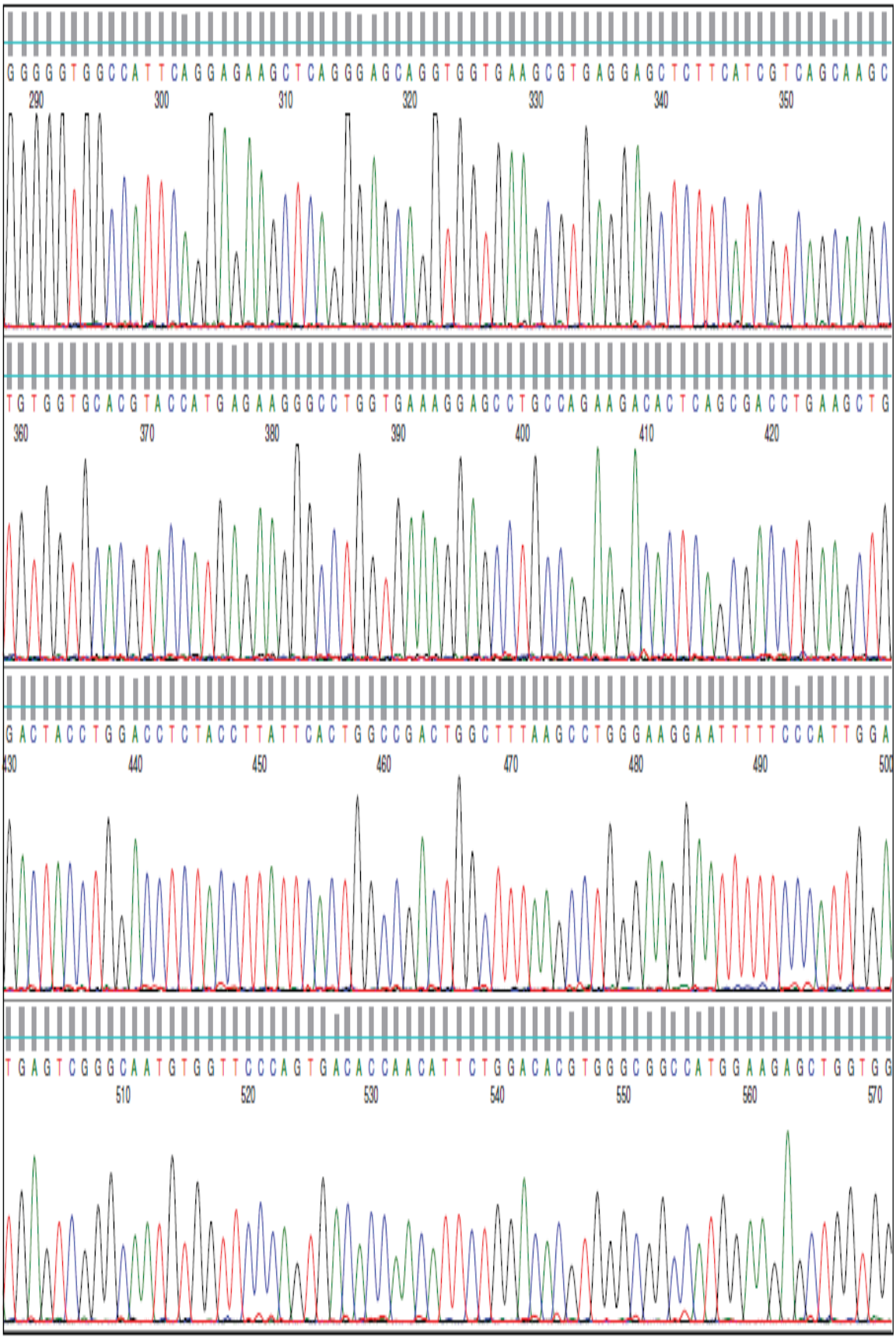
GGGGGTGGCCATTCAGGAGAAGCTCAGGGAGCAGGTGGTGAAGCGTGAGGAGCTCTTCATCGTCAGCAAGC
290
300
310
320
330
340
350
TGTGGTGCACGTACCATGAGAAGGGCCTGGTGAAAGGAGCCTGCCAGAAGACACTCAGCGACCTGAAGCTG
360
370
380
390
400
410
420
GACTACCTGGACCTCTACCTTATTCACTGGCCGACTGGCTTTAAGCCTGGGAAGGAATTTTTCCCATTGGA
430
440
450
460
470
480
490
TGAGTCGGGCAATGTGGTTCCCAGTGACACCAACATTCTGGACACGTGGGCGGCCATGGAAGAGCTGGTGG
510
520
530
540
550
560
570

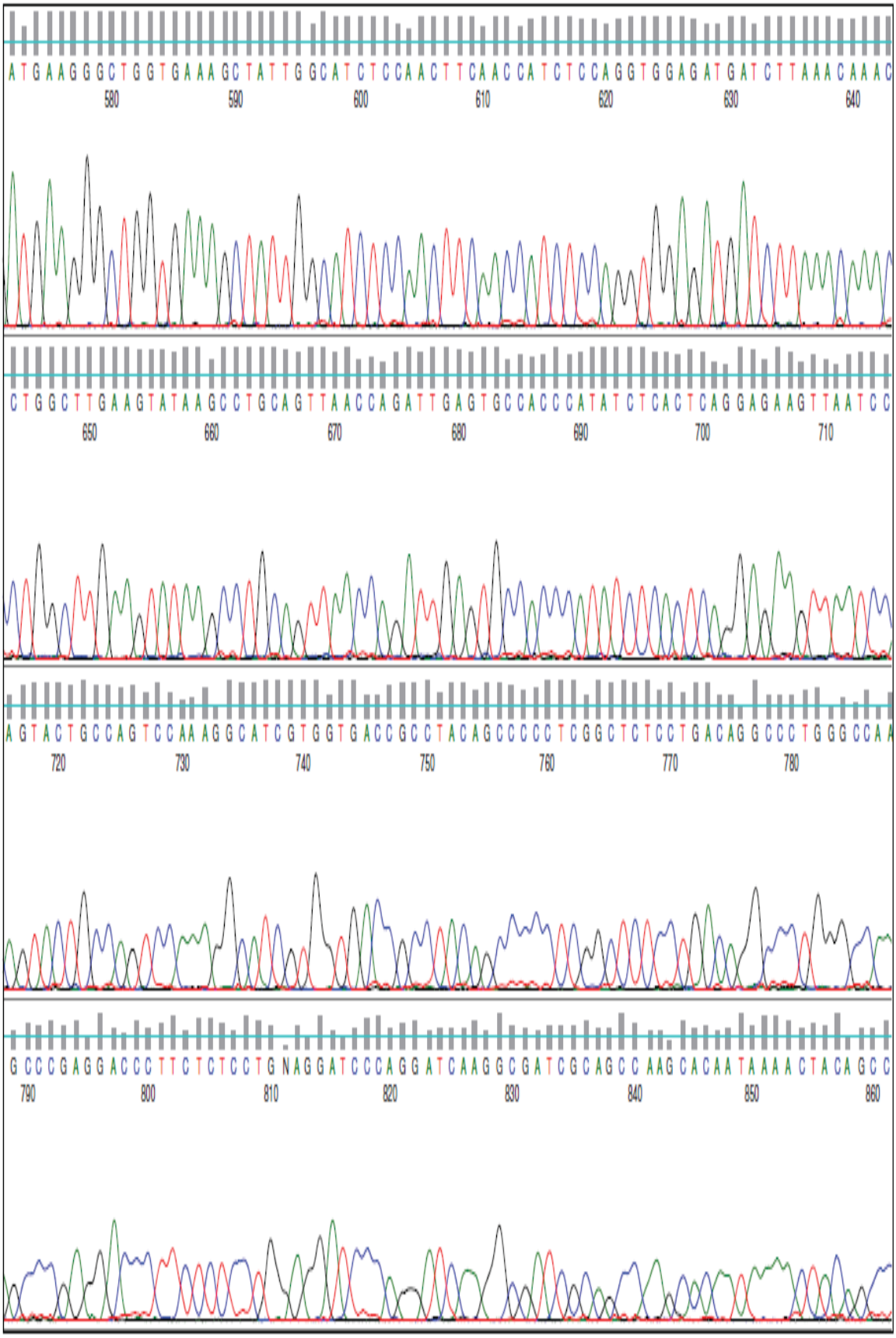
ATGAAGGGCTGGTGAAAGCTATTGGCATCTCCAACTTCAACCATCTCCAGGTGGAGATGATCTTAAACAAAC
580
590
600
610
620
630
640
CTGGCTTGAAGTATAAGCCTGCAGTTAACCAGATTGAGTGCCACCCATATCTCACTCAGGAGAAGTTAATCC
650
660
670
680
690
700
710
AGTACTGCCAGTCCAAAGGCATCGTGGTGACCGCCTACAGCCCCCCTCGGCTCTCCTGACAGGCCCTGGGCCAA
720
730
740
750
760
770
780
GCCCGAGGACCCTTCTCTCCTGNAGGATCCCAGGATCAAGGCGATCGCAGCCAAGCACAATAAAACTACAGCC
790
800
810
820
830
840
850
860

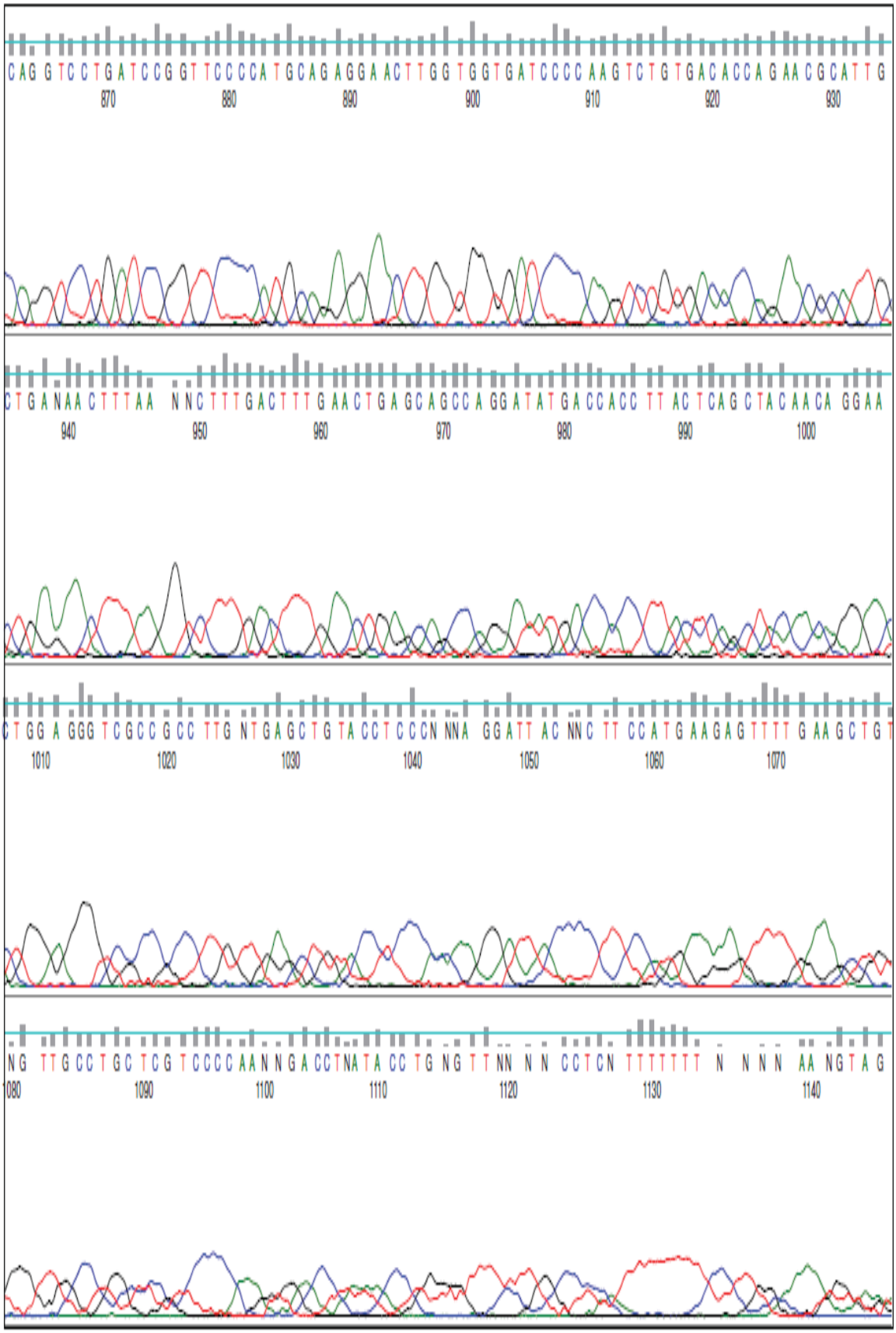
CAGGTCCTGATCCGGTTCCCCATGCAGAGGAACTTGGTGGTGATCCCCAAGTCTGTGACACCAGAACGCATTG
870 880 890 900 910 920 930
CTGANAACTTTAA NNCTTTGACTTTGAACTGAGCAGCCAGGATATGACCACCTTACTCAGCTACAACAGGAA
940 950 960 970 980 990 1000
CTGGAGGGTCGCCGCCTTGNTGAGCTGTACCTCCCNNNAGGATTACNNCTTCCATGAAGAGTTTTGAAGCTGT
1010 1020 1030 1040 1050 1060 1070
NGTTGCCTGCTCGTCCCCAANNGACCTNATACCTGNGTTNNNNNCCTCNTTTTTTTNNNNAANGTAG
1080 1090 1100 1110 1120 1130 1140

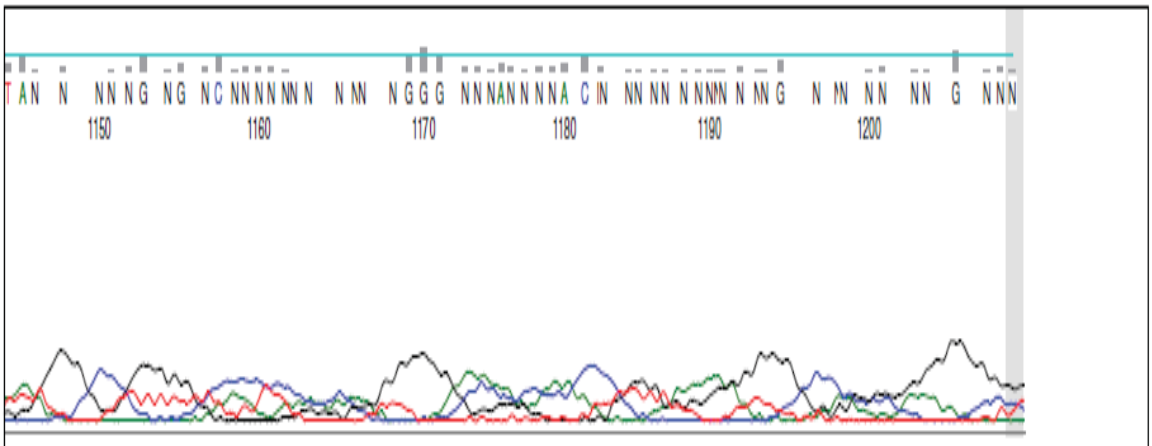
1150
1160
1170
1180
1190
1200

Figure 5.7: C298D Tube 2 Reverse Sequence

NNNNNNNNNNNTNNNTTCGGGCTTTGTTAGCAGCCGGATCCTCGAGGCAAAG
AGAAGTCTTGCTGAAAGGATTCCAGTTCCAAGCAGTCAAAACTCAACCGTTA
GTGGCACTATTTTGACCTGGTAGATTTTGCTTCTCTTTGGTCAGAAAAGGGTA
TTCAGGTTGTACTTTCCCCAGCAGGGTAGAAAGAAGGGCAAAGCAAACTGGA
AGAGACTTCTACTCTACTGACAGGGCTCTTGAGATCAAACATCAAGCTAGAC
ACGCCCTCGCTGGCCACTCTACAGGTTGCTGTCCCACTGCTGAGTGACACAG
GCCATACTACATTTGCAAGGAAAAAAATGAGGCAAGAAACACAGGTATAGG
TCACTTGGGGACGAGCAGGCAACCACAGCTTCAAAACTCTTCATGGAAGGGG
TAATCCTTGTGGGAGGTACAGCTCAACAAGGC**GTC**GACCCTCCAGTTCCTGT
TGTAGCTGAGTAAGGTGGTCATATCCTGGCTGCTCAGTTCAAAGTCAAAGAC
CTTAAAGTTCTCAGCAATGCGTTCTGGTGTCACAGACTTGGGGATCACCACCA
AGTTCCTCTGCATGGGGAACCGGATCAGGACCTGGGCTGTAGTTTTATTGTGC
TTGGCTGCGATCGCCTTGATCCTGGGATCCTCCAGGAGAGAAGGGTCCTCGG
GCTTGGCCCAGGGCCTGTCAGGAGAGCCGAGGGGGCTGTAGGCGGTCACCAC
GATGCCTTTGGACTGGCAGTACTGGATTAACTTCTCCTGAGTGAGATATGGGT
GGCACTCAATCTGGTTAACTGCAGGCTTATACTTCAAGCCAGGTTTGTTTAAG
ATCATCTCCACCTGGAGATGGTTGAAGTTGGAGATGCCAATAGCTTTCACCA
GCCCTTCATCCACCAGCTCTTCCATGGCCGCCCACGTGTCCAGAATGTTGGTG
TCACTGGGAACCACATTGCCCGACTCATCCAATGGGAAAAATTCCTTCCCAG
GCTTAAAGCCAGTCGGCCAGTGAATANNNAGAGGTCCAGGTAGTCCAGCTTC
AGGTCGCTGAGTGTCTTCTGGCAGNTNCTTTCACCAGGCCCTNNTNNTGGNAC
NNGCANNNAGCTGCTGACGATNAANAGCTNNTCACGCTTCACNNCNNNNNC
NNANCTTNNNCNNAATNNNNNCNNNNCTCATNNNCNNTNNNNNNNNNGNNN
NNNNCNNNNNNNNNNNNCNNNNNNNNNGNNNNNNNNNNGNGNCNNNNNN
NNNNNNCNNNNNNNNNNGTNNNNNNNNN

Figure 5.8: C298D Reverse DNA Chromatogram

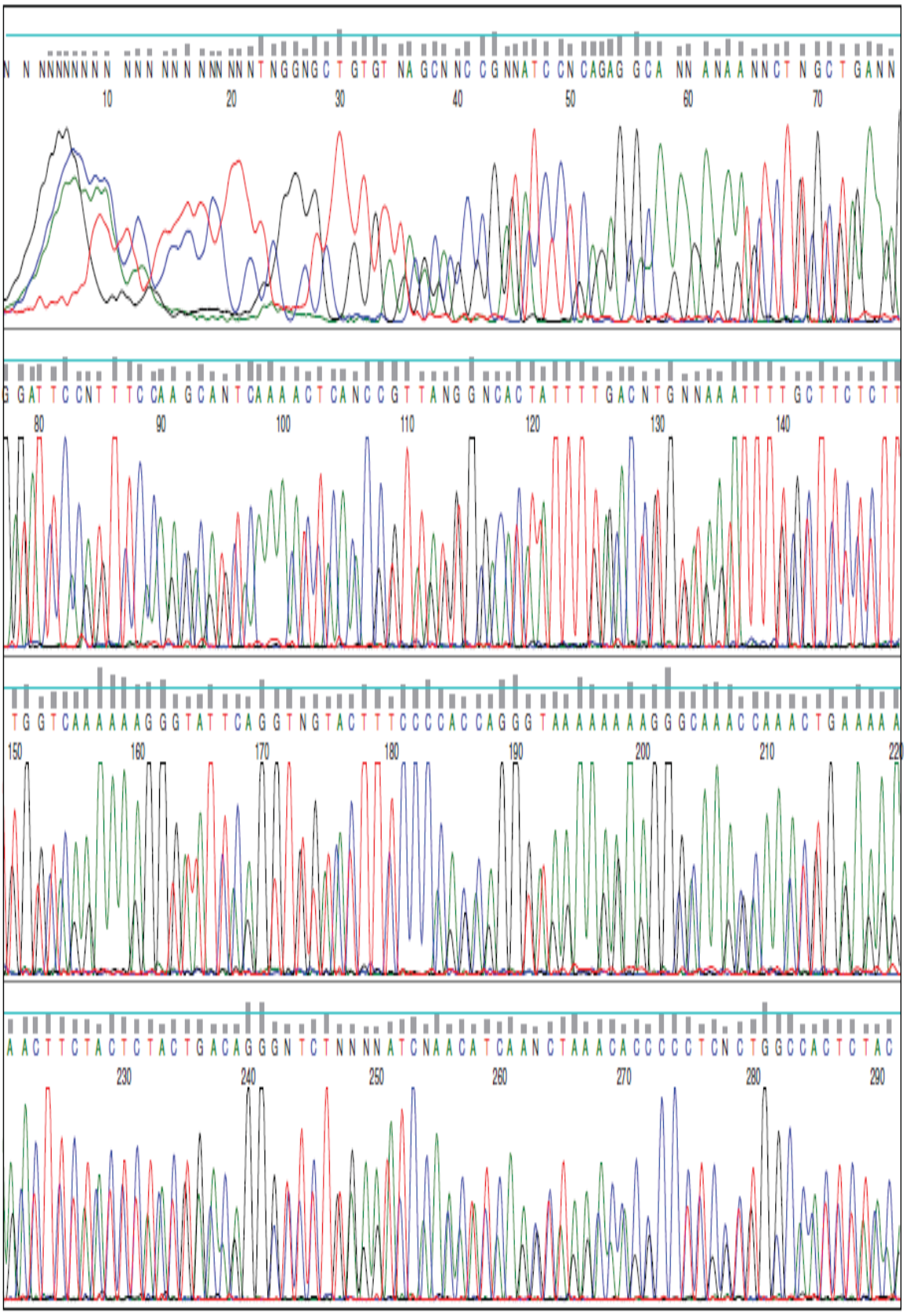

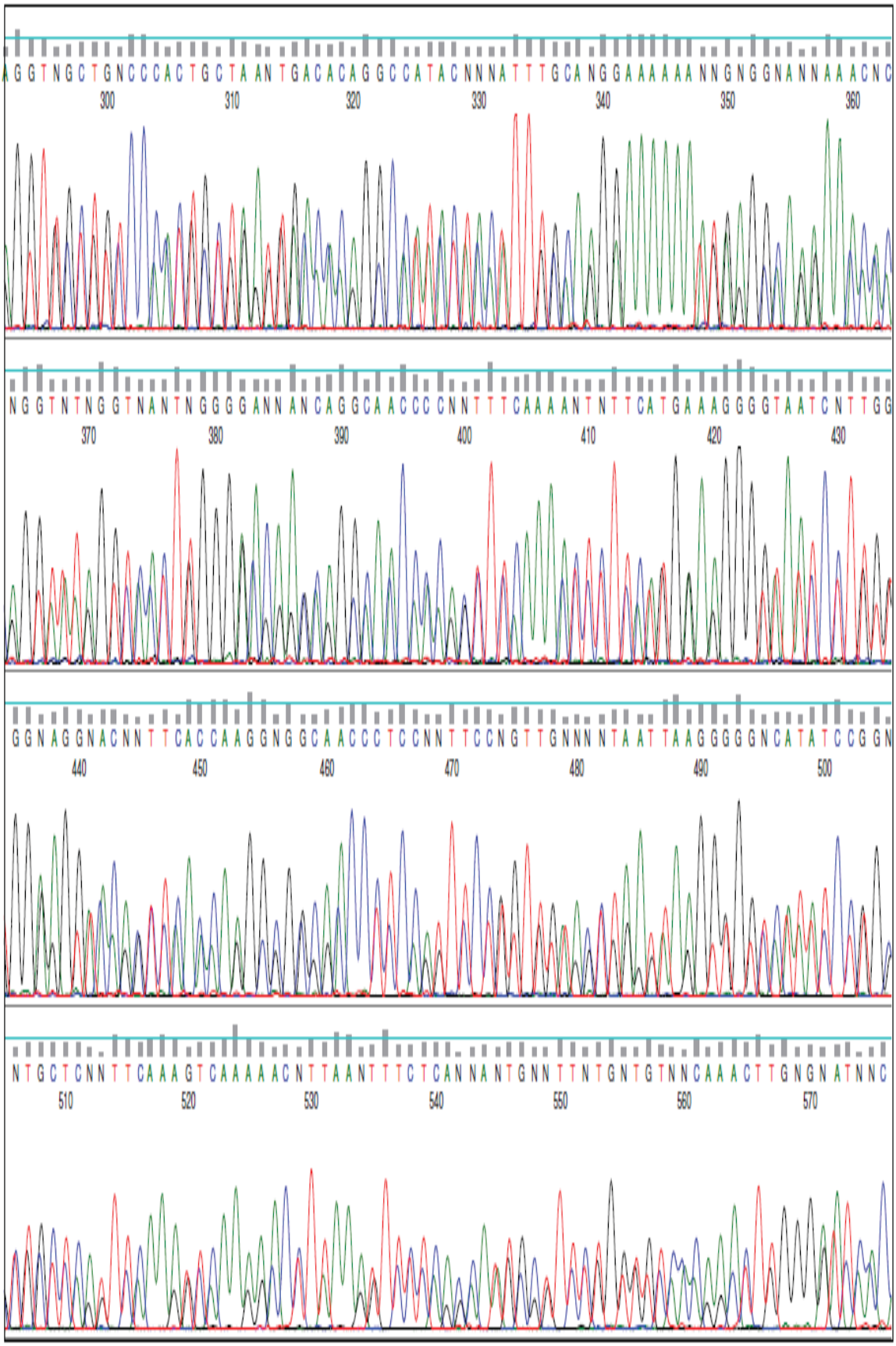
AGGTNGCTGNCCCACTGCTAANTGACACAGGCCATACNNNATTTGCANGGAAAAAANNGNGGNANNAAACNC
300 310 320 330 340 350 360
NGGTNTNGGTNANTNGGGGANNANCAGGCAACCCCNNTTTCAAAANTNTTCATGAAAGGGGTAATCNTTGG
370 380 390 400 410 420 430
GGNAGGNACNNTTCACCAAGGNGGCAACCCTCCNNTTCCNGTTGNNNNTAATTAAGGGGGNCATATCCGGN
440 450 460 470 480 490 500
NTGCTCNNTTCAAAGTCAAAAAACNTTAANTTTCTCANNANTGNNTTNTGNTGTNNCAAACTTGNGNATNNC
510 520 530 540 550 560 570

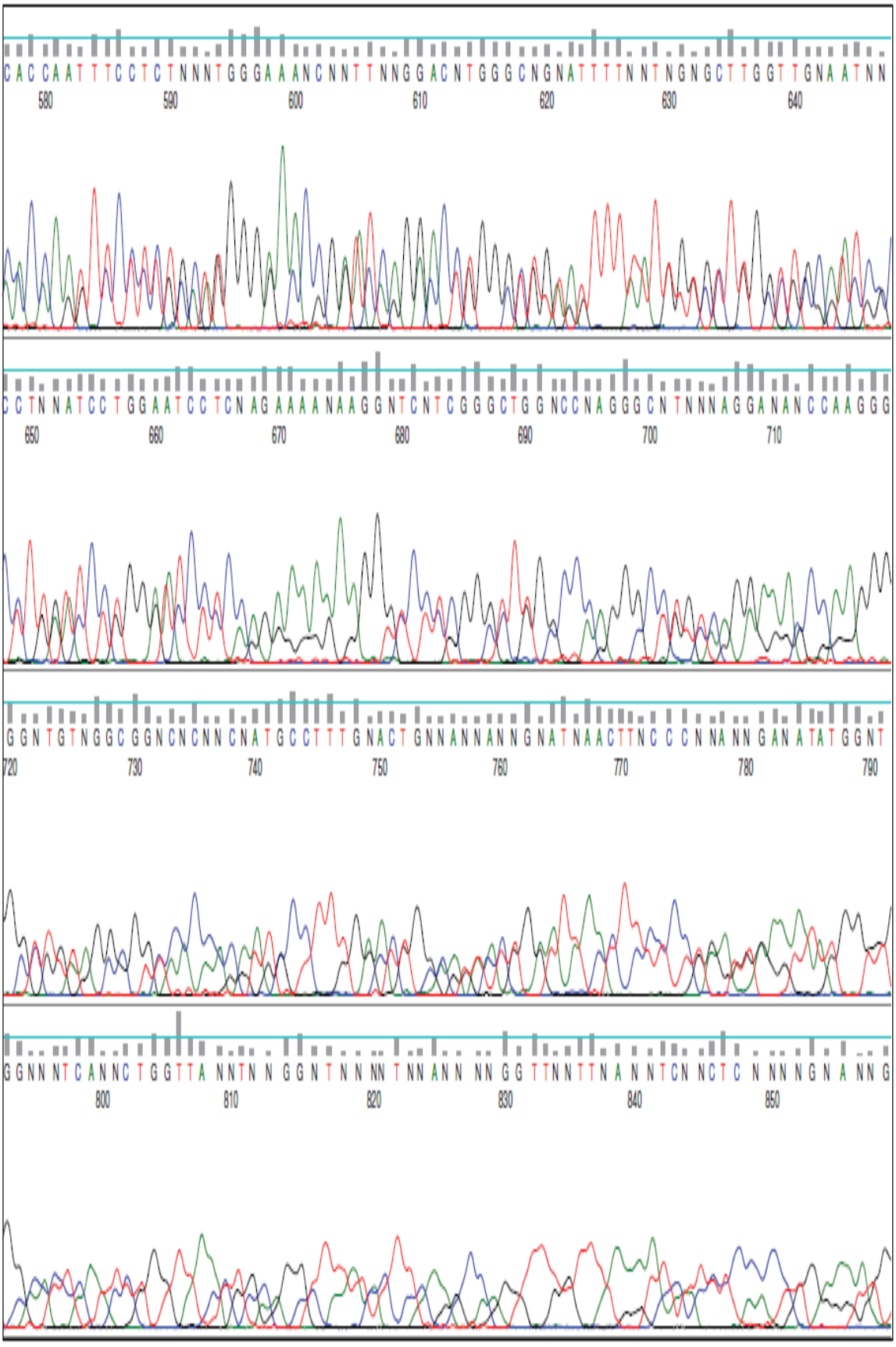
CACCAATTTCCTCTNNNTGGGAAANCNNTTNNGGACNTGGGCNGNATTTTNNTNGNGCTTGGTTGNAATNN
580
590
600
610
620
630
640
CCTNNATCCTGGAATCCTCNAGAAAANAAGGNTCNTCGGGCTGGNCCNAGGGCNTNNNAGGANANCCAAGGG
650
660
670
680
690
700
710
GGNTGTNGGCGGNCNCNNCNATGCCTTTGNACTGNNANNANNGNATNAACTTNCCCNNANNGANATATGGNT
720
730
740
750
760
770
780
790
GGNNNTCANNCTGGTTANNTNNGGNTNNNNTNNANNNNGGTTNNTTNANNTCNNCTCNNNNGNANNG
800
810
820
830
840
850

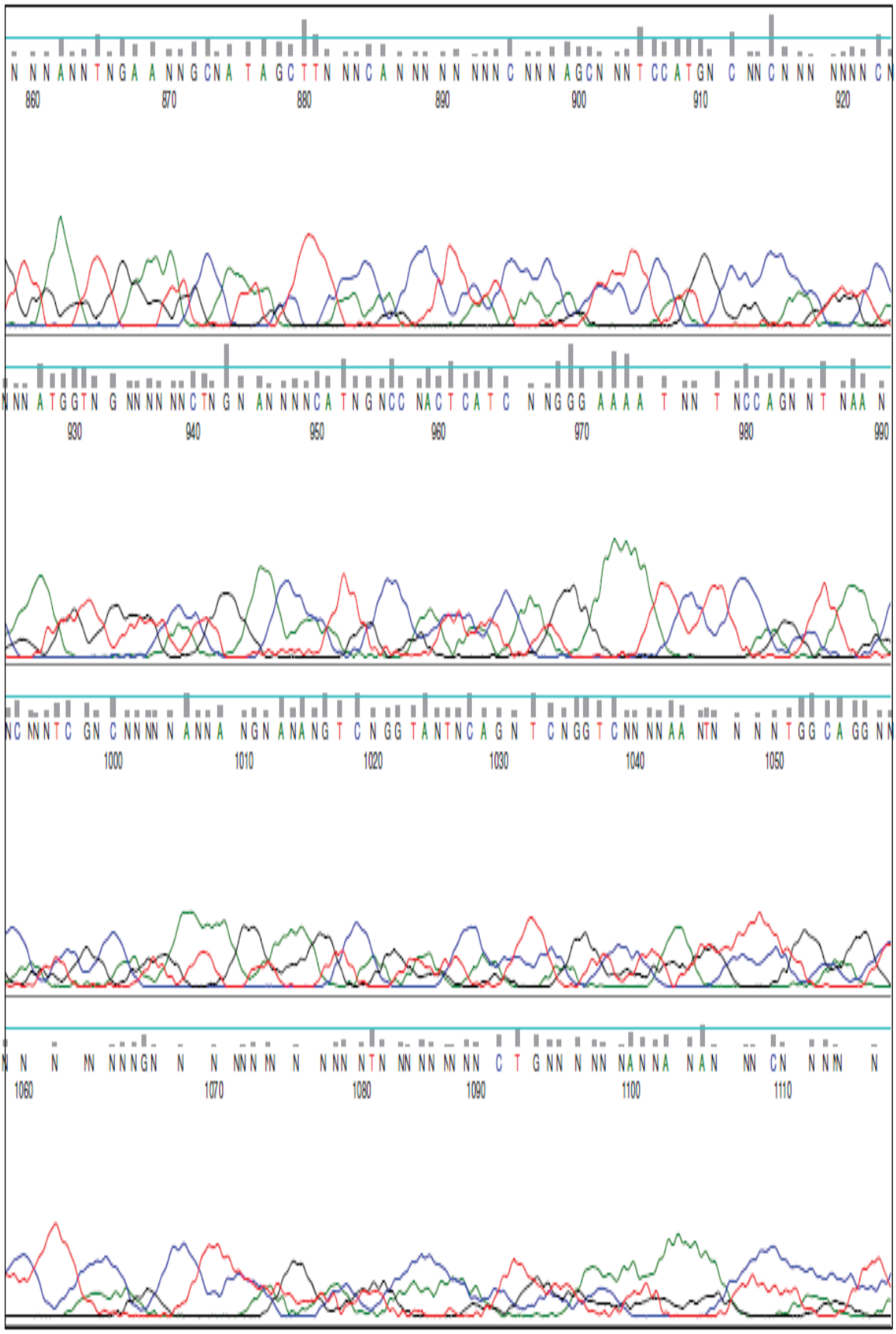

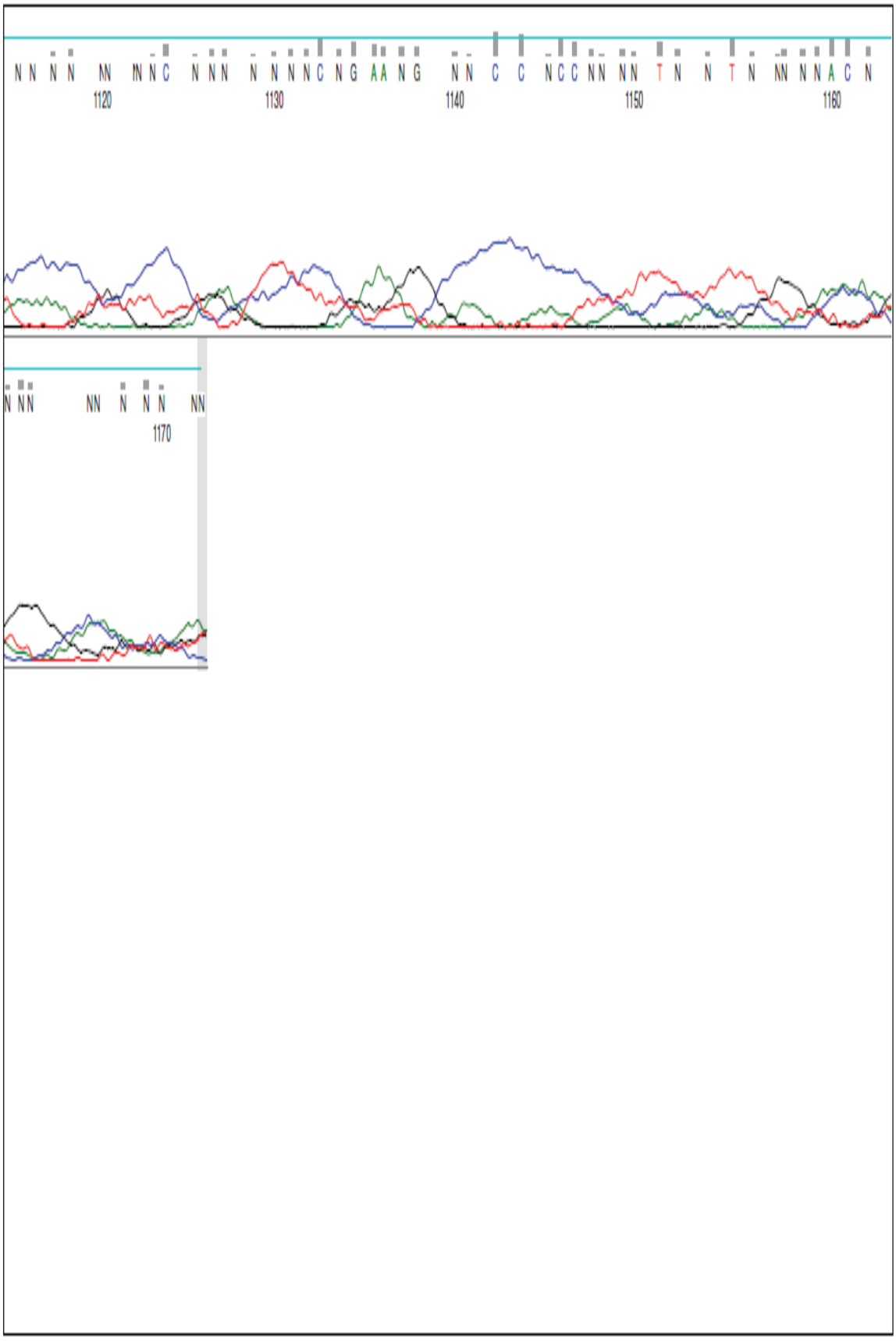
1120
1130
1140
1150
1160
1170

Figure 5.9: C298G Tube 1 Forward Sequence

NNNNNNNNNNNNNNNNNNNNNCTAGNNTAATTTTGTTTAACTTTAAGAAG
GAGATATACCATGGGCAGCAGCCATCATCATCATCACAGCAGCGGCCTG
GTGCCGCGCGGCAGCCATATGGCTAGCCGTATCCTGCTCAACAACGGCGCCA
AGATGCCCATCCTGGGGTTGGGTACCTGGAAGTCCCCTCCAGGGCAGGTGAC
TGAGGCCGTGAAGGTGGCCATTGACGTCGGGTACCGCCACATCGACTGTGCC
CATGTGTACCAGAATGAGAATGAGGTGGGGGTGGCCATTCAGGAGAAGCTCA
GGGAGCAGGTGGTGAAGCGTGAGGAGCTCTTCATCGTCAGCAAGCTGTGGTG
CACGTACCATGAGAAGGGCCTGGTGAAAGGAGCCTGCCAGAAGACACTCAG
CGACCTGAAGCTGGACTACCTGGACCTCTACCTTATTCACTGGCCGACTGGCT
TTAAGCCTGGGAAGGAATTTTTCCCATTGGATGAGTCGGGCAATGTGGTTCCC
AGTGACACCAACATTCTGGACACGTGGGCGGCCATGGAAGAGCTGGTGGATG
AAGGGCTGGTGAAAGCTATTGGCATCTCCAACTTCAACCATCTCCAGGTGGA
GATGATCTTAAACAAACCTGGCTTGAAGTATAAGCCTGCAGTTAACCAGATT
GAGTGCCACCCATATCTCACTCAGGAGAAGTTAATCCAGTACTGCCAGTCCA
AAGGCATCGTGGTGACCGCCTACAGCCCCCTCGGCTCTCCTGACAGGCCCTG
GGCCAAGCCCGAGGACCCTTCTCTCCTGGAGGATCCCAGGATCAAGGCGATC
GCAGCCAAGCACAATAAAACTACAGCCCAGGTCCTGATCCGGTTCCCCATGC
AGAGGAACTTGGTGGTGATCCCCAAGTCTGTGACACCAGAACGCATTGCTGA
GAACTTTNAGGTCTTTGACTTTGAACTGAGCAGCCAGGATATGACCACCTTAC
TCAGCTACAACAGGAACTGGGAGGGTC**GGA**GCCTTGTTGAGCTGTACCTCCC
ACAAGGATTACCCCTTTCCATGAANNNTTTNAAGCTGTGGTTNCNGCTCGTCC
CNAGTGACCTATACNNNNTTTCNTGCNCNTTTTTTNCNNCAANGNAGTANGG
NCCNGNNTNACTNANNNNNNNNNNGCANNNTNNNNNNNNNNNNNNNNTA
NNNTGANNNTNGANTNNNANNNNNCCNGTNNNNNNNNNNNNANNNANANN
CNCNNNNNNNNN

Figure 5.10: C298G Forward DNA Chromatogram

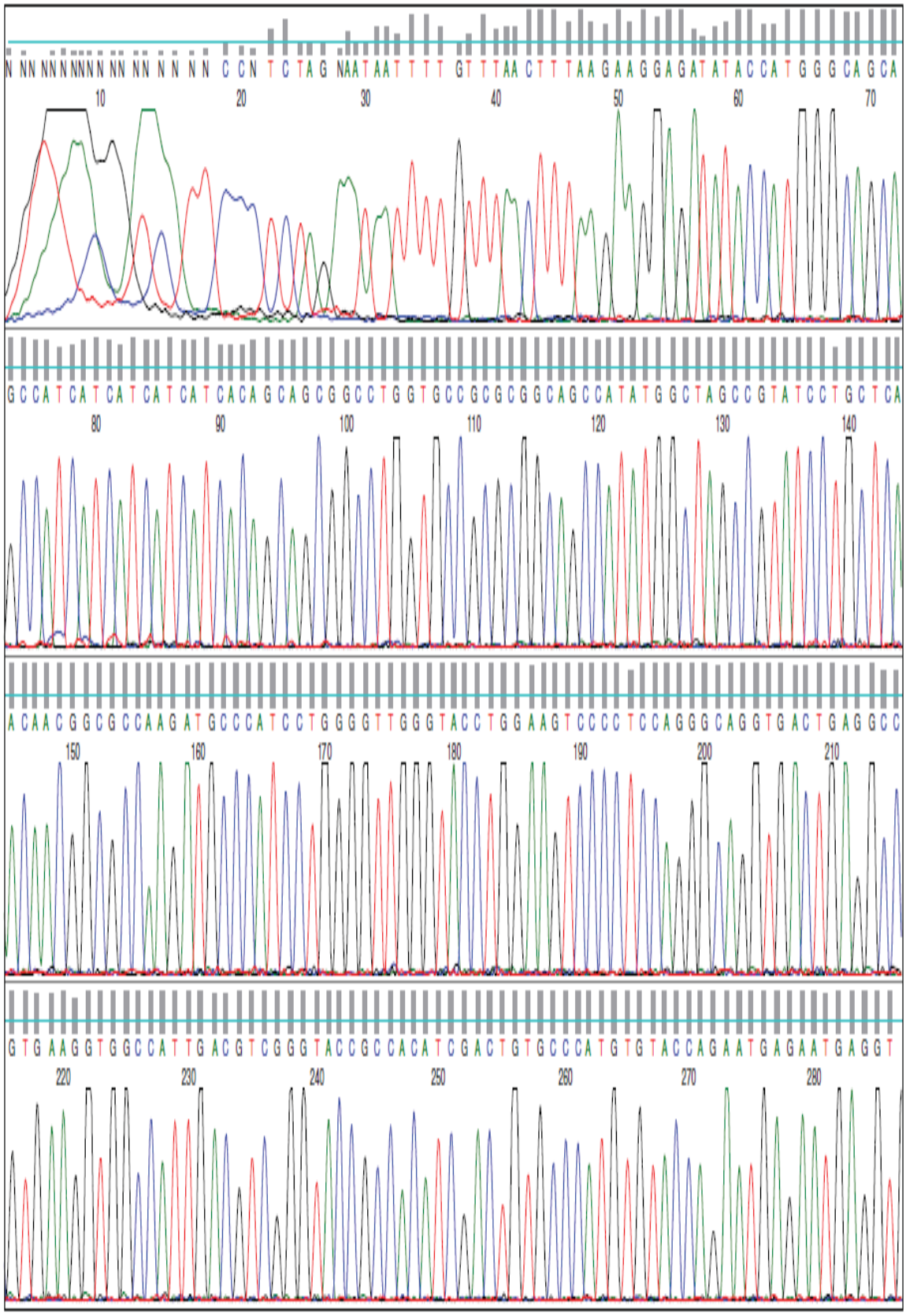

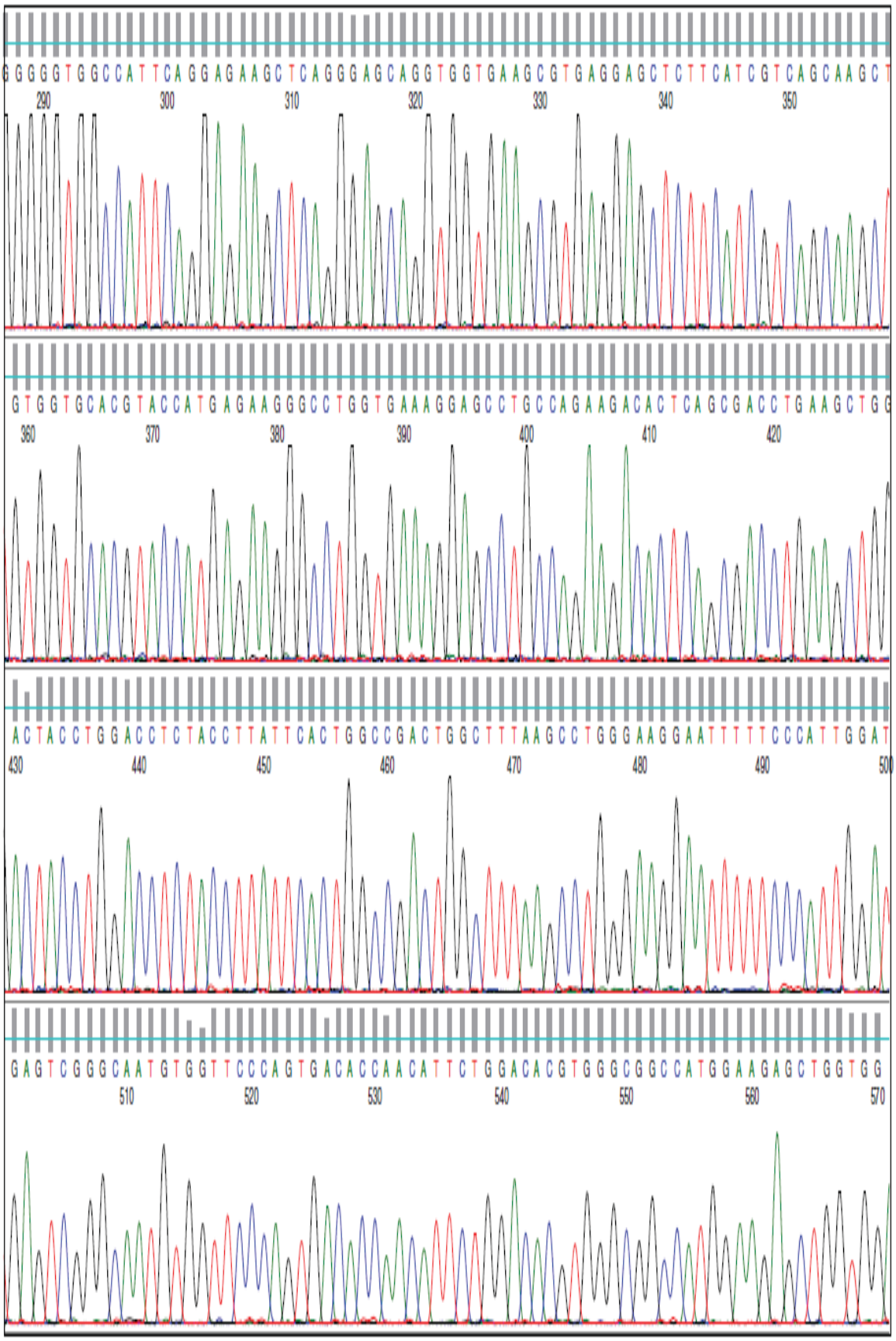
GGGGGTGGCCATTCAGGAGAAGCTCAGGGAGCAGGTGGTGAAGCGTGAGGAGCTCTTCATCGTCAGCAAGCT
290 300 310 320 330 340 350
GTGGTGCACGTACCATGAGAAGGGCCTGGTGAAAGGAGCCTGCCAGAAGACACTCAGCGACCTGAAGCTGG
360 370 380 390 400 410 420
ACTACCTGGACCTCTACCTTATTCACTGGCCGACTGGCTTTAAGCCTGGGAAGGAATTTTTCCCATTGGAT
430 440 450 460 470 480 490 500
GAGTCGGGCAATGTGGTTCCCAGTGACACCAACATTCTGGACACGTGGGCGGCCATGGAAGAGCTGGTGG
510 520 530 540 550 560 570

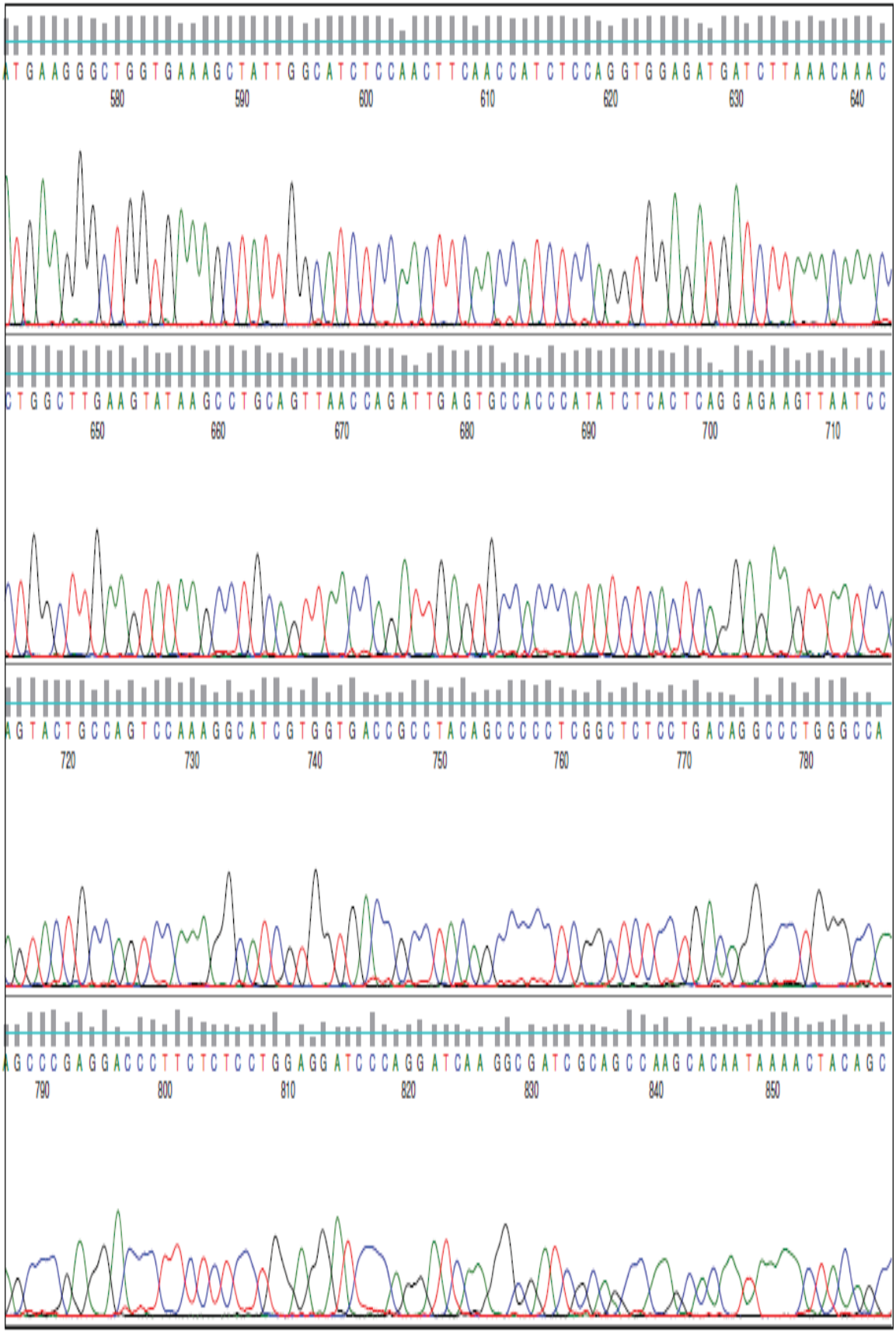
ATGAAGGGCTGGTGAAAGCTATTGGCATCTCCAACTTCAACCATCTCCAGGTGGAGATGATCTTAAACAAAC
580
590
600
610
620
630
640
CTGGCTTGAAGTATAAGCCTGCAGTTAACCAGATTGAGTGCCACCCATATCTCACTCAGGAGAAGTTAATCC
650
660
670
680
690
700
710
AGTACTGCCAGTCCAAAGGCATCGTGGTGACCGCCTACAGCCCCCTCGGCTCTCCTGACAGGCCCTGGGCCA
720
730
740
750
760
770
780
AGCCCGAGGACCCTTCTCTCCTGGAGGATCCCAGGATCAAGGCGATCGCAGCCAAGCACAATAAAACTACAGC
790
800
810
820
830
840
850

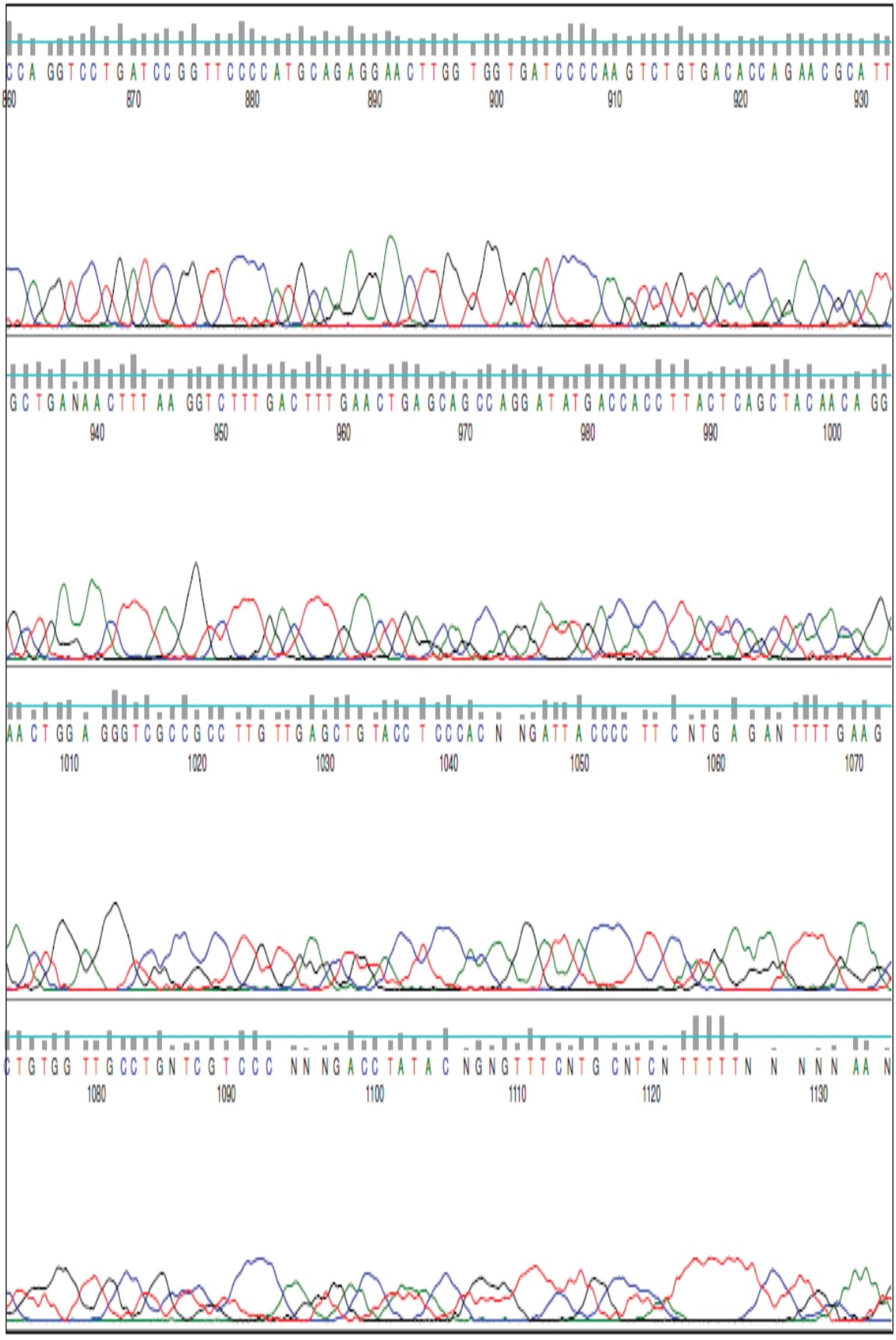
C C A GG T C C T G A T C C G G T T C C C C A T G C A G A G G A A C T T GG T GG T G A T C C C C A A G T C T G T G A C A C C A G A A C G C A T T
860 870 880 890 900 910 920 930
G C T G A N A A C T T T A A GG T C T T T G A C T T T G A A C T G A G C A G C C A G G A T A T G A C C A C C T T A C T C A G C T A C A A C A GG
940 950 960 970 980 990 1000
A A C T GG A GGG T C G C C G C C T T G T T G A G C T G T A C C T C C C A C N NG A T T A C C C C TT C N T G A G A N T T T T G A A G
1010 1020 1030 1040 1050 1060 1070
C T G T G G TT G C C T G N T C G T C C C NN NG A C C T A T A C NG N G T T T C N T G C N T C N T T T T T N N NN N A A N
1080 1090 1100 1110 1120 1130

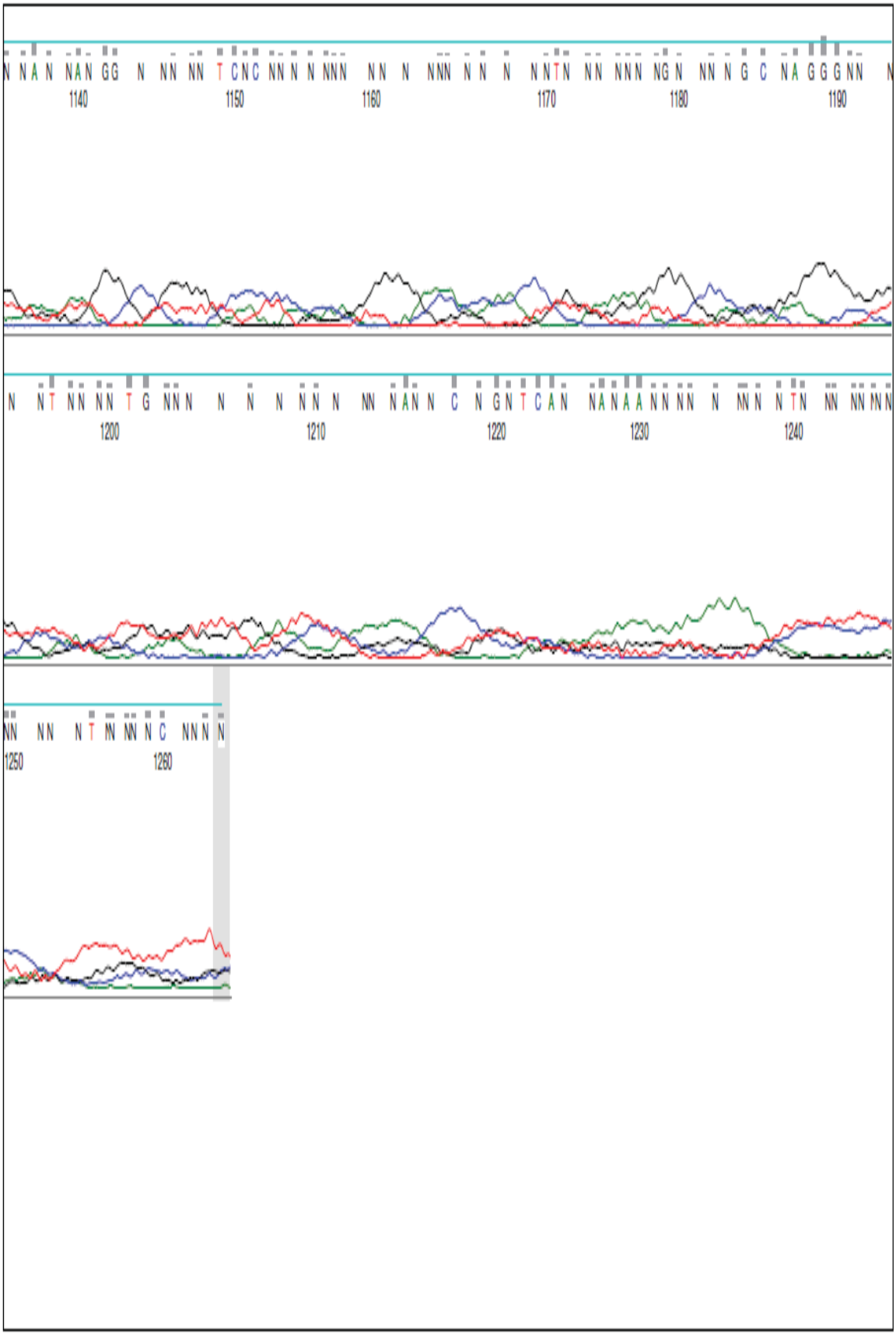
1140
1150
1160
1170
1180
1190
1200
1210
1220
1230
1240
1250
1260

Figure 5.11: C298G Tube 1 Reverse Sequence

NNNNNNNNNNNNNNNNNNNNCTTTCGGGCTTTGTTAGCAGCCGGATCCTC
GAGGCAAAGAGAAGTCTTGCTGAAAGGATTCCNGTTCCAAGCAGTCAAAACT
CAACCGTTAGTGGCACTATTTTGACCTGGTAGATTTTGCTTCTCTTTGGTCAG
AAAAGGGTATTCAGGTTGTACTTTCCCCAGCAGGGTAGAAAGAAGGGCAAAG
CAAACTGGAAGAGACTTCTACTCTACTGACAGGGCTCTTGAGATCCAACATC
AAGCTAGACACGCCCTCGCTGGCCACTCTACAGGTTGCTGTCCCACTGCTGA
GTGACACAGGCCATACTACATTTGCAAGGAAAAAAATGAGGCAAGAAACAC
AGGTATAGGTCACTTGGGGACGAGCAGGCAACCACAGCTTCAAAACTCTTCA
TGGAAGGGGTAATCCTTGTGGGAGGTACAGCTCAACAAGGC**TCC**GACCCTCC
AGTTCCTGTTGTAGCTGAGTAAGGTGGTCATATCCTGGCTGCTCAGTTCAAAG
TCAAAGACCTTAAAGTTCTCAGCAATGCGTTCTGGTGTCACAGACTTGGGGAT
CACCACCAAGTTCCTCTGCATGGGGAACCGGATCAGGACCTGGGCTGTAGTT
TTATTGTGCTTGGCTGCGATCGCCTTGATCCTGGGATCCTCCAGGAGAGAAGG
GTCCTCGGGCTTGGCCCAGGGCCTGTCAGGAGAGCCGAGGGGGCTGTAGGCG
GTCACCACGATGCCTTTGGACTGGCAGTACTGGATTAACTTCTCCTGAGTGAG
ATATGGGTGGCACTCAATCTGGTTAACTGCAGGCTTATACTTCAAGCCAGGTT
TGTTTAAGATCATCTCCACCTGGAGATGGTTGAAGTTGGAGATGCCAATAGCT
TTCACCAGCCCTTCATCCACCAGCTCTTCCATGGCCGCCCACGTGTCCAGAAT
GTTGGTGTCACTGGGAACCACATTGCCCGACTCATCCAATGGGAAAAATTCC
TTCCCAGGCTTAAAGCCAGTCGGCCAGTGAATANNNAGAGGTCCANGTAGTC
CAGCTTCNNNCGCTGANTGNNNTTCTGGCNGNTCCTTTCNCCAGNCCTTCTCA
TGGNACGTGCACCACAGCTNGCTGACGANNANAGCTCCNNNNNNTTNNCCA
NCNGCNCCCNNNNCTTCNNCNNNNGNNNNCCCCNNCNNNNTNNNATNNGGN
NNNANGGNNNNANTCNANNNNGNNNGNNNCCNNNNNTCANNNNN

Figure 5.12: C298G Reverse DNA Chromatogram

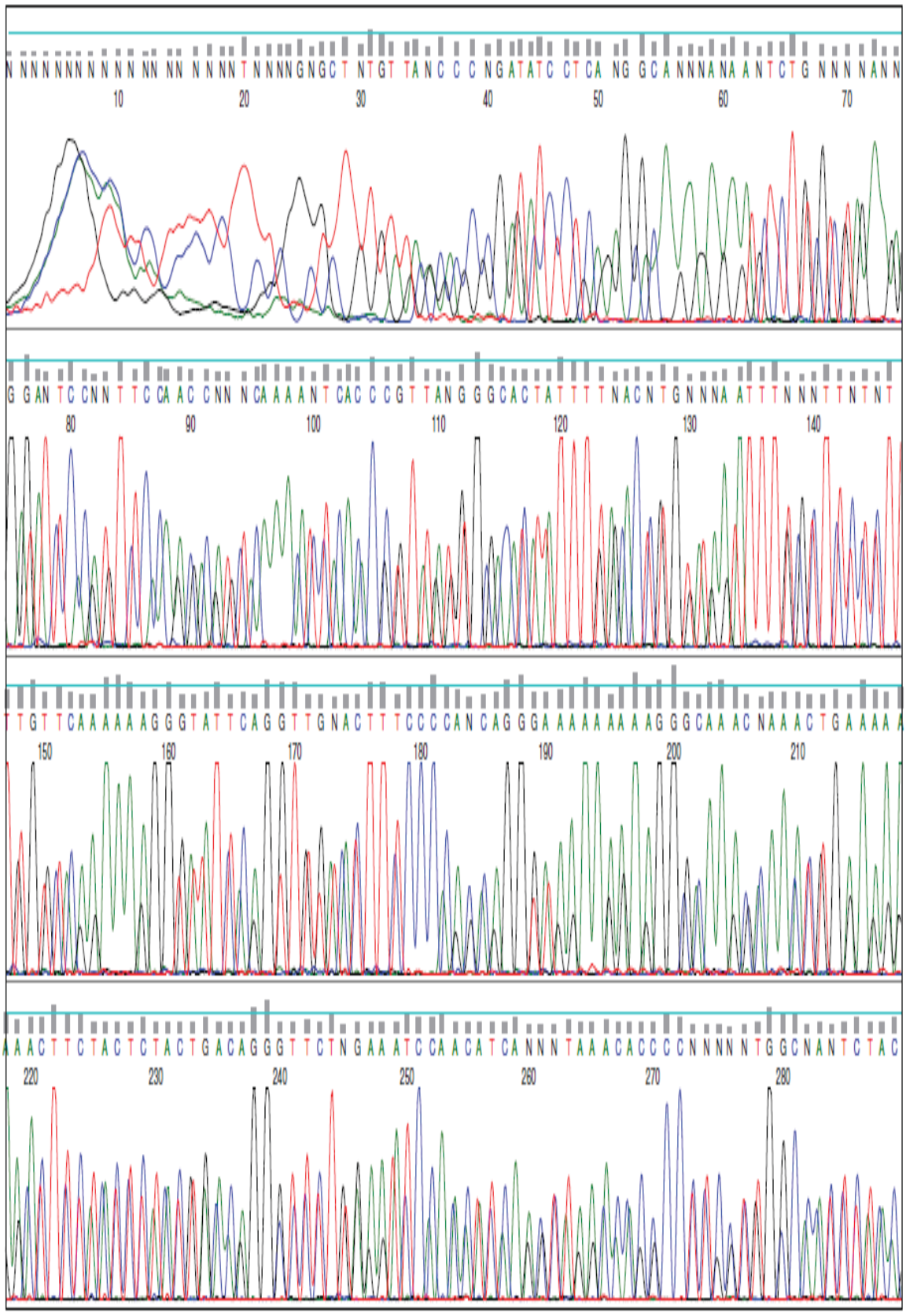

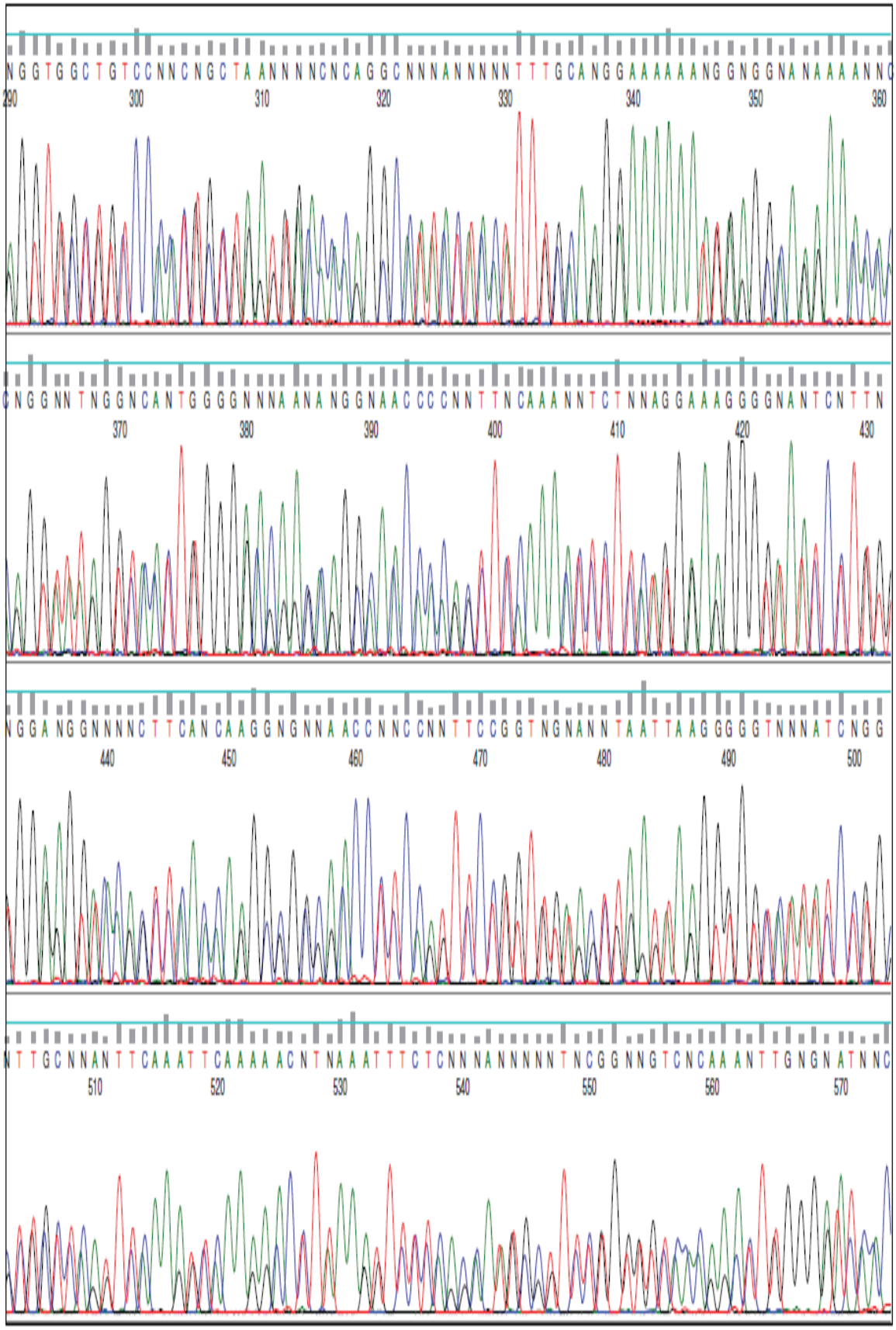

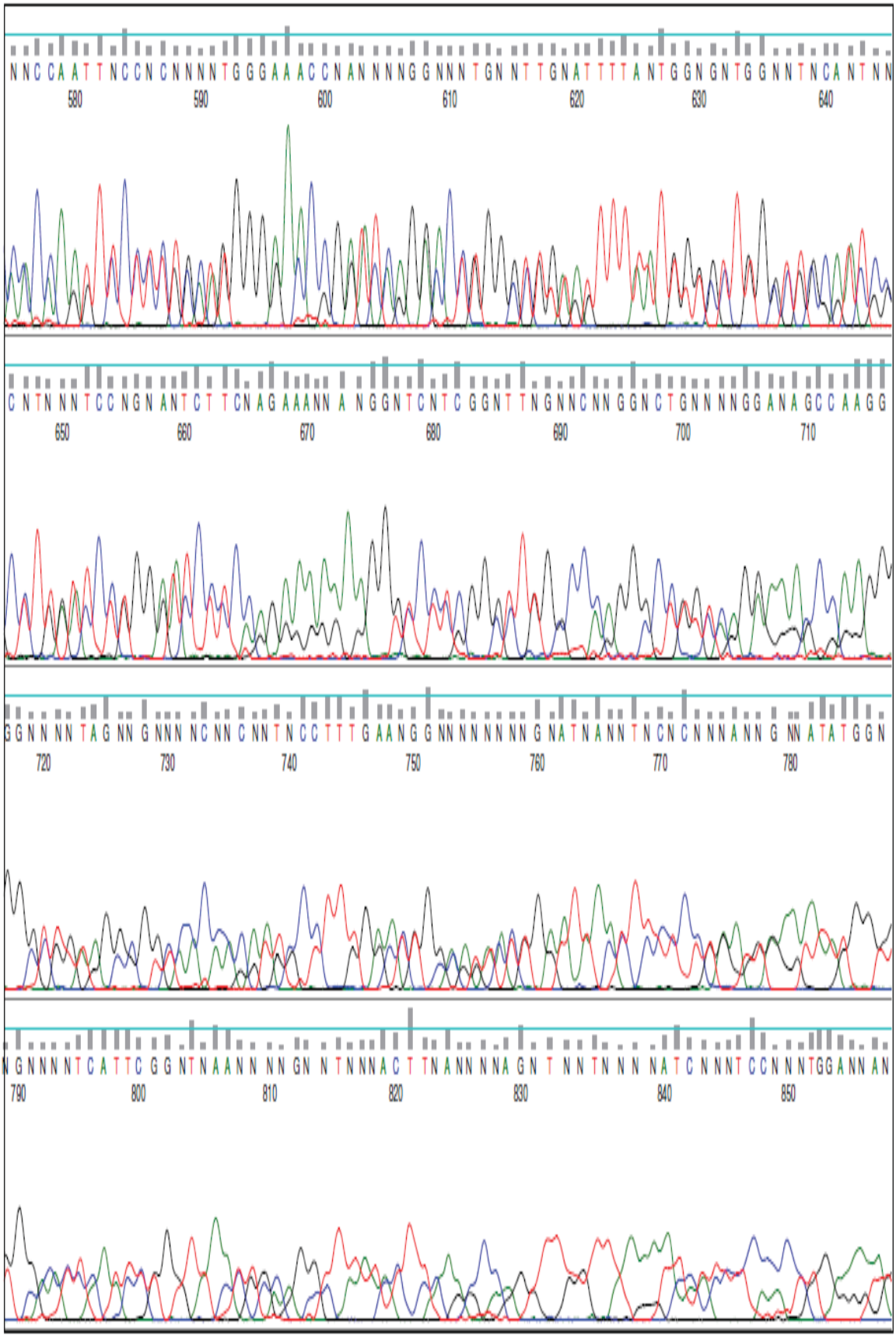
580
590
600
610
620
630
640
650
660
670
680
690
700
710
720
730
740
750
760
770
780
790
800
810
820
830
840
850

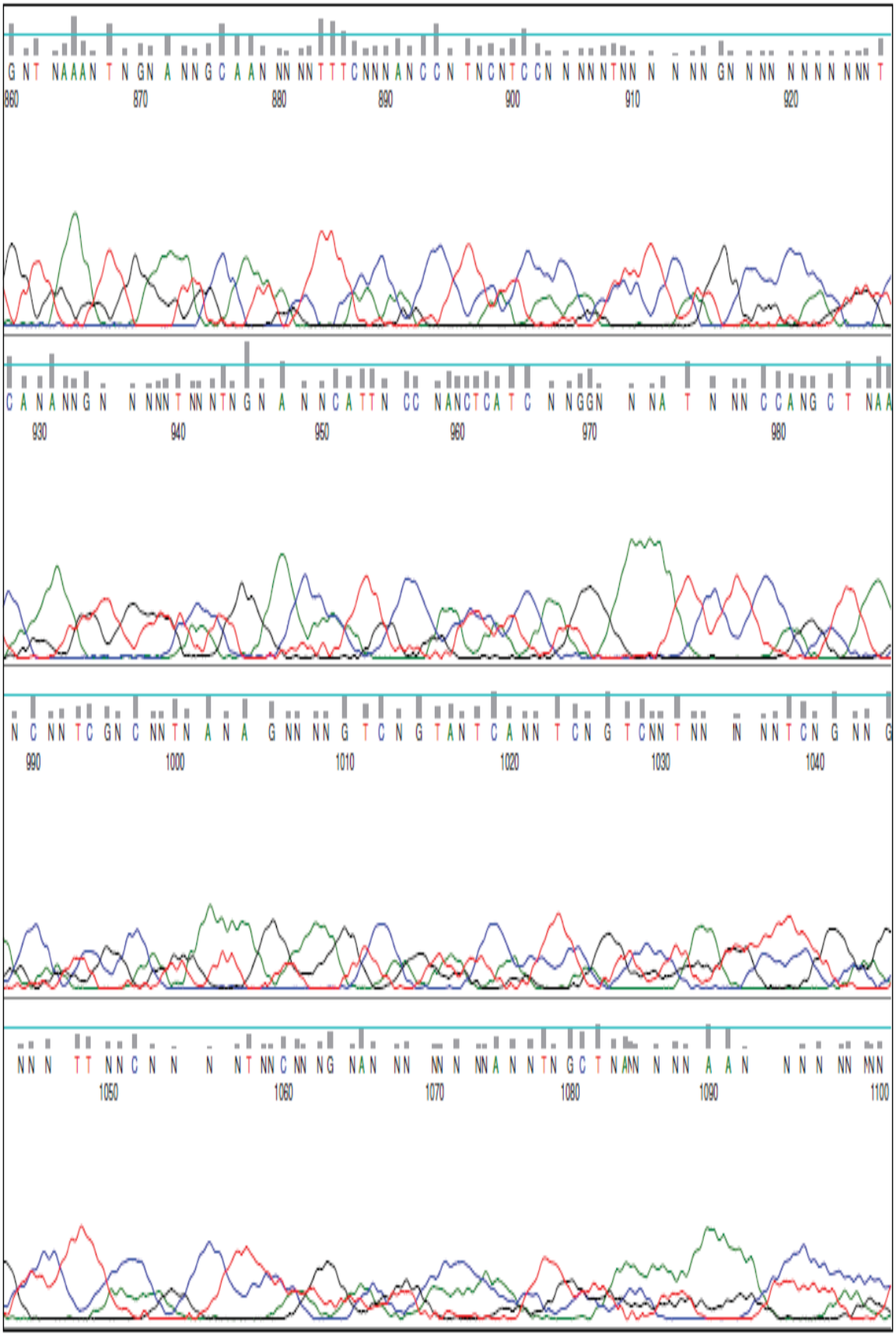

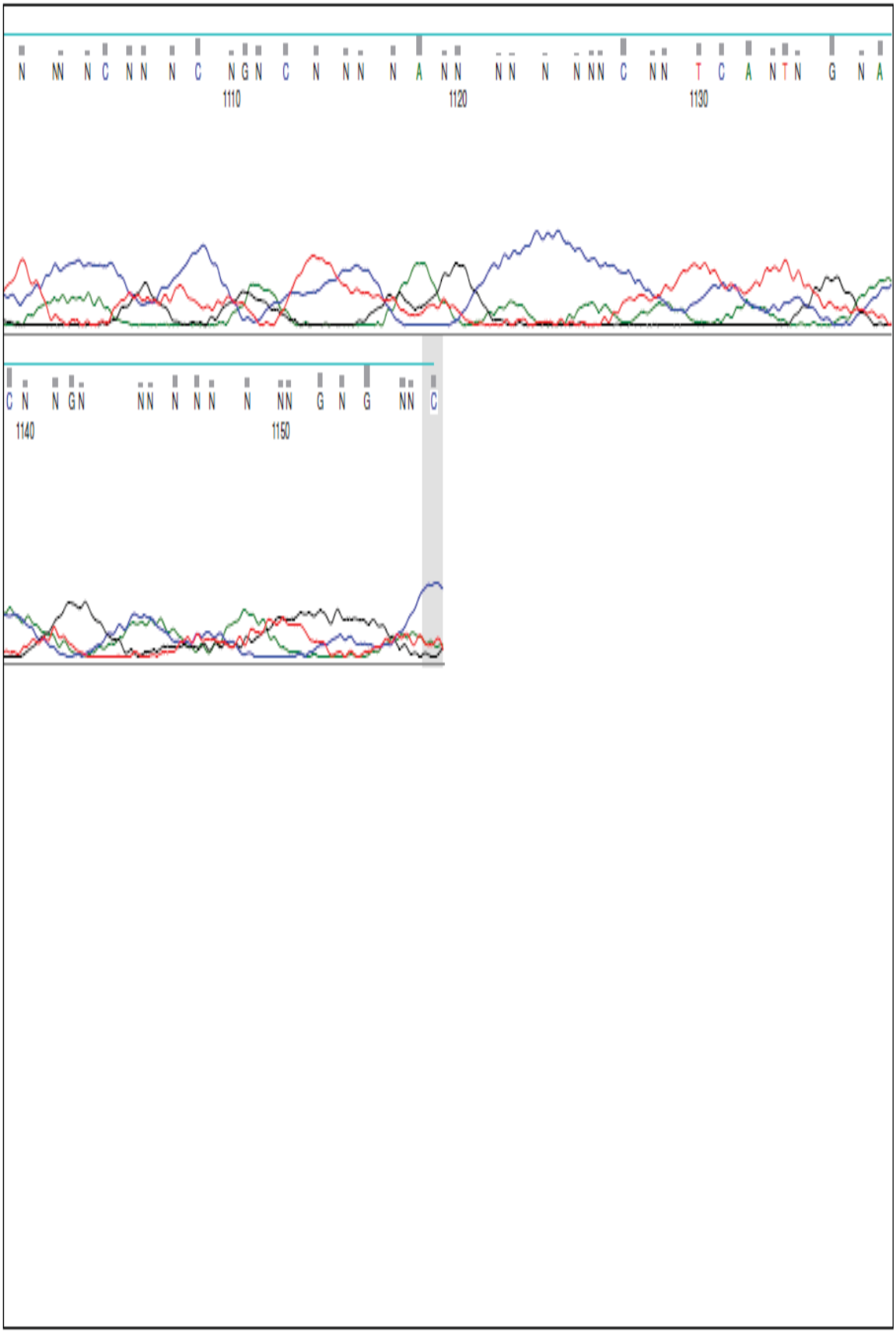
1110
1120
1130
1140
1150

II. Protein Expression

This gel (Figure 5.13) corresponds to the expression of C298G. Lanes 3-5 are the induced samples with a noticeable band at around 35 kDa. Lane 2 is the uninduced sample with no noticeable band at 35 kDa. The 36 kDa is the size of hAR so a band in the 35 kDa region confirms that aldose reductase has been expressed.

Figure 5.13: Uninduced/Induced Samples of C298G

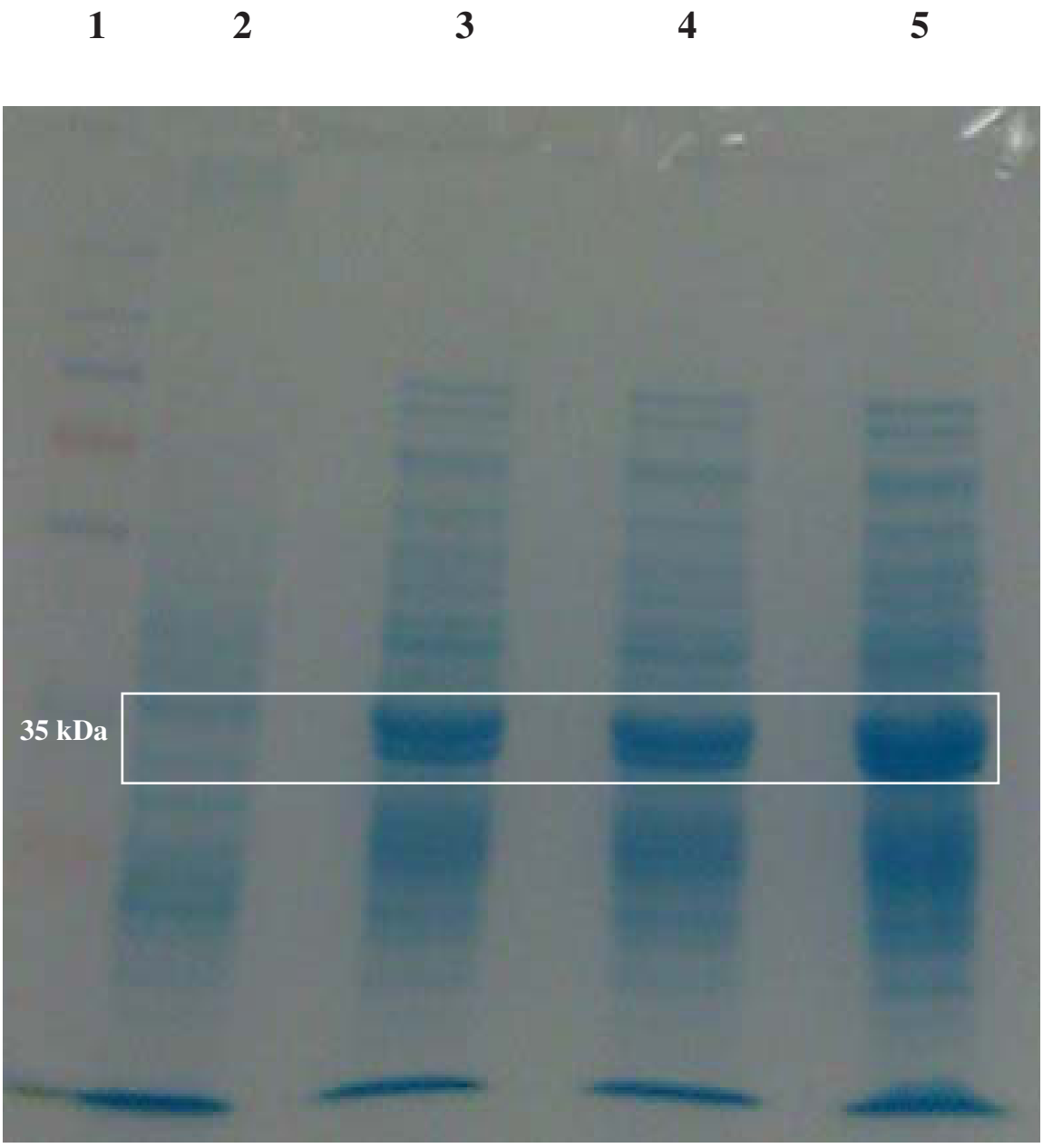

III. Immobilized Metal Affinity Chromatography

This is the samples from protein purification of C298A (Figure 5.14). Lane 10 is the supernatant, lane 9 is the flow-through, lane 8 is wash 1, lane 7 is wash 2, lanes 2 -6 are the eluates from the elution buffer. Eluate 3 (lane 4), eluate 2 (lane 5) and eluate 1 (lane 6) were chosen for dialysis because they had thicker bands in the 35 kDa region.

Figure 5.14: IMAC Column Samples of C298A

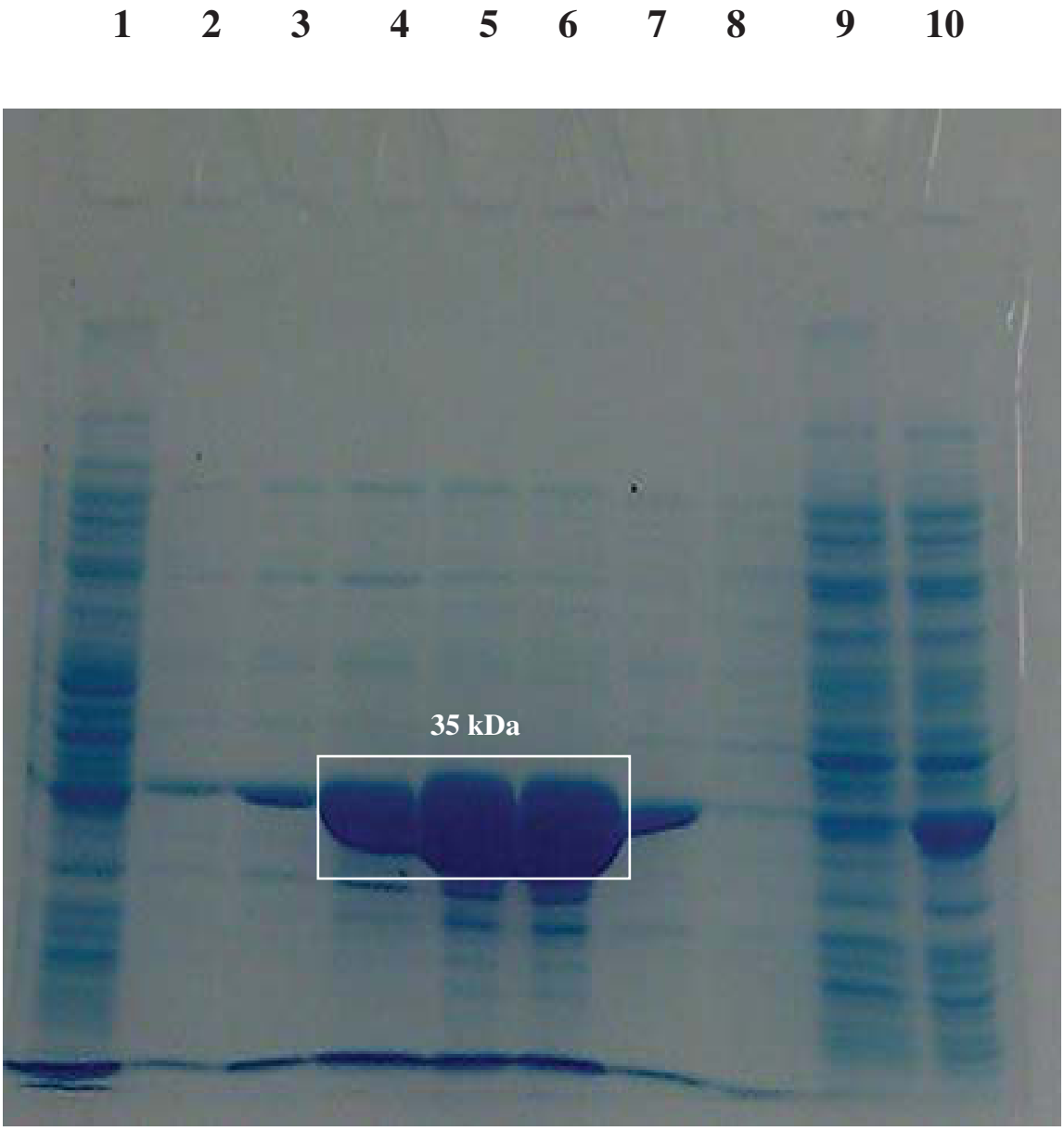

IV. Dialysis and Thrombin Cleavage of Histidine Tag

This is a gel from C298D (Figure 5.15) showing samples from dialysis and thrombin digestion. Lane 1 is the protein after dialysis and lane 2 is the protein after thrombin digestion. There is a slight decrease in the size of the protein band due to the cleavage of the histidine tag.

Figure 5.15: Dialysis and Thrombin Digestion Samples of C298D

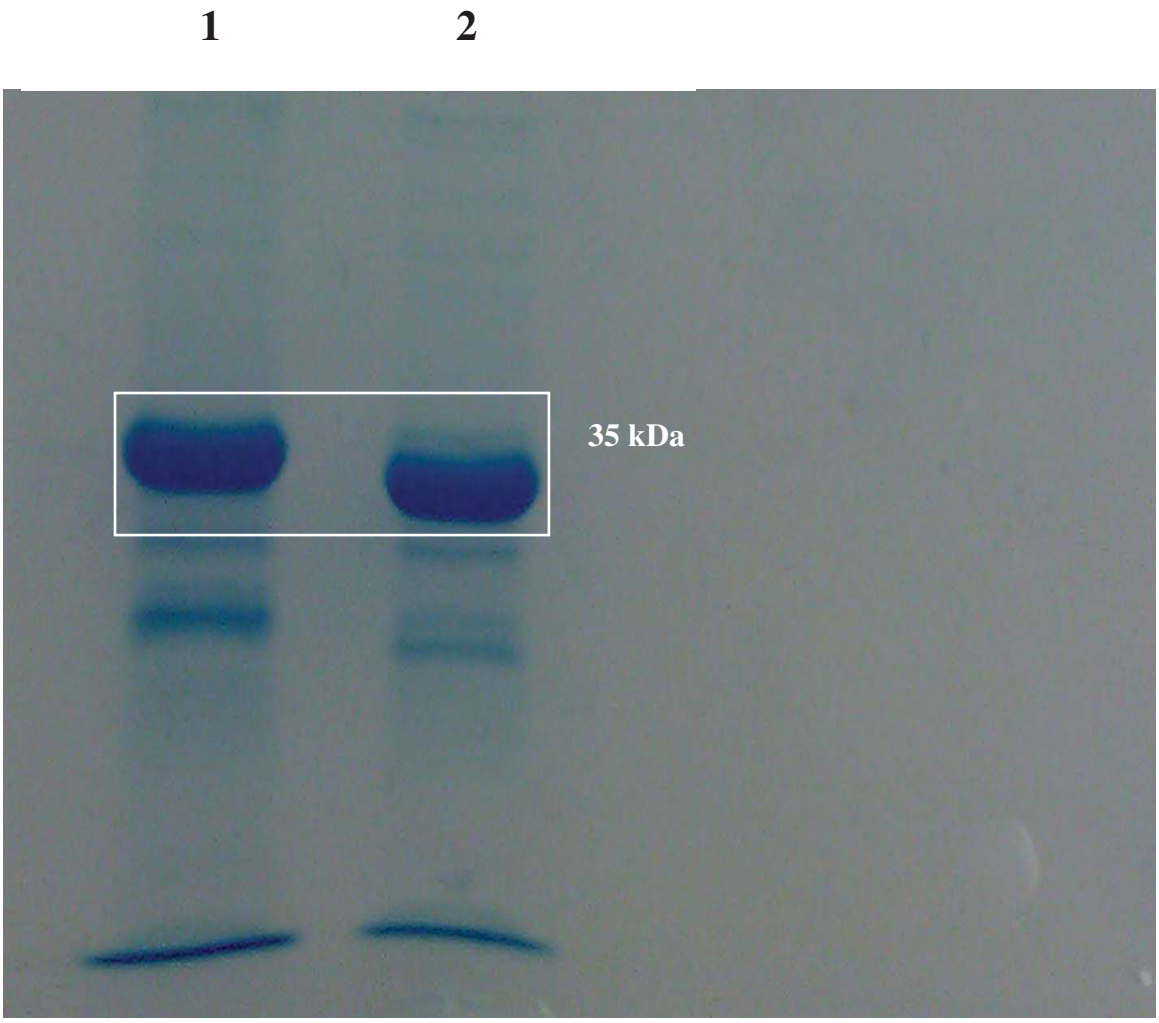

Chapter VI: Conclusion

The thesis project was a great learning experience and fortunately the mutagenesis, expression and purification of the Cys298 hAR mutants was successful. Several methods were used at each part of the project and some parts were more challenging than others due to unforeseen hurdles. Nonetheless, the set goals of this project provides the foundation for future kinetic, structure, and function studies.

During mutagenesis, primers were designed for synthesizing the mutant hAR DNA and later this DNA was amplified for transformation into *E. coli* bacteria. DNA sequencing and BioEdit software was used to analyze the quality of the mutant DNA and verify that correct mutations had been made.

Protein expression was induced with IPTG and incubation at 37°C for 4 hours. Optimal expression was achieved with 2X YT media and it was confirmed by the presence of a 36 kDa band on SDS-PAGE gels. Protein purification was carried out through sonication, immobilized metal affinity chromatography and thrombin cleavage of the histidine tag. Finally, protein quantification was completed through Bradford Reagent Assay with bovine γ-globulin standards. Overall, the procedures have been optimized for the reproducible production of recombinant cells of hAR mutants (C298A, C298D, C298G) for their overexpression and purification.

Future work would include measuring the Michaelis-Menten parameters of these mutants with forward reaction substrates, reverse reaction substrates, and inhibitors. Also, van't Hoff analysis could be used to study the thermodynamics of enzyme-inhibitor and enzyme-substrate interaction. Additionally, Arrhenius analysis could be performed to examine the activation energy differences between the wild-type and mutant enzymes.

The kinetic and thermodynamic properties of the C298A and C298G mutants may be similar to that of the wild-type. Both amino acids have neutral, non-polar side chains that are expected to minimally destabilize the NADPH and substrate binding sites. For the C298D mutant, the kinetic and thermodynamic properties should be more pronounced than that of the wild-type. Aspartate has an acidic, polar side chain that may significantly destabilize both binding sites.

Chapter VII: References

1. Barski, O. A.; Tipparaju, S. M.; Bhatnagar, A. The Aldo-Keto Reductase Superfamily and its Role in Drug Metabolism and Detoxification. *Drug Metabolism Reviews*. **2008**, 40, 553-624.
2. Gueraud, M. A.; Bresgen, N. Cipak, A.; Eckl, P. M.; Huc, L.; Jouanin, I.; Siems, W.; Uchida, K. Chemistry and biochemistry of lipid peroxidation products. *Free Radical Res*. **2010**, 44, 1098-1124.
3. Goldin, A.; Beckman, J. A.; Schmidt, A. M.; Creager, M. A. Advanced Glycation End Products Sparking the Development of Diabetic Vascular Injury. *Circulation*. **2006**, 114, 597-605.
4. Nagai, R. Accumulation of Advanced Glycation End Products in Age-Dependent Disorders. *Med. Hypotheses Res*. **2004**, 1, 161-170.
5. Ramasamy, R.; Goldberg, I. J. Aldose Reductase and Cardiovascular Diseases Creating Human-Like Diabetic Complications in an Experimental Model. *Circ. Res*. **2010**, 106, 1449-1458.
6. Yabe-Nishimura, C. Aldose Reducatase in Glucose Toxcicity: A Potential Target for the Prevention of Diabetic Complications. *Pharmacol. Rev*. **1998**, 50, 21-33.
7. Ramana, K. V. Aldose reductase: new insights for an old enzyme. *Biomol. Concepts*. **2011**, 2, 103-114.
8. Grimshaw, C. E.; Lai, C-J. Oxidized Aldose Reductase: In Vivo Factor, Not in Vitro Artifact. Arch. *Biochem. Biophys.* **1996**, 327, 89-97.
9. Wood, S.; Trayhurn, P. Glucose transporters (GLUT and SGLT): expanded families of sugar transport proteins. *Brit. J. Nutr*. **2003**, 89, 3-9.

10. Deponte, M. Glutathione catalysis and the reaction mechanisms of glutathione-dependent enzymes. *Biochim. Biophys. Acta*. **2013**, 1830, 3217-3266.
11. Petrash, J. M.; Harter, T. M.; Devine, C. S.; Olins, P. O.; Bhatnagar, A.; Liu, S-Q.; Srivastava, S. K. Involvement of Cysteine Residues in Catalysis and Inhibition of Human Aldose Reductase: Site-Directed Mutagenesis of Cys-80, -298, and -303. *J. Biol. Chem*. **1992**, 267, 24833-24840.
12. Chung, H. S.; Wang, S-B.; Venkatraman, V.; Murray, C. I.; Van Eyk, J. E. Cysteine Oxidative Posttranslational Modifications: Emerging Regulation in the Cardiovascular System. *Circ. Res*. **2013**, 112, 382-392.
13. Balendiran, G. K.; Sawaya, M. R.; Schwarz, F. P.; Ponniah, G.; Cuckovich, R.; Verma, M.; Cascio, D. The Role of Cys-298 in Aldose Reductase Function. *J. Biol. Chem*. **2011**, 286, 6336-6344.
14. Qiagen. https://www.qiagen.com/us/resources/resourcedetail?id=89bfa021-7310-4c0f-90e0-6a9c84f66cee&lang=en (accessed April 4, 2015).
15. Bhatnagar, A.; Liu, S-Q.; Ueno, N.; Chakrabarti, B.; Srivastava, S. K. Human placental aldose reductase: role of Cys-298 in substrate and inhibitor binding. *Biochim. Biophys. Acta*. **1994**, 1205, 207-214.
16. Brownlee, J. M.; Carlson, E.; Milne, A.; Pape, E.; Harrison, D. H. T. Structural and Thermodynamic Studies of Simple Aldose Reductase-Inhibitor Complexes. *Bioorg. Chem*. **2006**, 34, 424-444.
17. Cappiello, M.; Voltarelli, M.; Cecconi, I.; Vilardo, P. G.; Dal Monte, M.; Marini, I.; Del Corso, A.; Wilson, D. K.; Quiocho, F. A.; Petrash, J. M.; Mura, U.

Specifically Targeted Modification of Human Aldose Reductase by Physiological Disulfides. *J. Biol. Chem*. **1996**, 271, 33539-33544.

18. Chandra, A.; Srivastava, S.; Petrash, J. M.; Bhatnagar, A.; Srivastava, S. K. Active site modification of aldose reductase by nitric oxide donors. *Biochim. Biophys. Acta*. **1997,** 1341, 217-222.
19. Grimshaw, C. E.; Bohren, K. M.; Lai, C-J.; Gabbay, K. H.; Human Aldose Reductase: Subtle Effects Revealed by Rapid Kinetic Studies of the C298A Mutant Enzyme. *Biochemistry*. **1995**, 34, 14366-14373.
20. Koch, C.; Heine, A.; Klebe, G. Tracing the Detail: How Mutations Affect Binding Modes and Thermodynamic Signatures of Closely Related Aldose Reductase Inhibitors. *J. Mol. Biol*. **2011**, 406, 700-712.
21. Kubiseski, T. J.; Flynn, T. G.; Studies on Human Aldose Reductase: Probing the Role of Arginine 268 by Site-Directed Mutagenesis. *J. Biol. Chem*. **1995**, 270, 16911-16917.
22. Kurono, M.; Fujiwara, I.; Yoshida, K. Stereospecific Interaction of a Novel Spirosuccinimide Type Aldose Reductase Inhibitor, AS-3201, with Aldose Reductase. *Biochemistry.* **2001**, 40, 8216-8226.
23. Petrova, T.; Steuber, H.; Hazemann, I.; Cousido-Siah, A.; Mitschler, A.; Chung, R.; Oka. M.; Klebe, G.; El-Kabbani, O.; Joachimiak, A.; Podjarny, A. Factorizing Selectivity Determinants of Inhibitor Binding toward Aldose and Aldehyde Reductases: Structural and Thermodynamic Properties of the Aldose Reductase Mutant Leu300Pro-Fidarestat Complex. *J. Med. Chem*. **2005**, 48, 5659-5665.

24. Steuber, H.; Heine, A.; Klebe, G. Structural and Thermodynamic Study on Aldose Reductase: Nitro-substituted Inhibitors with Strong Enthalpic Binding Contribution. *J. Mol. Biol.* **2007**, 368, 618-638.

25. Steuber, H.; Heine, A.; Podjarny, A.; Klebe, G. Merging the Binding Sites of Aldose and Aldehyde Reductase for Detection of Inhibitor Selectivity-determining Features. *J. Mol. Biol*. **2008**, 379, 991-1016.